July 2018

Evaluation of trace-metal and isotopic records as techniques for tracking lifetime movement patterns in fishes

Jennifer E. Granneman
University of South Florida, jgranneman@mail.usf.edu

Evaluation of trace-metal and isotopic records as techniques for tracking lifetime movement patterns in fishes

by

Jennifer E. Granneman

A dissertation submitted in partial fulfillment
of the requirements for the degree of
Doctor of Philosophy
with a concentration in Marine Resource Assessment
College of Marine Science
University of South Florida

Co-Major Professor: Ernst B. Peebles, Ph.D.
Co-Major Professor: Steven A. Murawski, Ph.D.
William F. Patterson, III, Ph.D.
Cameron H. Ainsworth, Ph.D.
David J. Hollander, Ph.D.

Date of Approval:
April 9, 2018

Keywords: otolith microchemistry, eye lens, stable isotopes, trace elements, diet switch, meta-analysis

Dedication

This work is dedicated to Dr. David Jones for his guidance, patience, and pursuit of the significant truth.

Acknowledgements

I could not have achieved all I set out to do without the love and support of my family. My husband is my cornerstone and I am deeply appreciative of all the love, patience, and guidance he has provided throughout this trial. I would also like to thank my soul sisters and aunt for their constant empathy; they helped me through the times when I wasn't sure if it was worth continuing to pursue this degree. My parents helped to instill the grit I needed to achieve this goal, and for that I will be eternally thankful.

I must thank my co-advisors, Dr. Ernst Peebles and Dr. Steve Murawski, for their financial support and mentorship offered to me during my time at USF. I also thank the members of my dissertation committee - Dr. Cameron Ainsworth, Dr. David Hollander, and Dr. William Patterson, III - for their feedback on this research. I would especially like to acknowledge the late Dr. David Jones, my friend and committee member, for his support and kindness throughout this academic journey.

This research was made possible in part by financial support provided by the William and Elsie Knight Endowed Fellowship Fund for Marine Science, the Paul Getting Endowed Memorial Fellowship in Marine Science, the Gulf of Mexico Research Initiative/C-IMAGE I and II (SA 15-16), the State of Louisiana (S203-4S-2121), and the National Fisheries Institute.

Table of Contents

List of Tables

List of Figures

Abstract

The focus of this work was on the use of otolith microchemistry and fish eye lens chemical profiles to measure fish movement and provided indirect support for the use of otolith microchemistry to examine exposure to crude oil. Chapter 1 provides an introduction to the applications of otolith microchemistry and eye lens isotopic profiles. In the second chapter, which examined associations between metal exposure and lesion formation in fishes collected after the *Deepwater Horizon* (DWH) oil spill, I did not observe any change in oil-associated metal concentrations in otoliths coinciding with the timing of the DWH oil spill. This suggests that either the technique used is not sensitive enough to detect any transient changes that may have occurred because of exposure to the oil spill or that the fish examined were not exposed to the oil spill. However, I did find that lesioned fish may have been exposed to a persistent source of trace-metals in the GoM prior to, during, and after the oil spill, and metal-induced immunomodulation may have occurred in these fish. These interactions between the physiological and environmental modulation of otolith element incorporation were explored further in Chapter 3 in which multiple tests demonstrated that physiology explained more of the variation in otolith chemical tags than ambient water chemistry. These findings suggest that the use of otolith microchemistry alone to track fish movement and potential exposure to harmful metals may be complicated by physiological control of otolith microchemistry. Thus, in Chapter 4, I pursued a novel method to evaluate the movement of fish across isoscapes of varying $\delta^{15}N$. I

validated the use of fish eye lenses as potential lifetime recorders of isotopic histories and in Chapter 5 compared the use of fish eye lens $\delta^{15}N$ profiles to otolith microchemistry profiles to examine fish movement. Both techniques suggested similar patterns of movement in Red Snapper from the northern GoM to the West Florida Shelf. This is the first study to use these complimentary techniques to track fish movement.

Chapter 1. Introduction

The field of otolith microchemistry incorporates information about fish biology and the physicochemistry of water bodies that fish move through. The fact that this has rapidly evolved and expanded since its beginnings in the 1970s is testament to the application of this research in fisheries management. There are several calcified structures within fish that produce identifiable growth increments that can be used to determine the age of fish. These include opercula, fin rays, cleithra, scales, vertebrae, and otoliths, although otoliths are most commonly used to determine age in most species (Panfili et al. 2002). Otoliths are highly suitable for age determination because, unlike other calcified structures contained within the fish, they are metabolically inert once formed, which means that they are not mobilized for homeostasis during times of stress (Campana 1999). The sagittal otolith is the largest of the three types of otoliths that are part of the vestibular apparatus of fishes, which functions in the acoustico-lateralis system (Popper and Fay 1973). Otoliths are primarily composed of aragonite, a form of crystalline calcium carbonate, which is precipitated on a protein matrix (Degens et al. 1969). The initial deposition of calcium carbonate material occurs during the latter part of the egg stage and becomes the core of the otolith. As a juvenile fish grows, calcium carbonate is deposited daily in a manner that results in a zone high in organic material that appears opaque and a translucent mineral-rich zone. The deposition of these alternating layers of optically dense and translucent zones usually occurs in a diel cycle and results in identifiable daily growth rings that are discernible in young (<100 days post-hatch) fish (Pannella 1971). Additionally, faster

growth during the summer and slower growth during the winter results in the appearance of seasonal and annual growth rings which can be counted to determine fish age (Pannella 1971).

Minor and trace elements from the surrounding water are incorporated into the otolith as a fish grows at three sites within the otolith: as a substitution for calcium in the crystal structure, within the interstitial spaces of the otolith at crystal defects, and by covalent bonding with the organic molecules that make up the protein matrix (Campana 1999). Therefore, environmental reconstruction based on the incorporation of trace elements in the otoliths is possible if fish movement occurs through waters with differing physicochemical properties. However, differences can only be detected in the otolith chemistry of fish migrating between different water bodies if the fish reside in these environments for long enough to incorporate a chemical tag. The ecosystems that fish occupy are often spatially and temporally variable in their physicochemistry and this has provided considerable insight into the movement patterns of fish.

The emphasis of research involving otoliths has evolved and shifted focus with the development of new technology. The dominant use of otoliths was for age and growth studies of fish until about the 1980s. Prior to 1999, 80% of papers published on otolith research were focused on annual age-and-growth studies (Campana 2005). However, in a review of otolith studies published between 1999 and 2004, Campana (2005) found that age-and-growth papers only accounted for 40% of the publications. During the 1980s and 1990s, a shift occurred and the proportion of studies on otolith chemistry rapidly increased with the development of more sensitive mass spectrometers (Campana and Thorrold 2001). In a review of the otolith literature from 1999-2004, otolith chemistry, otolith microstructure, and other non-ageing applications of otolith studies each accounted for between 15 and 20% of the studies on fish otoliths (Campana 2005). In the beginning of the 21st century, the analytical constraints associated with otolith

chemistry were mostly overcome with the development of more sensitive technologies. For example, high-resolution laser ablation inductively coupled plasma mass spectrometry (HR-LA-ICPMS) can detect parts per trillion trace element concentrations within precise locations in otoliths.

Researchers investigating chemical tags within otoliths take two general approaches: examination of the whole otolith or of different life-history stages using selected portions of the otoliths. Whole-otolith analysis is accomplished by dissolving the entire otolith and measuring the resulting solution using solution-based ICPMS. This technique provides a chemical tag that integrates the entire life of the fish, but is only stable over a short period of time (months to years). A different approach is to cut a thin section of an otolith and sample a selected time period within the otolith corresponding to the life-history stage of interest. This approach can be further divided into two different techniques: the analysis of a single location within an otolith using spot-sampling or the analysis of a chemical profile within an otolith to relate changes in chemistry to fish movement. Laser ablation ICPMS (LA-ICPMS), x-ray fluorescence, micro-proton induced x-ray emission (PIXE), micromilling and mass spectrometry, and electron microprobe are all techniques that can be used to analyze a specific portion of an otolith section (Panfili et al. 2002).

In contrast, the use of fish eye lenses as chronological recorders of microchemical constituents is a relatively recent development (reviewed by Tzadik et al. 2017). Fish eye lenses consist of concentric cell layers (laminae) (Zampighi et al. 2000). All laminae except the outermost ones are made up of lens fiber cells (LFC) that have undergone attenuated apoptosis, a process in which all the DNA and organelles are removed from the LFCs (Wride 2011). The process of attenuated apoptosis improves the optical properties of the LFCs by minimizing the

absorbance and scattering of light and prevents LFCs from synthesizing any new proteins (Greiling and Clark 2012). Laminae are gradually added to the exterior of the eye lens as a fish ages, with interior laminae becoming increasingly hardened and less water-soluble with age.

Unlike otoliths, which contain very little protein, the primary constituent of lens fiber cells is the protein crystallin (Horwitz 2003). Thus, the abundance of crystallin protein in eye lens laminae makes them well-suited for the analysis of stable isotopes, $\delta^{13}C$ and $\delta^{15}N$. Additionally, because eye lens laminae form through a sequential cessation of organic synthesis, eye lens laminae are potential recorders of lifetime histories of $\delta^{13}C$ and $\delta^{15}N$. Individual eye lens laminae are carefully removed for analysis through the process of delamination. In this process, each lamina is removed by starting near one lens pole and working towards the other. After drying and homogenizing the laminae, they can be analyzed using an isotope ratio mass spectrometer.

The use of fish eye lenses as potential long-term recorders of stable isotopes was introduced by Wallace et al. (2014). Red Snapper and Gag Grouper eye lens laminae were observed to exhibit enough isotopic variation to detect broad-scale changes in the isotopic histories of individuals (Wallace et al. 2014). In addition, Wallace et al. (2014) matched the isotopic histories of these fish collected on the West Florida Shelf (WFS) to isotopic baselines created for the WFS by Radabaugh et al. (2013).

The following chapters explore the utility of otolith microchemistry and eye lens stable isotopes as techniques to examine fish movement and exposure to *Deepwater Horizon* (DWH) oil-associated metals. In Chapter 2, otolith microchemistry was used to determine whether fish were exposed to metals associated with the DWH oil spill. In Chapter 3, a meta-analysis of

otolith microchemistry was conducted to evaluate the relative contribution of physiological and environmental effects on otolith element incorporation. Chapter 4 validates the use of fish eye lenses as stable isotope recorders through an experimental step-change in dietary $\delta^{15}N$. Finally, Chapter 5 compares the otolith microchemistry and eye lens $\delta^{15}N$ profiles of Red Snapper to examine their movement in the Gulf of Mexico.

Chapter 2. Associations between metal exposure and lesion formation in offshore Gulf of Mexico fishes collected after the *Deepwater Horizon* oil spill

2.1 Research Overview

The *Deepwater Horizon* (DWH) drilling platform explosion resulted in the release of approximately 4.9 million barrels of crude oil into the Gulf of Mexico (GoM). The unprecedented extent of subsurface and benthic oil from the DWH oil spill substantially overlapped with the known distributions of many species of adult and larval fishes in the GoM. The purpose of this study was to determine whether the unique, metal signatures recorded within fish otoliths could potentially serve as oil-exposure biomarkers that would not degrade over time. We took advantage of the chronological deposition of metals in otoliths in order to examine the metal-exposure histories and establish baseline conditions for offshore fish species collected after the DWH oil spill occurred. The main objectives of this study were to: (1) examine patterns of short- and long-term metal exposure within the otoliths of six offshore fish species in varying states of health, as indicated by the presence of external skin lesions, and (2) determine if there was a change in otolith metal concentrations concurrent with the DWH oil spill. Otoliths collected from 2011 to 2013 in the Gulf of Mexico (GOM) were analyzed for a suite of trace-metals known to be associated with DWH oil. The short-term analysis of trends in otolith metal concentrations revealed no significant differences among the years prior to, during, or after the DWH oil spill for all of the species analyzed. We found that lesioned fish often had elevated

levels of otolith ^{60}Ni and ^{64}Zn before, during, and after the DWH oil spill. In addition, metal exposure varied according to species-specific life history patterns. These findings indicate that lesioned individuals were exposed to a persistent source of trace-metals in the GoM prior to the oil spill.

2.2 Note to Reader

This chapter was published in the peer-reviewed Elsevier journal *Marine Pollution Bulletin* and is included here in Appendix A. The full citation is Granneman, J.E., D.L. Jones, and E. B. Peebles. 2017. Associations between metal exposure and lesion formation in offshore Gulf of Mexico fishes collected after the *Deepwater Horizon* oil spill. *Marine Pollution Bulletin* 117(1-2): 462-477.

Chapter 3. Otolith Microchemistry Meta-Analysis including the Gulf of Mexico, West Atlantic, and Caribbean Sea

Abstract

Otolith microchemistry is not a function of ambient water chemistry alone. Temperature and salinity as well as species-specific ontogenetic processes and biochemical processes can influence otolith element incorporation. This fact does not invalidate the use of otolith element fingerprints that can be studied as natural tags of habitat use; however, it does make interpretation of the results more complex. The purpose of this study was to quantify otolith multi-element environmental, taxonomic, and ecological patterns of all fish species in the Gulf of Mexico (GoM), along the West Atlantic coast, and in the Caribbean Sea for which this information is available. A search of the relevant literature identified 63 studies of otolith chemistry conducted on 45 species within 23 families within the GoM, Caribbean Sea, and West Atlantic. A total of 415 data points were extracted from these studies, including 36 elements. The following 8 constituents were found to potentially be indicative of ambient water chemistry in both the freshwater and marine environment: $\delta^{18}O$, Li, Mg, Ba, Mn, Sr, Fe, and $\delta^{13}C$. The only analytes that were found to be indicative of ambient water chemistry without being under some degree of physiological control were $\delta^{18}O$ and $\delta^{13}C$. In comparison, 70% of the elements tested to determine the extent of physiological control on otolith element concentrations indicated some degree of biological influence and the most important of these included: Ba, Sr,

Cu, Li, Na, Mg, Mn, Fe, and Pb. Multiple tests demonstrated that taxonomic effects explained more of the variation in otolith chemical tags than regional effects. Although physiology apparently is frequently more important in controlling otolith element concentrations than the environment, regional patterns were observed in otolith element concentrations and region was repeatedly observed to significantly affect otolith multielement patterns. Patterns of otolith element concentrations among regions included a noticeable enrichment in element concentrations from South Florida to the Mississippi Delta and the Central/North Atlantic.

3.1 Introduction

Advances in technology have been instrumental in obtaining detailed analyses of otolith chemistry, but the ability to determine fish movements through different environments relies on the ability to recognize the dynamic changes in water chemistry, temperature, and salinity that vary in space and time among different water bodies. Fresh water chemistry can be affected by a number of factors such as hydrologic processes, groundwater retention, heterogeneity of the basement catchment, and the presence of evaporate minerals. In estuaries and marine systems water chemistry may be affected by tides, water currents, evaporation, precipitation, temperature, salinity, and upwelling. The primary sources of elements that contributed to localized increased in these elements include atmospheric deposition, river discharge, or anthropogenic input. Differences in otolith chemistry as a result of spatial variation in water chemistry have been observed over a scale of several meters, while other studies found no differences in otolith chemistry among locations separated by up to 3000 km (Elsdon et al. 2008). Temporal variation in water chemistry may occur over short time periods in dynamic environments (Elsdon and Gillanders 2006). Intra-annual variation in otolith chemistry has been observed in many studies;

thus, a sampling design that takes into account spatial and temporal variation in water chemistry is needed in order to interpret chemical tags and make inferences about fish movement.

The proportion of studies on otolith structure and chemistry rapidly increased after 1999 with the development of more sensitive mass spectrometers (Campana and Thorrold 2001). The ability to trace fish movement through waters with differing physicochemical properties has a variety of fishery management applications; for instance, the method provides a useful tool for discriminating fish stocks. Heidemann (2012) analyzed 12 element/calcium ratios in the otoliths of Baltic cod to determine if significant differences could be detected in the otoliths of cod collected from the eastern and western Baltic Sea and between the North Sea and Baltic Sea. They found that adult cod collected from those areas could be separated based on their otolith chemistry and additionally the core regions of otoliths from juveniles indicated that exchange among stocks is limited. The use of otolith chemical tags to discriminate between fish stocks has also been demonstrated for Orange Roughy (Edmonds et al. 1991), Atlantic Cod (Syedang et al. 2010), Spanish mackerels (Begg 1998), and Pink Snapper (Edmonds et al. 1991). Syedang (2010) observed that differences in otolith element composition among sites provided even better discrimination among populations than genetic studies.

Otolith microchemistry has also been remarkably successful in describing the migratory routes and timing of fish migration, especially for diadromous species. Life history profiles of otoliths can reveal the transition between fresh and marine habitats after identification of the freshwater and marine end members (Hoover et al. 2012). Analyzing otolith chemical tags has led to the discovery that groups of individuals, or contingents, within the same species may exhibit facultative diadraomy. Otolith microchemistry has confirmed that some populations of

diadromous species of Anguilliformes, Salmoniformes, Perciformes and others consist of residents and migrants (Walther and Limburg 2012).

Dispersal of larval fish and connectivity within metapopulations can also be examined using otolith microchemistry. The otolith chemistry of the adult Scotia Sea Icefish was analyzed in the Antarctic Peninsula and South Georgia to measure connectivity along the Antarctic Peninsula shelf (Ashford et al. 2010). Analysis of otolith material deposited in the core of larval otoliths indicated a population boundary between the Antarctic Peninsula and South Georgia. Additionally, similarity in otolith core composition between the eastern and northern shelves of South Georgia indicated a single, self-recruiting population in that region. Simulated particle transport using a Lagrangian circulation model confirmed the population boundary suggested by the otolith chemistry of larval Scotia Sea Icefish. Used in conjunction, particle simulations and otolith chemistry can provide a useful technique for testing hypotheses related to larval dispersal and connectivity.

Otoliths are used as natural tags to measure the fraction of adults that originate from different nursery areas to identify important habitats and focus conservation efforts. This technique was applied by Reis-Santos et al. (2012) to address the movement of juvenile flounder and European sea bass from estuaries that function as nursery areas to offshore areas. Spatial variation in otolith chemistry between these species and among estuaries enabled accurate classification of the fish to their estuarine nursery of origin. However, seasonal and annual temporal variation in otolith element fingerprints was identified for both species. Variation among years hindered spatial discrimination, however seasonal variation did not and incorporating seasonal data increased correct classification of estuaries. This study suggests the importance of establishing year specific libraries of natural tags to account for temporal variation

in otolith chemistry and demonstrates the ability to estimate the contribution of estuarine nursery areas to adult fish populations.

Clearly, otolith microchemistry can be used to differentiate fish movement among differing water bodies, but how these patterns of element chemistry should be interpreted and whether they are reflections of local water chemistry is less clear. In many studies of otolith microchemistry, it was unnecessary for the authors to understand the mechanisms generating geographic variability in the otolith chemical tags. Because significant spatial and temporal variation in water chemistry often exists among the bodies of water being tested, this information was unnecessary, provided it was possible for the authors to construct a library of the chemical tags for the species and areas of interest. Yet, these studies could benefit from an understanding of why such variation exists in otolith chemistry because the ability to predict that variation would undoubtedly improve the spatial discrimination of the study and reduce repeated sampling costs. Unfortunately, the complex interactions between the environmental and physiological influences on the deposition of trace elements in otoliths in different fish species are not well understood.

Otolith microchemistry is not a function of ambient water chemistry alone; temperature and salinity as well as species-specific ontogenetic processes and biochemical processes can influence otolith element incorporation. This fact does not invalidate the use of otolith element fingerprints that can be studied as natural tags of habitat use; however, it does make interpretation of the results more complex. The validation that species-specific variation exists in the biological and geographical influences on otolith composition has stimulated the development of research efforts that compare multispecies element fingerprints among different locations (Swearer et al. 2003; Reis-Santos et al. 2008; Chang and Geffen 2012; Patterson et al.

2014). Such studies have consistently identified element fingerprints that were most similar between species that are closely related in terms of phylogeny and ecology. In principle, species that are phylogenetically closer will have the most analogous physiological processes. Although laboratory experiments have yet to confirm similarity in otolith composition among closely related species, they have identified species-specific biochemical control on element assimilation due to differences in element discrimination at the interfaces of incorporation into the otolith (Hamer and Jenkins 2007).

Chang and Geffen (2012) conducted a meta-analysis of otolith chemical tag data from several species in European and North Atlantic waters in order to evaluate the relative contributions of regional versus taxonomic factors in otolith multi-element patterns. Most studies of otolith microchemistry occur over relatively short spatial and temporal scales, but this meta-analysis provided a method for examining larger trends in otolith microchemistry data. Chang and Geffen (2012) revealed that taxonomic patterns in otolith composition were often stronger than regional patterns. This novel approach also suggested elements that may be subject to greater physiological rather than environmental influences.

The purpose of the present study was to quantify otolith multi-element environmental, taxonomic, and ecological patterns of all fish species in the Gulf of Mexico (GoM), along the Western Atlantic Ocean, and in the Caribbean Sea for which this information is available. Comparisons of otolith microchemistry among species and/or families within a geographic region were used to determine if physiology has a significant effect on otolith microchemistry. Fish that live within the same geographical area would likely be exposed to relatively similar element concentrations and thus should have similar otolith microchemistry, unless there is substantial species-specific physiological control on otolith element incorporation. Similarly,

fish species living across multiple geographic regions were used in this study to determine the relative contribution of environmental, or geographic, effects on element incorporation. Mean element concentrations from published otolith microchemistry studies were used to compare otolith multi-element signals among species. This meta-analysis has the potential to inform future studies of otolith microchemistry in the GoM and southwest Atlantic by revealing elements that are more likely to show geographical, taxonomic, and/or ecological effects.

3.2 Methods

A literature search was conducted for otolith chemistry in the Gulf of Mexico, West Atlantic, and Caribbean Sea within Cambridge Scientific Abstracts' Natural Sciences Database (www.csa.com). Searches were conducted for "otolith chemistry", "Gulf of Mexico", "West Atlantic", and "Caribbean Sea" from 1970-2016. Additional searches were also conducted for each species with measured otolith chemistry to identify otolith chemistry studies of the same species outside these areas, including in the relevant watersheds. Only studies of modern, not fossilized, otoliths were used in this meta-analysis. The following information was recorded for each relevant study identified in the literature search: species name, family name, species habitat type from Fishbase (e.g. demersal, reef-associated, pelagic, pelagic-neritic, or benthopelagic), species migration type from Fishbase (amphidromous, anadromous, catadromous, non-migratory, or oceanodromous), sampling site, salinity regime from which fish were sampled (freshwater or saltwater), sampling time (month and year), life-history stage (adult, juvenile, young of the year, or larval stage), and element and/or stable isotope names and mean concentrations.

The methods used in this study were similar to those used in the meta-analysis conducted by Chang and Geffen (2013). Arithmetic mean element or isotope concentrations or ratios were

extracted from the selected studies either as mean values from a specific site location, time, and/or life-history stage. These concentrations were all converted to either μmol/mol Ca or delta notation relative to Vienna Pee Dee Belemnite (VPDB) for elements and isotope ratios, respectively. All element concentrations were converted to ratios to Ca because most studies reported element concentrations using this convention. Sampling site was placed into one of 9 regions which were defined based on the overlap among sampling sites to evenly distribute studies among the regions and based on differences in the environmental, element concentrations among these regions (Fig. 3.1). For instance, the Mississippi River delta was designated as a separate region because the annual flux of elements to the GoM from the Mississippi River is 13.03 billion kg (Trefry 1977). In addition, there are two distinct sediment zones along the northern GoM that affect the concentrations of trace metals in these regions: (1) west of the Mississippi River sediments are primarily siliclastic and (2) east of the Mississippi River calcium carbonate sediments dominate (Martinec et al. 2014). The 9 regions that were designated in this study (Fig. 3.1) were the following: Caribbean Sea, West GoM, Mississippi Delta, Northeast GoM, West Florida, South Florida, South Atlantic, Central Atlantic, and North Atlantic. Migration- and habitat-type was taken from Fishbase (www.fishbase.org) for each species in this study. Migration-type for the fishes in this study were benthopelagic, demersal, pelagic, pelagic-neritic, or reef-associated. Habitat-type was either amphidromous, anadromous, catadromous, non-migratory, or oceanodromous. Ecological niches were defined as unique combinations of migration- and habitat-type (e.g. benthopelagic-amphidromous). There were 15 ecological niches, defined as unique combinations of migration- and habitat-type, that were identified for the species investigated. Many studies of otolith microchemistry were excluded from this meta-analysis because element concentrations were not provided by the study and the authors could

not be reached to provide this information. Some studies were additionally excluded because the same data were provided in multiple studies (e.g. Dorval et al. 2005, 2007) [31,32].

3.2.1 Trends in Concentrations of the Most Common Constituents ($\delta^{13}C$, $\delta^{18}O$, Ba, Mg, Mn, and Sr)

To determine whether physiology or the environment has a larger effect on otolith constituent incorporation, multi-constituent concentrations were made among species, families, regions, and ecological niches. Comparisons among species were used to determine the relative contribution of species-specific vital effects on constituent incorporation in otoliths; while comparisons among families were similarly used to examine phylogenetic differences between taxonomic groups. Regions were used in this study to determine the relative contribution of environmental, or geographic, effects on constituent incorporation. Although differences in otolith constituent concentrations are often observed over smaller spatial scales than those used in this study, because data were compared over broad time periods and multiple life history stages, the use of broad regions was necessary to determine whether differences among regions were legitimate. Finally, the comparisons among ecological niches were used to determine whether migration and habitat significantly affected otolith constituent concentrations.

The distributions of otolith constituent values among families, regions, and ecological niches were compared using boxplots for the constituents that were most commonly reported in the studies included in the meta-analysis. In addition, mean concentrations for each constituent among regions, families, and ecological niches were calculated to provide additional comparisons across levels of these factors.

3.2.2 One-way ANOVAs of Regions and Species

All statistical analyses were conducted with the Fathom toolbox for Matlab (Jones 2012) and PRIMER 7 (Clarke and Gorley 2006). Because the underlying data distributions were often not reported and could not be assumed to be normal, all data were analyzed using non-parametric, permutation-based methods. One-way, permutation-based, ANOVAs were conducted within regions among multiple species for each constituent for which there was enough available data, defined as a minimum of three data points. For each constituent, values were square-root transformed and a resemblance matrix was generated using Bray-Curtis similarity (Bray and Curtis 1957). These analyses were conducted to test whether there was a species-specific, or vital, effect on otolith microchemistry. For instance, if there were no significant differences in the otolith constituent concentrations among species within a region, this would indicate that the local environment, had a more substantial impact on otolith microchemistry than physiological processes exerted at the species level. Additionally, one-way, permutation-based ANOVAs were also conducted within species among multiple regions for individual constituents to determine if the environment has a significant effect on otolith microchemistry. Accordingly, non-significant findings in these analyses could indicate that physiology is more important than geography in regulating otolith constituent concentrations. A lack of significant results could alternatively be attributed to Type II error; however, as the same methods are being employed to evaluate environmental and physiological influences on otolith trace constituent composition this error should be the same for all the tests conducted. The relative proportion of significant results from each test was compared to determine whether the environment or species was more important in regulating otolith microchemistry. Finally, one-way, permutation-based ANOVAs were also conducted among ecological niches to determine if migration- and habitat-type significantly affected otolith microchemistry.

3.2.3 Multiple Comparison Tests of Regions and Families

To determine whether the environment or species-specific physiology has a larger effect on otolith microchemistry, two-way, permutation-based ANOVAs of family versus region were conducted for all constituents for which there were sufficient data, defined as a minimum of three data points for a family tested within each region. Again, constituent values were square-root transformed and a resemblance matrix was generated using Bray-Curtis similarity. The partial eta-squared method was used to compare the magnitudes of the effect sizes.

Otolith constituents for permutation-based, two-way multivariate analyses of variance (PERMANOVAs (Anderson 2001)) were selected to maximize the number of comparisons among families and regions (i.e. constituents that are most commonly reported will be given preference) and to maximize the number of constituents that are most often found to be significantly different in the two-way, permutation-based ANOVAs. For each constituent, concentrations were square-root transformed and a resemblance matrix was generated using Bray-Curtis similarity. Stable isotope elemental ratios and element concentrations were analyzed using separate PERMANOVAs. PERMANOVAs were conducted on the suite of selected constituents to determine whether family or region significantly affects otolith microchemistry and the partial eta-squared method was used to calculate the relative magnitude of the effect sizes.

Exploratory data analysis was conducted using hierarchical cluster analysis, and the divisions were tested using Type 1 similarity profile analysis (SIMPROF,(Clarke et al. 2008)) in Primer 7 to detect significant multivariate structure within the same datasets used for the PERMANOVAs. For each SIMPROF analysis, I standardized the data to give equal weight to

each constituent and a Bray-Curtis similarity was used to generate a resemblance matrix. Non-metric multi-dimensional scaling (nMDS) plots were used to visually compare SIMPROF groups among families, regions, and ecological niches.

3.3 Results

A search of the relevant literature identified 63 relevant studies of otolith microchemistry conducted on 45 species within 23 families within the GoM, Caribbean Sea, and West Atlantic (Fig. 3.1). A total of 415 data points were extracted from these studies, involving 36 constituents (Table 3.1). The constituents with the most data points were Sr, Ba, Mg, Mn, $\delta^{18}O$, and $\delta^{13}C$; thus, these constituents were used in additional multivariate analyses. The data for these analyses was collected from fishes that lived anytime from 1992-2011. A lack of replicate data points from overlapping time frames, species, and regions precluded a temporal meta-analysis of otolith microchemistry.

3.3.1 Trends in Concentrations of the Most Common Constituents ($\delta^{13}C$, $\delta^{18}O$, Ba, Mg, Mn, and Sr)

Average values were calculated for each of the 36 otolith constituents analyzed in this study by family (n=322 individual fish), region (n=178), and ecological niche (n=230), although constituent values were not available for all levels of each factor (Table 3.2). The Caribbean Sea and Central Atlantic were most frequently the regions with the highest average constituent values, while West GoM and North Atlantic consistently had the lowest constituent values. The ecological niches that were observed to have the lowest constituent values were the benthopelagic-anadromous followed by the reef-associated-oceanodromous ecological niche; however, this result is potentially misleading as there were only 3 elements reported for the

benthopelagic-anadromous group and 32 for the reef-associated-oceanodromous ecological niche. The reef-associated-non-migratory and demersal-anadromous ecological niches frequently had the highest otolith constituent values. The Balistidae had a relatively large range of constituent values and was frequently observed to have both the minimum and maximum constituent values in comparison to other families. Excluding the Balistidae, the lowest constituent values were observed most frequently in Lutjanidae and Haemulidae; The families with the highest constituent values were the Salmonidae and Labridae, respectively.

An examination of $\delta^{13}C$ values by family and region (Fig. 3.2) reveal that this isotope is apparently at its lowest value in the North and Central Atlantic. Additionally, the families with relatively low $\delta^{13}C$ appear to be the Clupeidae, Istiophoridae, Labridae, Moronidae, and Scombridae. Yet, these families are the only ones reported from the North and Central Atlantic for $\delta^{13}C$; thus, it is not possible to determine for these fish whether family, region, or some combination of these factors, were responsible for the relatively low $\delta^{13}C$. In contrast, there is an apparent separation among ecological niches, with pelagic species appearing to have lower $\delta^{13}C$ in comparison to demersal and reef-associated species, although the demersal-anadromous ecological niche does not follow this trend. These trends in $\delta^{13}C$ among regions, families, and ecological niches were repeated for $\delta^{18}O$, with slight variations (Fig 3.3). The Istiophoridae and Scombridae families had relatively high $\delta^{18}O$, and the range of $\delta^{18}O$in the South Atlantic was similar to the Central and North Atlantic regions.

An increase in Ba and Sr occurred from South Florida north to the Central Atlantic and north to the Mississippi Delta (Fig. 3.4). This geographic trend in element concentrations also occurred for Mn and Mg, although the peak in Mn occurred in the North Atlantic, while the peak in Mg occurred in the West GoM. Additionally, concentrations of Ba, Mg, and Mn in the

Caribbean Sea were similar or lower than in South Florida. Sr concentrations in the Caribbean Sea had a relatively large range in comparison to the other regions, with both the minimum and maximum Sr values observed in this region.

Demersal species tended to have relatively higher Sr, Ba, Mg, and Mn concentrations and larger ranges in concentration; the top 2-3 ecological niches with the highest element concentrations observed belonged to a demersal ecological niche (Fig. 3.5). In a comparison of average element concentrations among migration-types, anadromous species had the highest concentrations, while catadromous species had the lowest (Table 3.3). In a comparison of habitat-type only, demersal species had the highest element concentrations and pelagic/benthopelagic species were observed to consistently have the lowest concentrations.

The families Moronidae and Sciaenidae had relatively high concentrations of Sr, Ba, Mg, and Mn and large ranges for all the elements examined (Fig. 3.6). In addition, clupeids and eleotrids were observed to have relatively high concentrations of Sr and Ba, although this was not true for Mg and Mn. There were no other consistent trends across elements in the remaining families.

3.3.2 One-way ANOVAs of Regions and Species

There were 72 one-way ANOVAs conducted to determine if there was a significant difference in otolith constituent concentrations among marine species within a region, thus examining biological effects on otolith chemical tags (Table 3.4). These tests included 19 species collected in the marine environment from 9 regions. Because a minimum of 3 data points were required for each species within a region tested, tests were only conducted on 23 of the total 36 constituents and between 2 and 6 species were tested within a region. Between 45

and 100% of the constituents tested within a region were found to be significantly different among species. There were 16 constituents that were significantly different among the species tested within a region: B, Ba, Rb, Sn, V, Y, Sr, Cu, Li, Na, Mg, Mn, Fe, Pb, $\delta^{13}C$, and $\delta^{18}O$. Although five of these constituents were significantly different among species in 100% of the tests conducted, these constituents were only compared in 1or 2 tests. The constituents that were most frequently (i.e., in more than 2 comparisons) observed to vary significantly among species within a region in more than 50% of the tests conducted were Ba, Sr, Cu, Li, Na, Mg, Mn, Fe, and Pb. Of the 72 tests conducted, 63% of the tests indicated a significant difference among species within a region, suggesting a relatively large amount of physiological control on otolith microchemistry.

Comparatively fewer one-way ANOVAs were conducted for freshwater species among regions and only West Atlantic regions were included in these analyses (Table 3.4). These tests compared the values of 2-4 constituents for 2-5 species, depending on the region being tested. Half of the 10 tests that were conducted indicated a significant difference in otolith constituent values among species within a region, with the North Atlantic having the highest number of significant tests. Of the four elements tested, three were significantly different among species within a region in 50% or more of the tests conducted: Ba, Sr, and $\delta^{18}O$.

To determine if ambient water chemistry had a significant influence on otolith constituent values, otolith microchemistry was compared among regions for individual marine species (Table 3.5). These analyses were conducted for 6 marine species across different combinations of 7 different regions. The number of regions included within a species range that also contained enough data points to be tested ranged from 2-4 regions. The tests of species-constituent concentrations included 25 constituents, but ranged from 2-18 constituents, depending on

species. Approximately 30% of the constituents tested were found to be significantly different among regions for a single species and included $\delta^{18}O$, Li, Mg, Ba, Mn, Sr, Fe, and $\delta^{13}C$. Of those constituents that varied significantly among regions, only $\delta^{18}O$, Li, and Mg were significantly different among regions in over 50% of the tests conducted. In total, only 26% of the 57 tests conducted that compared constituent concentrations across regions were significant. Spotted Seatrout otolith constituent concentrations were observed to be different among the regions tested (Central Atlantic, Mississippi Delta, and West GoM) with the highest frequency.

Comparisons of freshwater species' constituent concentrations occurred for the three regions in the West Atlantic. There were three freshwater species with enough data to make comparisons among regions and for each species a range of 2-4 constituents were tested. Only 25% of the tests (n = 8) identified a significant difference in otolith constituent concentrations among regions. Sr and $\delta^{18}O$ were significantly different among regions; however, only $\delta^{18}O$ was significantly different in over 50% of the tests conducted.

A total of 147 tests were conducted for both freshwater and marine species combined. Of those tests of constituent values for species within a region, 61% of the tests were significant. In comparison, 26% of the tests comparing multiple regions for a single species were significant. Thus, otolith constituent values may be more strongly affected by species-specific, physiological processes than by differences in water chemistry among geographical regions.

3.3.3 Multiple Comparison Tests of Regions and Family

Two-way ANOVAs comparing otolith constituent values among all regions and families (marine and freshwater) were completed for 27 of the 36 constituents (Table 3.6). There was either a significant effect of family, region, or both on the concentrations of 78% of the

constituents tested, and only three constituents had significant interactions between region and family (Sr, Mn, and Y). Additionally, the family effect was larger than the effect of region on otolith constituent values in two-thirds of the constituents tested.

Nonparametric two-way MANOVAs for $\delta^{13}C$ and $\delta^{18}O$ combined compared constituent concentrations among 8 families, while the NP-MANOVA of Sr, Ba, Mg, and Mn tested for differences among 12 families. In both tests, families were compared among all 9 regions in the study. Both family and region explained variation in both sets of multivariate otolith constituent values ($p < 0.001$) and there were no significant interactions between family and region ($p > 0.05$). Again, the partial eta-squared method showed that family assignment explained more of the variation in constituent values than did region assignment in both multi-constituent analyses (Sr/Ba/Mg/Mn-region: 0.649, family: 0.706; $\delta^{13}C/\delta^{18}O$-region: 0.223, family: 0.374).

The SIMPROF analysis of $\delta^{13}C$ and $\delta^{18}O$ combined revealed both taxonomic and regional groupings within the multi-constituent data. Grouping of the multi-constituent data among families primarily occurred between Moronidae and Clupeidae, Lutjanidae and Scombridae, and Labridae and Sciaenidae (Fig. 3.7). The regions that were placed into the same SIMPROF groups and visualized using nMDS were the following: Central Atlantic; North Atlantic, Mississippi Delta, West GoM, and West Florida; and North Atlantic, West Florida, and South Florida. ANOSIM identified that the differences among groups were larger among families ($R = 0.438$, $p < 0.001$) than among regions ($R = 0.359$, $p < 0.001$).

The multi-element patterns in Sr, Ba, Mg, and Mn were also analyzed using SIMPROF and groupings were visualized with nMDS. The only families that clearly grouped together for these multi-element data were the Malacanthidae and Moronidae, although both families also

formed separate groups (Fig. 3.8). In addition, the two clearest groupings among regions occurred between West Florida with the Northeast GoM and between the North and Central Atlantic. ANOSIM of this multi-element dataset revealed that while there were significant differences among both families and regions ($p < 0.001$), the family effect ($R = 0.535$) was larger than the region effect ($R = 0.256$).

3.3.4 Tests of Ecological Niches

There were 27 constituents tested to determine if there was a significant difference among ecological niches (Table 3.7). Although there were 15 ecological niches identified in the dataset, only 11 of the ecological niches had enough data to be tested. Of the constituents tested, the only non-significant tests occurred for Ge and P; thus, 93% of the constituents tested varied significantly among ecological niches.

Non-parametric MANOVAs for $\delta^{13}C$ and $\delta^{18}O$ combined compared isotope ratios among 8 ecological niches, while the NP-MANOVA of Sr, Ba, Mg, and Mn tested for differences among 9 ecological niches. Ecological niche explained the variation in both sets of multivariate otolith element concentrations ($p < 0.001$). The effect size of family, region, and ecological niche were compared in Figure 3.9, showing that physiology and ecological niche had relatively large effect sizes for the combination of Sr, Ba, Mg, and Mn. In comparison, the effect sizes of physiology, environment, and ecological niche were similar for $\delta^{13}C$ and $\delta^{18}O$. The multi-constituent patterns in both datasets were also analyzed using SIMPROF and groupings were visualized with nMDS. The only ecological niches that clearly grouped together for $\delta^{13}C$ and $\delta^{18}O$ were demersal-anadromous with pelagic-neritic-oceanodromous and reef-associated-amphidromous with pelagic-oceanodromous (Fig. 3.10). For the multivariate analysis of Sr, Ba,

Mg, and Mn, there were 3 ecological niches that formed SIMPROF groups separate from other niches: demersal-non-migratory, demersal oceanodromous, and demersal anadromous (Fig. 3.10). An ANOSIM of both multi-constituent datasets revealed that there were significant differences among ecological niches for both datasets ($p < 0.001$); however, this effect was more pronounced in the Sr, Ba, Mg, and Mn dataset ($R = 0.452$) compared to the $\delta^{13}C$ and $\delta^{18}O$ dataset ($R = 0.316$).

3.4 Discussion

Multiple tests demonstrated that taxonomic effects explained more of the variation in otolith chemical tags than regional effects. These findings suggest that physiological regulation of constituent incorporation into otoliths is more important than has previously been recognized. Although physiology apparently can be more important in controlling otolith constituent values than the environment (Table 3.6), regional patterns were observed in otolith constituent values (Figures 3.2 and 3.3), and region was repeatedly observed to significantly affect otolith multi-constituent patterns. Thus, while otolith constituent values may reflect the water chemistry that differs among water bodies, the concentrations or ratios are likely not an accurate representation of water chemistry, but are more likely the result of complex physiological processes occurring in response to differing water chemistries.

Relatively little is known about the physiological regulation of constituent incorporation in otoliths in relation to their concentration in the surrounding water. Constituents that are incorporated into otolith material must first be absorbed across the gills or gut and then enter the bloodstream of the fish. Then the constituent must move from the blood plasma into the endolymph fluid of the inner ear canal and finally be incorporated into either the mineral

structure or protein matrix of the otolith (Campana 1999). Constituent discrimination can occur to varying degrees at any of the interfaces in this multi-step process, although little is known about the degree of discrimination. Several studies have observed differences in the constituent fingerprints of different species inhabiting the same environment, suggesting species-specific biochemical processes on constituent incorporation into otoliths (Swearer et al. 2003; Reis-Santos et al. 2008; Chang and Geffen 2012; Reis-Santos et al. 2012).

In addition to the biochemical processes on mineralization, there are also species-specific ontogenetic processes that may lead to alterations of otolith microchemistry. Trace constituent concentrations in the otolith have been shown to vary with age, possibly as a result of changes in metabolic rate subsequently affecting growth and incorporation of constituents into the otolith (Morales-Nin et al. 2005). Age-related changes in otolith microchemistry may also be related to changes in diet because dietary uptake of trace constituents has been shown to influence otolith constituent composition (Buckel et al. 2004). Metamorphosis, reproduction, and maternal contribution are all age-related events that have also been demonstrated to affect the uptake of trace constituents into the otolith (Thorrold et al. 2006). Additionally, Sturrock et al. (2014) observed ontogenetic, temporal, and sex-specific differences in blood plasma element concentrations, especially among more thiophilic 'soft acid metal ions' (Mn, Cu, Zn, Se, and Pb). These observations suggest that whole otolith analysis used to differentiate fish stocks must take into account age and sex structure or else risk mistaking age- and sex-related trends for stock differences.

Studies between salinity and temperature effects on otolith trace-constituent incorporation have alternately observed no relationship, positive relationships, and negative relationships (Martin and Wuenschel 2006). In addition, these relationships have been shown to

vary depending on the fish species and the constituent examined in the otolith. For instance, Elsdon and Gillanders (2002) found a positive relationship between Sr:Ca and Ba:Ca ratios and temperature, but no relationship between Mn:Ca and temperature for black bream, *Acanthopagrus butcheri*. Temperature-salinity interactive effects and salinity alone have generally been found to be more influential on trace-constituent incorporation than temperature alone (Martin and Wuenschel 2006). There is a need for more laboratory-based validation experiments to evaluate the potential effect of differences in water temperature and salinity on otolith constituent incorporation because these effects are unknown for most fish species.

Although there were 25 constituents used to determine the extent to which the environment significantly affects otolith microchemistry, only the following 8 constituents were found to potentially be indicative of ambient water chemistry in both the freshwater and marine environments: $\delta^{18}O$, Li, Mg, Ba, Mn, Sr, Fe, and $\delta^{13}C$ (Table 3.4). Furthermore, $\delta^{18}O$, Li, and Mg were the only constituents most consistently (i.e., over 50% of the time) observed to be different among regions. In comparison, 70% of the constituents tested to determine the extent of physiological control on otolith constituent values indicated some degree of biological influence on constituent incorporation. Ba, Sr, Cu, Li, Na, Mg, Mn, Fe, and Pb were most frequently different among both freshwater and marine species within the same region (Table 3.5). Interestingly, B, Rb, Sn, V, and Y were also observed to differentiate marine fishes in the same region; yet, there were only 1-2 tests conducted for each of these elements, so further testing may be necessary to determine whether these elements perform consistently. Thus, the only analytes that were found to be indicative of ambient water chemistry without being under some degree of physiological control were $\delta^{18}O$ and $\delta^{13}C$. Additionally, $\delta^{18}O$ is likely to be a

better indicator of ambient water chemistry, as it differentiated regions in 75% of the tests, while differences in $\delta^{13}C$ were observed in 25% of the tests conducted.

Chang and Geffen (2013) observed that Li, Ba, Sr, Pb, and Cu were likely to demonstrate differences among environments, while Mg, Mn, Sr, and Ba were affected by species-specific physiological effects. Unfortunately, $\delta^{18}O$ and $\delta^{13}C$ were not included in their meta-analysis. Thus, the results from the Chang and Geffen (2013) meta-analysis suggest that Li, Pb, and Cu are the best elements to use to distinguish species among different environments. Although the present study also suggested that Li, Sr, and Ba were different among regions, these elements were additionally observed to be significantly affected by species-specific physiology.

Both $\delta^{18}O$ and $\delta^{13}C$ were observed to have relatively low concentrations in the North and Central Atlantic, although this was less apparent for $\delta^{13}C$ (Figures 3.2 and 3.3). Depletion of $\delta^{18}O$ and $\delta^{13}C$ occurs with decreasing salinity and temperature; thus, $\delta^{18}O$ and $\delta^{13}C$ follow the predicted pattern and decrease from South Florida to the North Atlantic. In addition, the $\delta^{13}C$ baseline is higher in shallow, nearshore regions due to the dependence on benthic algae in these systems (Radabaugh 2013). Although differences in $\delta^{13}C$ among depth were not explicitly tested in this study, the enriched values of $\delta^{13}C$ in demersal species compared to pelagic species could be explained by differences in the reliance on benthic primary production. Yet, kinetic and metabolic effects on the incorporation of $\delta^{13}C$ into otoliths have been documented (Hoie et al. 2003); thus, $\delta^{13}C$ would not be expected to be as useful a discriminatory isotope among regions.

Sr was different among some regions in this study (Fig. 3.4) and is often assumed to be one of the more useful elements for differentiating environments because ambient concentrations are often related to salinity and geological differences. Yet, in this study it failed to distinguish

between large geographic regions for the Red Snapper (Northeast GoM, West GoM, West Florida, and South Atlantic), even though it has been repeatedly used to track Red Snapper movement throughout the GoM. This fact is surprising given the fact that Sr concentrations are affected by sediment type and Florida, the Yucatan, and the Bahamas are primarily derived from calcium carbonate, while the northern GoM and West Atlantic are composed of siliclastic sediments (Taft and Harbaugh 1964). In this study, Sr was also affected by biology, which is in agreement with several studies indicating that Sr otolith concentration is affected by a variety of physiological processes.

Patterns of otolith constituent values among regions included a noticeable enrichment in constituent values from South Florida to the Mississippi Delta and the Central/North Atlantic. The substantial flux of metals to the GoM from the Mississippi River (Trefry 1977) could explain the enrichment in constituent values observed from south to north along the West Florida Shelf. The increase in constituent values from South Florida to the North Atlantic could be due, in part, to transport and accumulation of metals via the Gulf Stream. The peak in constituent values that was frequently observed in the Central Atlantic could also be attributed to the presence of both the Chesapeake and Delaware bays in this region.

Otolith chemical tags indicated that the Caribbean Sea was one of the regions, along with the Central Atlantic, that was relatively enriched in most of the constituents examined in this meta-analysis and additionally exhibited the largest distributions in concentrations for some elements (i.e., Sr). The Caribbean Sea was the largest region included in this meta-analysis; thus, the relatively wide range in constituent values is likely the result of the large geographical area this region encompasses. In addition, extractions of mineral deposits in the Caribbean Sea have resulted in pollutants such as Pb, Cu, and Zn reaching the marine environment (Fernandez

et al. 2007). In contrast, the West GoM was observed to have relatively low constituent values in comparison to other areas in the GoM. Martinec et al. (2014) demonstrated that trace-metal concentrations west of the Mississippi River are primarily of a lithogenic, and not anthropogenic origin.

Ecological niche explained a significant portion of the variation in otolith microchemistry. Overall, pelagic species tended to have the lowest constituent values, while demersal species had relatively higher values of most of the constituents examined. Demersal species are closely associated with sediments that may harbor elevated constituent values in comparison to the water column; thus, this finding is consistent with expectations. Additionally, anadromous species were typically associated with higher concentrations of Sr, Ba, Mg, and Mn in comparison to catadromous species. Dissolved concentrations of Ba are typically highest at low salinities due to desorption from particles in estuaries (Coffey et al. 1997) while Sr is typically elevated in marine habitats (Kraus and Secor 2004).

Family also had a relatively strong effect on otolith microchemistry. The Lutjanidae and Haemulidae families were observed to have the lowest constituent values. The Salmonidae and Labridae families were observed to have the highest constituent values examined; although, there is no obvious explanation for this pattern. The Salmonidae and Labridae are in separate orders and the species within each family inhabit different ecological niches. Additionally, the SIMPROF plots revealed that the Malacanthidae and Moronidae were grouped together. These families are in the same order, Perciformes, and the species within each of these families are demersal.

There were many species in this study that exhibited similar patterns in otolith microchemistry. For instance, the French Grunt and Schoolmaster in the Caribbean Sea inhabit the same ecological niche and were observed to have similar values of $\delta^{18}O$, $\delta^{13}C$, Mg, Co, Cu, Sr, and Ba. Within the Central Atlantic, the Spotted Seatrout and Weakfish, which are both demersal species, did not have significantly different concentrations of Mg, Mn, Sr, and Ba. Future research should focus on the analysis of sympatric species that are more likely to have similar otolith chemical tags. For instance, Brown (2006) identified similarities in the otolith microchemistry of two species of flatfish along the central California coast and used the chemical tag of one species as a proxy for classifying estuarine use of the other species. The use of a species-specific chemical tag as a proxy for another phylogenetically close species could reduce the number of fishes and analyses required to investigate fish movement.

Although most studies of otolith microchemistry focus on a relatively short time frame and small spatial scale, this meta-analysis examined trends in otolith chemistry throughout the GoM, Caribbean Sea, and West Atlantic over an aggregated time span of decades. This study has clearly demonstrated the comparatively large effect that physiology has on the incorporation of constituents into fish otoliths. In multiple tests, the effect of species and/or family was found to be substantially more informative than regional effects on otolith microchemistry. Although most of the constituents tested were significantly affected by physiological processes, there were two isotopes that were reliably different among regions: $\delta^{13}C$ and $\delta^{18}O$. In addition, the ratios of these isotopes within the otoliths included in this meta-analysis followed the patterns in $\delta^{13}C$ and $\delta^{18}O$ that would be predicted from ambient water chemistry alone, although this was more consistent for $\delta^{18}O$. Future otolith microchemistry studies should take into consideration that metal concentrations in the water are not likely to align with those measured in otoliths.

Although differences in otolith microchemistry may be detected over short spatial and temporal scales, those differences are most likely the result of complex physiological responses to differences in the physicochemical properties of the water in which they reside, rather than true reflections of metal concentrations measured within that water body. Consequently, there is a need for more laboratory studies to measure the effects of differing physiochemical water properties on otolith constituent incorporation rates before otolith chemical tags can be accurately interpreted.

3.5 Tables

Table 3.1 Summary of the constituents, studies, families, and regions included in the study listed by species.

Common Name	Study	Family	Migration Type	Habitat Type	Region	Salinity Regime	Sample Size	Elements
Alabama Shad	Schaffler et al. 2015	Clupeidae	Anadromous	Pelagic-neritic	Northeast GOM	FW	20	Mn, Y, Ba, Pb
Alewife	Turner and Limburg 2014	Clupeidae	Anadromous	Pelagic-neritic	North Atlantic	SW	72	$\delta^{18}O$, Sr87/86, Sr, Ba
	Turner et al. 2015	Clupeidae	Anadromous	Pelagic-neritic	North Atlantic	FW	20	Sr87/86, Sr
American Shad	Walther and Thorrold 2008	Clupeidae	Anadromous	Pelagic-neritic	North Atlantic	FW	58	δ18O, Sr87/86, Sr, Ba
Atlantic Bluefin Tuna	Rooker et al. 2001	Scombridae	Oceanodromous	Pelagic	Central Atlantic	SW	69	Li, Na, Mg, K, Mn, Sr, Ba
	Rooker et al. 2003	Scombridae	Oceanodromous	Pelagic	North Atlantic	SW	12	Li, Mg, Mn, Sr, Ba
	Rooker et al. 2008	Scombridae	Oceanodromous	Pelagic	North Atlantic	SW	81	δ13C, δ18O
	Rooker et al. 2014	Scombridae	Oceanodromous	Pelagic	North Atlantic	SW	115	δ13C, δ18O
Atlantic Croaker	Hanson and Zdanowicz 1999	Sciaenidae	Non-migratory	Demersal	West GOM	SW	10	Li, Na, Mg, K, Cr, Mn, Ni, Cu, Ga, Rb, Sr, Ba
	Limburg et al. 2015	Sciaenidae	Non-migratory	Demersal	West GOM	SW	10	Mn
	Schaffler et al. 2009	Sciaenidae	Non-migratory	Demersal	South Atlantic	SW	28	Mg, Mn, Rb, Sr, Y, Ba, Pb
	Thorrold et al. 1997	Sciaenidae	Non-migratory	Demersal	Central Atlantic	FW	N/A	Mg, Zn, Sr, Ba
Atlantic Menhaden	Schaffler et al. 2014	Clupeidae	Oceanodromous	Pelagic-neritic	Central Atlantic	FW	52	δ13C, δ18O, Li, Mg, Mn, Rb, Sr, Y, Ba
Atlantic Salmon	Kennedy et al. 2002	Salmonidae	Anadromous	Benthopelagic	North Atlantic	SW	4	Sr87/86
Bicolor damselfish	Chittaro and Hogan 2013	Pomacentridae	Non-migratory	Reef-associated	Caribbean Sea	SW	328	Mg, Mn, Zn, Sr, Ba, La, Pb, Tl
	Chittaro et al. 2006a	Pomacentridae	Non-migratory	Reef-associated	Caribbean Sea	SW	66	Li, Mg, Mn, Zn, Sr, Sn, Ba, Ce, Pb
	Chittaro et al. 2006b	Pomacentridae	Non-migratory	Reef-associated	Caribbean Sea	SW	40	Mn, Zn, Sr, Ba, Ce, Pb
Bigmouth Sleeper	Smith and Kwak 2014	Eleotridae	Amphidromous	Demersal	Caribbean Sea	FW	N/A	Sr, Ba
Blackfin Tuna	Rooker et al. 2001	Scombridae	Oceanodromous	Pelagic	West GOM	SW	56	Li, Na, Mg, K, Mn, Sr, Ba
Blue marlin	Wells et al. 2010	Istiophoridae	Oceanodromous	Pelagic	Northeast GOM	SW	26	δ13C, δ18O
Blueback Herring	Turner and Limburg 2014	Clupeidae	Anadromous	Pelagic-neritic	North Atlantic	SW	48	δ18O, Sr87/86, Sr, Ba
	Turner et al. 2015	Clupeidae	Anadromous	Pelagic-neritic	North Atlantic	FW	20	Sr87/86, Sr

Table 3.1 (Continued)

Common Name	Study	Family	Migration Type	Habitat Type	Region	Salinity Regime	Sample Size	Elements
Bluefish	Buckel et al. 2004	Pomatomidae	Oceanodromous	Pelagic	North Atlantic	SW	9	Na, Mg, K, Mn, Sr, Ba
Bluehead Wrasse	Hamilton and Warner 2009	Labridae	Non-migratory	Reef-associated	Caribbean Sea	SW	46	Mg, Mn, Sr, Ba
	Ruttenberg et al. 2005	Labridae	Non-migratory	Reef-associated	Caribbean Sea	SW	121	Mg, Mn, Sr, Ba
	Sandin et al. 2005	Labridae	Non-migratory	Reef-associated	Caribbean Sea	SW	100	Mg, Mn, Sr, Ba, Pb
	Swearer et al. 1999	Labridae	Non-migratory	Reef-associated	Caribbean Sea	SW	232	Mn, Cu, Zn, Ba, Pb
Common Snook	Patterson et al. 2005	Centropomidae	Amphidromous	Reef-associated	South Florida	SW	20	Mg, Mn, Cu, Zn, Sr, Ba
	Rolls 2014	Centropomidae	Amphidromous	Reef-associated	West Florida	SW	N/A	V, Co, Sr, Y
French Grunt	Chittaro et al. 2004	Haemulidae	Non-migratory	Reef-associated	Caribbean Sea	SW	44	Sr, Ba
	Chittaro et al. 2005	Haemulidae	Non-migratory	Reef-associated	Caribbean Sea	SW	162	Li, Mg, Cu, Zn, Rb, Sr, Sn, Ba, Pb
	Mateo et al. 2010a	Haemulidae	Non-migratory	Reef-associated	Caribbean Sea	SW	45	δ13C, δ18O, Na, Mg, Co, Cu, Sr, Ba
Gag Grouper	Hanson et al. 2004	Serranidae	Oceanodromous	Reef-associated	West Florida	SW	20	δ13C, δ18O, Li, Na, Mg, K, Mn, Cu, Sr, Ba, Pb
	Jones et al. 2013	Serranidae	Oceanodromous	Reef-associated	Northeast GOM	SW	N/A	Li, Na, Mg, Sc, V, Cr, Fe, Mn, Co, Ni, Cu, Zn, Ge, Rb, Sr, Y, Cd, Sn, Ba, Au, Pb
Gray Snapper	Gerard and Muhling 2010	Lutjanidae	Amphidromous	Reef-associated	South Florida	SW	70	δ13C, δ18O
	Lounder 2009	Lutjanidae	Amphidromous	Reef-associated	Northeast GOM	SW	97	δ13C, δ18O, Li, Mg, Mn, Sr, Ba
Gray Triggerfish	Sluis 2011	Balistidae	Non-migratory	Reef-associated	Northeast GOM	SW	15	Li, B, V, Fe, Mn, Co, Cu, Zn, Mo, Cd, Sn, Ba, Pb, Tl, Bi
Gulf Killifish	Nelson et al. 2014	Fundulidae	Non-migratory	Benthopelagic	Mississippi Delta	SW	N/A	Fe, Mn, Rb, Sr, Ba, U
King Mackerel	Grady et al. 1989	Scombridae	Oceanodromous	Reef-associated	West GOM	SW	15	Cu, Zn, Pb
	Patterson et al. 2004	Scombridae	Oceanodromous	Reef-associated	West Florida	SW	140	Mg, Mn, Sr, Ba
Lane Snapper	Patterson et al. 2010/Sluis et al. 2012	Lutjanidae	Non-migratory	Reef-associated	West Florida	SW	N/A	δ13C, δ18O Li, Mg, Mn, Sr, Ba
Largemouth Bass	Farmer et al. 2013	Centrarchidae	Non-migratory	Benthopelagic	Northeast GOM	FW	28	Sr

Table 3.1 (Continued)

Common Name	Study	Family	Migration Type	Habitat Type	Region	Salinity Regime	Sample Size	Elements
Moutain Mullet	Smith and Kwak 2014	Mugilidae	Catadromous	Pelagic-neritic	Caribbean Sea	FW	N/A	Sr, Ba
Nassau grouper	Patterson et al. 1999	Serranidae	Oceanodromous	Reef-associated	Caribbean Sea	SW	15	Zn, Sr, Ba
Red Drum	Houston 2015	Sciaenidae	Oceanodromous	Demersal	Mississippi Delta	SW	N/A	Mg, V, Cr, Fe, Co, Ni, Cu, Zn, Pb
	Patterson et al. 2004	Sciaenidae	Oceanodromous	Demersal	Northeast GOM	SW	20	Mg, Mn, Zn, Sr, Ba
	Rolls 2014	Sciaenidae	Oceanodromous	Demersal	West Florida	SW	N/A	Na, P, Cr, Cu, Sr
	Rooker et al. 2010	Sciaenidae	Oceanodromous	Demersal	West GOM	SW	34	δ13C, δ18O
Red Grouper	Granneman et al. 2017	Serranidae	Non-migratory	Reef-associated	Northeast GOM	SW	4	Li, Na, Mg, P, Sc, V, Cr, Fe, Mn, Co, Ni, Cu, Zn, Ge, Rb, Sr, Y, Cd, Sn, Ba, Au, Pb, U
Red Porgy	Granneman et al. 2017	Sparidae	Oceanodromous	Benthopelagic	Northeast GOM	SW	8	Li, Na, Mg, P, Sc, V, Cr, Fe, Mn, Co, Ni, Cu, Zn, Ge, Rb, Sr, Y, Cd, Sn, Ba, Au, Pb, U
Red Snapper	Barnett et al. 2015	Lutjanidae	Oceanodromous	Reef-associated	South Atlantic	SW	3	δ13C, δ18O, Mg, Mn, Sr, Ba
	Granneman et al. 2017	Lutjanidae	Oceanodromous	Reef-associated	Northeast GOM	SW	89	Li, Na, Mg, P, Sc, V, Cr, Fe, Mn, Co, Ni, Cu, Zn, Ge, Rb, Sr, Y, Cd, Sn, Ba, Au Pb, U
	Nowling et al. 2011	Lutjanidae	Oceanodromous	Reef-associated	Northeast GOM	SW	32	V, Co, Ni, Cu, Zn Ag, Cd, Pb U
	Patterson et al. 2001	Lutjanidae	Oceanodromous	Reef-associated	Northeast GOM	SW	N/A	Mg, Sr, Cd, Ba
	Patterson et al. 2008	Lutjanidae	Oceanodromous	Reef-associated	Northeast GOM	SW	30	Mg, Mn, Sr, Ba
	Patterson et al. 2010/Sluis et al. 2012	Lutjanidae	Oceanodromous	Reef-associated	West Florida	SW	20	δ13C, δ18O, Li, Mg, Mn, Sr, Ba
	Sluis 2011	Lutjanidae	Oceanodromous	Reef-associated	Northeast GOM	SW	377	Li, B, V, Fe, Mn, Co, Cu, Zn, Mo, Cd, Sn, Ba, Pb, Tl, Bi
	Sturgeon et al. 2005	Lutjanidae	Oceanodromous	Reef-associated	Northeast GOM	SW	N/A	Li, Na, Mg, Mn, Sr, Ba

Table 3.1 (Continued)

Common Name	Study	Family	Migration Type	Habitat Type	Region	Salinity Regime	Sample Size	Elements
River goby	Smith and Kwak 2014	Gobiidae	Non-migratory	Benthopelagic	Caribbean Sea	FW	N/A	Sr, Ba
Schoolmaster	Chittaro et al. 2006c	Lutjanidae	Non-migratory	Reef-associated	Caribbean Sea	SW	118	Li, Mg, Cu, Zn, Rb, Sr, Sn, Ba, Pb
	Mateo et al. 2010a	Lutjanidae	Non-migratory	Reef-associated	Caribbean Sea	SW	45	δ13C, δ18O, Na, Mg, Co, Cu, Sr, Ba
Sirajo goby	Smith and Kwak 2014	Gobiidae	Amphidromous	Benthopelagic	Caribbean Sea	FW	N/A	Sr, Ba
Southern Flounder	Farmer et al. 2013	Paralichthyidae	Non-migratory	Demersal	Northeast GOM	FW	8	Sr
Southern Hake	Granneman et al. 2017	Phycidae	Non-migratory	Demersal	Northeast GOM	SW	7	Li, Na, Mg, P, Sc, V, Cr, Fe, Mn, Co, Ni, Cu, Zn, Ge, Rb, Sr, Y, Cd, Sn Ba, Au, Pb, U
Spotted Seatrout	Beharry 2011	Sciaenidae	Non-migratory	Demersal	Central Atlantic	SW	43	δ13C, Li, Mg, Sr, Y, Ba
	Comyns et al. 2008	Sciaenidae	Non-migratory	Demersal	Mississippi Delta	SW	N/A	δ13C, δ18O, Li, Mg, Mn, Sr, Ba
	Curtis et al. 2014	Sciaenidae	Non-migratory	Demersal	West GOM	SW	N/A	δ13C, δ18O, B, Na, K, Mn, Rb, Sr, Ba
	Dorval et al. 2005	Sciaenidae	Non-migratory	Demersal	Central Atlantic	SW	22	δ13C, Mn, Sr, Ba, La, Ce
Striped Bass	Mohan et al. 2012	Moronidae	Anadromous	Demersal	Central Atlantic	SW	6	Mg, Mn, Sr, Ba
	Mohan et al. 2015	Moronidae	Anadromous	Demersal	Central Atlantic	SW	19	Mg, Mn, Sr, Ba
Summer Flounder	Kellison and Taylor 2007	Paralichthyidae	Oceanodromous	Demersal	Central Atlantic	SW	28	Mg, Mn, Zn, Sr, Ba
Tautog	Mateo et al. 2010b	Labridae	Non-migratory	Reef-associated	North Atlantic	SW	20	δ13C, δ18O, Mng, Co, Rb, Sr, Ba
Tilefish	Granneman et al. 2017	Malacanthidae	Non-migratory	Demersal	Northeast GOM	SW	30	Li, Na, Mg, P, Sc, V, Cr, Fe, Mn, Co, Ni, Cu, Zn, Ge, Rb, Sr, Y, Cd, Sn, Ba, Au, Pb, U
Weakfish	Thorrold et al. 1998	Sciaenidae	Oceanodromous	Demersal	South Atlantic	SW	N/A	Mg, Mn, Sr, Ba
White marlin	Wells et al. 2010	Istiophoridae	Oceanodromous	Pelagic	Northeast GOM	SW	13	δ13C, δ18O

Table 3.1 (Continued)

Common Name	Study	Family	Migration Type	Habitat Type	Region	Salinity Regime	Sample Size	Elements
White Perch	Kerr et al. 2007	Moronidae	Anadromous	Demersal	Central Atlantic	FW	6	δ13C, δ18O, Sr
	Kerr et al. 2009	Moronidae	Anadromous	Demersal	Central Atlantic	SW	27	Sr
Yellowedge Grouper	Granneman et al. 2017	Serranidae	Non-migratory	Demersal	Northeast GOM	SW	29	Li, Na, Mg, P, Sc, V, Cr, Fe, Mn, Co, Ni, Cu, Zn, Ge, Rb, Sr, Y, Cd, Sn, Ba, Au Pb, U
Yellowfin Tuna	Rooker et al. 2001	Scombridae	Oceanodromous	Pelagic	Central Atlantic	SW	92	Li, Na, Mg, K, Mn, Sr,
Yellowtail Snapper	Huijber et al. 2013	Lutjanidae	Non-migratory	Reef-associated	Caribbean Sea	SW	89	δ13C, δ18O
	Verweij et al. 2008	Lutjanidae	Non-migratory	Reef-associated	Caribbean Sea	SW	17	δ13C

Table 3.2 Average constituent values separated by regions, families, and ecological niches.

Region	$\delta^{13}C$	δ18O	Sr87/86	Li	B1-11	Na	Mg	Al	P	K	Sc	V	Cr	Fe	Mn	Co	Ni	Cu
Caribbean Sea	-3.02E+00	-7.83E-01		2.48E+00		3138.38739	48.21104			2685.53876			5.77E-01		9.23589	4.64E-01	1.70E+00	2.23E+00
Central Atlantic	-6.21E+00	-6.95E+00	7.12E-01	3.82E+00		16442.09628	165.22129			1308.24102					22.51472			
Mississippi Delta	-5.48E+00	-2.87E+00		2.28E+00			124.54269					7.85E-03	4.26E-01	438.11198	32.80545	2.76E-01	1.54E-01	6.13E-01
North Atlantic	-6.85E+00	-6.44E+00	7.12E-01	1.73E+00		14920.33242	77.29863			2180.65747					20.38962	3.68E-01		
Northeast GOM	-4.04E+00	-1.30E+00		7.37E+00	1.21E+01	11279.20849	120.69126	2.56E+03	3.97E+02	1042.88422	1.96E-01	5.22E-02	8.39E-01	541.50699	11.60866	1.87E-01	4.17E-01	7.06E-01
South Atlantic	-3.31E+00	-2.40E+00	7.10E-01				128.48018								7.35294			1.51E-01
South Florida	-3.54E+00	-5.58E-01	7.10E-01	3.35E+00			91.75798								1.60834			2.60E-01
West Florida	-5.66E+00	-1.30E+00		6.29E+00	6.69E+00	11804.20831	94.31553		3.81E+02	1108.29037	2.15E-01	1.09E-01	1.04E+00	363.07533	19.48818	2.87E-01	5.34E-01	1.29E+00
West GOM	-3.47E+00	-1.11E+00		4.85E+00	1.08E+01	11149.67045	188.41370	2.41E+03		1923.37032		3.63E-04	7.05E-01	221.05829	13.80597	2.42E-04	5.11E+00	6.02E-01
Family																		
Balistidae				9.42E+00	1.71E+01							1.26E-02		1968.78861	2.93094	2.55E-03		2.60E-01
Centrarchidae							130.92000								4.94000			1.90E-01
Centropomidae							124.22000					3.33E-01			4.47333	3.03E-01		2.10E-01
Clupeidae	-8.88E+00	-8.03E+00	7.12E-01	3.77E+00			76.66667								5.17778			
Eleotridae														626.73471	3.09439			
Fundulidae														706.32007	2.79102			
Gobiidae				1.73E+00			59.57622											2.57E+00
Haemulidae	-2.35E+00	-7.16E-01		2.31E+00		3192.67276	39.45078									5.12E-01		9.23E-01
Istiophoridae	-5.04E+00	-4.02E-01					57.00000								1.30000			
Labridae	-6.47E+00	-3.31E+00		1.87E+00			56.14232								5.31571	3.68E-01		1.42E+01
Lutjanidae	-3.97E+00	-7.17E-01		5.93E+00	7.55E+00	6076.67990	150.51222	2.46E+03	3.00E+02		2.04E-01	3.29E-02	1.03E+00	214.22107	5.28014	2.02E-01	3.37E-01	4.51E-01
Malacanthidae				1.18E+01		10351.72561	81.49369		1.75E+02		1.83E-01	1.02E-01	9.79E-01	362.42021	2.50860	2.53E-01	4.34E-01	1.12E+00
Moronidae	-1.15E+01	-7.21E+00					191.83054								43.49883			
Mugilidae																		
Paralichthyidae				6.26E+00		13766.79094	197.61223		9.42E+02		1.63E-01	7.06E-02	7.52E-01	392.67361	9.29687	3.43E-01	8.11E-01	3.57E-01
Phycidae				5.64E+00		14068.19367	96.48531		9.42E+02		1.64E-01	7.02E-02	7.07E-01	402.74024	18.61310	3.72E-01	1.06E+00	3.52E-01
Pomacentridae				2.88E+00		14688.70765	86.85456			2059.68034					3.60933			
Pomatomidae			7.18E-01			15151.95719	135.77453			2301.63460					4.55058			
Salmonidae				3.60E+00		6742.12943	115.20263			2685.53876			5.77E-01		63.70813		1.70E+00	9.44E-01
Sciaenidae	-3.88E+00	-1.84E+00		3.08E+00	1.33E+01	11538.20804	130.52384		4.17E+02	1923.37032		8.15E-03	6.99E-01	352.45907	45.17340	2.49E-01	1.08E+00	8.56E-01
Scombridae	-8.56E+00	-1.48E+00		2.68E+00		16442.09628	96.99422			1308.24102					1.12915			1.35E-01
Serranidae	-4.07E+00	-1.88E+00		6.65E+00		11580.87998	92.30632		2.73E+02	1079.22097	2.23E-01	9.53E-02	1.00E+00	379.72390	1.27931	3.11E-01	5.43E-01	1.74E+00
Sparidae				6.89E+00		9970.17322	116.57026		3.30E+02		2.03E-01	7.99E-02	9.15E-01	379.57703	0.62868	2.81E-01	4.23E-01	3.22E-01
Ecological Niche																		
Benthopelagic Amphidromous			7.18E-01															
Benthopelagic Anadromous																		
Benthopelagic Non-migratory				7.20E+00		8937.82645	88.55687		3.98E+02		2.37E-01	8.99E-02	9.82E-01	669.02279	2.58121	2.45E-01	4.62E-01	3.98E-01
Benthopelagic Oceanodromous				6.89E+00		9970.17322	116.57026		3.30E+02		2.03E-01	7.99E-02	9.15E-01	379.57703	0.62868	2.81E-01	4.23E-01	3.22E-01
Demersal Amphidromous							156.34643								3.64046			
Demersal Anadromous	-1.15E+01	-7.21E+00		3.60E+00		6742.12943	182.25206			2685.53876			5.77E-01		46.02500		1.70E+00	9.44E-01
Demersal Non-migratory	-4.28E+00	-2.14E+00		5.64E+00	1.33E+01	11158.50137	135.93473		4.56E+02	2022.55199	1.74E-01	8.28E-02	8.26E-01	376.49463	26.06971	2.86E-01	1.52E+00	8.10E-01
Demersal Oceanodromous	-2.67E+00	-1.29E+00				12833.33333	110.59666		4.17E+02			8.15E-03	6.98E-01	352.45907	66.12593	2.49E-01	1.54E-01	7.61E-01
Pelagic Oceanodromous	-5.92E+00	-6.70E-01		2.68E+00		15120.02995	124.39827			1601.70647					3.31160			
Pelagic-neritic Anadromous		-8.32E+00	7.12E-01												8.50000			
Pelagic-neritic Catadromous	-9.20E+00	-7.80E+00		3.10E+00			90.00000								5.00000			
Pelagic-neritic Oceanodromous	-7.93E+00	-5.62E+00		3.98E+00			80.83333								4.68333			
Reef-associated Amphidromous	-4.80E+00	-6.35E-01		3.47E+00			110.27088					3.33E-01			6.74437	3.03E-01		2.03E-01
Reef-associated Non-migratory	-3.88E+00	-1.57E+00		6.92E+00	1.97E+01	4043.37459	60.78383		2.68E+02		3.05E-01	1.14E-01	1.64E+00	936.99990	3.67409	3.85E-01	7.36E-01	1.93E+00
Reef-associated Oceanodromous	-3.83E+00	-9.23E-01		5.33E+00	7.55E+00	12552.06601	154.39267	2.46E+03	3.27E+02	1079.22097	2.03E-01	3.74E-02	8.20E-01	260.52153	3.82835	1.69E-01	4.08E-01	1.11E+00

Table 3.2 (Continued)

Region	Zn	Ga	Ge	Rb	Sr	Y	Mo	Ag	Cd	Sn	Ba	La	Ce	Au	Pb	Tl	Bi	U	% Min	% Max
Caribbean Sea	6.753	1.004		1.11E-01	2307.503					0.950	1.984	6.972	0.064		1.195	5.189E-02			19.0	47.6
Central Atlantic	5.752			1.08E-01	2413.974	1.122E-02					27.508	0.001	130.000		0.035				12.5	31.3
Mississippi Delta	0.408			1.23E-01	2832.851	2.000E-03					18.604				0.032			4.481E-04	16.7	11.1
North Atlantic				4.65E-01	2124.530						11.584								25.0	8.3
Northeast GOM	2.299		2.016E-01	2.30E-01	2347.602	9.363E-03	2.982E-03	3.585E-04	3.526E-02	0.199	5.256			6.325E-03	0.054	3.425E-04	5.024E-05	1.475E-03	12.5	28.1
South Atlantic	0.755			1.80E-02	2256.141	1.500E-03					16.990				0.014				25.0	0.0
South Florida	0.720				2205.079						6.339								20.0	10.0
West Florida	1.194		2.135E-01	1.46E-01	2200.613	8.893E-03	2.293E-03		6.006E-02	0.308	3.691			6.078E-03	0.079	2.593E-04	3.350E-05	2.889E-03	20.0	20.0
West GOM	0.738	0.956		9.65E-02	2215.900		2.392E-03		2.756E-02	0.002	9.368				0.006	2.642E-04	3.948E-05	3.571E-04	33.3	7.4
Family																				
Balistidae	27.006				1060.260		3.970E-03		8.451E-04	0.006	29.448				0.004	5.676E-04	5.264E-05		31.3	31.3
Centrarchidae	0.520				2197.522						2.650								0.0	0.0
Centropomidae	0.640				2588.600	1.700E-03					2.860				0.030				10.0	10.0
Clupeidae				4.16E-01	1943.311	7.429E-03					17.137				0.090				18.2	0.0
Eleotridae				1.40E-01	4764.873						6.270							3.571E-04	16.7	16.7
Fundulidae				1.27E-01	3818.676						4.212							3.734E-04	0.0	0.0
Gobiidae	1.670			1.40E-01	3673.577					0.649	1.181				0.072				11.1	0.0
Haemulidae				5.85E-02	1534.438					1.116	1.458				0.111				25.0	16.7
Istiophoridae					3250.000						0.030								16.7	16.7
Labridae	17.407			4.32E-01	2777.641					1.803	2.390				0.626				0.0	23.1
Lutjanidae	0.721		2.335E-01	1.33E-01	2143.902	9.810E-03	2.417E-03	3.585E-04	2.593E-02	0.093	5.902			8.270E-03	0.020	2.571E-04	4.147E-05	1.822E-03	25.8	16.1
Malacanthidae	0.816		2.184E-01	1.03E-01	3090.072	7.809E-03			5.593E-02	0.232	17.363			7.573E-03	0.056			2.666E-03	4.3	4.3
Moronidae					3458.716						43.285								16.7	16.7
Mugilidae					1303.049						0.160								0.0	0.0
Paralichthyidae	8.060		1.376E-01	1.28E-01	1785.698	6.238E-03			4.449E-02	0.239	3.669			5.596E-03	0.073			1.997E-03	8.7	8.7
Phycidae	2.256		1.390E-01	1.21E-01	2066.678	9.556E-03			4.513E-02	0.256	3.626	4.666		4.967E-03	0.118	1.557E-01		2.766E-03	4.0	8.0
Pomacentridae	3.268				2911.350					0.067	5.294	6.972	0.064		3.049	5.189E-02			7.7	15.4
Pomatomidae					1539.260						1.966								0.0	14.3
Salmonidae		1.004		1.05E-01	1769.003						14.564								8.3	33.3
Sciaenidae	0.733	0.956		7.36E-02	2304.715	1.192E-02					23.000	0.001	130.000		0.035				12.5	8.3
Scombridae	1.838				2021.645						1.824				0.015				8.3	8.3
Serranidae	1.970		2.145E-01	1.46E-01	2342.435	1.068E-02			6.815E-02	0.364	2.312			5.442E-03	0.098			2.684E-03	3.8	7.7
Sparidae	0.462		2.142E-01	1.56E-01	2585.154	1.116E-02			5.171E-02	0.249	5.610			6.536E-03	0.060			2.203E-03	8.7	0.0
Ecological Niche																				
Benthopelagic Amphidromous					1100.000						0.160								33.3	33.3
Benthopelagic Anadromous					410.000						0.980								50.0	0.0
Benthopelagic Non-migratory	0.552		2.246E-01	1.32E-01	3569.912	1.834E-02			5.872E-02	0.238	5.073			8.599E-03	0.054			6.184E-04	4.3	13.0
Benthopelagic Oceanodromous	0.462		2.142E-01	1.56E-01	1978.865	1.116E-02			5.171E-02	0.249	4.385			6.536E-03	0.060			2.203E-03	8.7	0.0
Demersal Amphidromous					5792.036						32.849								0.0	25.0
Demersal Anadromous		1.004		1.05E-01	3572.800						44.708								14.3	35.7
Demersal Non-migratory	1.044	0.956	1.789E-01	9.42E-02	2340.030	1.087E-02			5.308E-02	0.231	23.333	0.001	130.000	6.372E-03	0.057			2.469E-03	16.7	6.7
Demersal Oceanodromous	1.616				2017.571						6.944				0.036				12.5	12.5
Pelagic Oceanodromous					1432.588	2.000E-03					1.812				0.030				18.2	9.1
Pelagic-neritic Anadromous				1.25E+00	2020.515	3.500E-03					19.115				0.090				25.0	12.5
Pelagic-neritic Catadromous				2.00E-01	1128.500	6.800E-03					2.580								0.0	0.0
Pelagic-neritic Oceanodromous				1.25E-01	1341.667	8.340E-03					7.167								0.0	0.0
Reef-associated Amphidromous	1.024				2688.174	1.600E-03					4.556	4.666			0.211	1.557E-01			13.3	20.0
Reef-associated Non-migratory	8.015		3.193E-01	3.27E-01	2258.541	1.747E-02	4.002E-03		5.313E-02	0.533	3.229	6.972	0.064	1.006E-02	0.767	1.765E-02	5.981E-05	2.985E-03	12.9	48.4
Reef-associated Oceanodromous	1.373		1.946E-01	1.40E-01	2215.076	6.274E-03	2.417E-03	3.585E-04	3.405E-02	0.229	5.372			4.088E-03	0.059	2.571E-04	4.147E-05	1.767E-03	37.5	6.3

Table 3.3 Average element concentrations for Mg, Mn, Sr, and Ba separated by migration- and habitat-type.

Ecological Niche		**Mg**	**Mn**	**Sr**	**Ba**
Habitat Type	Benthopelagic	102.56	1.60	1764.69	2.65
	Demersal	146.28	35.47	3430.61	26.96
	Pelagic	98.41	5.37	1480.82	7.67
	Reef	108.48	4.75	2387.26	4.39
Migration Type	Amphidromous	133.31	5.19	3193.40	12.52
	Anadromous	182.25	27.26	2001.10	21.60
	Catadromous	90.00	5.00	1128.50	2.58
	Non-migratory	95.09	10.78	2722.83	10.55
	Oceanodromous	117.36	15.72	1797.15	5.14

Table 3.4 Results of one-way permutation-based ANOVAs to test whether there are significant differences among species within a region. Significant differences among species (marine and freshwater) within a region for each constituent tested are shown using different letters. Cells without letters indicate that a test was not conducted for that constituent because there were not sufficient data.

Region (salinity)	Species	$\delta^{13}C$	$\delta^{18}O$	Li	B	Na	Mg	K	V	Cr	Fe	Mn	Co	Ni	Cu	Zn	Rb	Sr	Y	Cd	Sn	Ba	Pb	U	Sr87/86
Caribbean Sea (SW)	Bicolor Damselfish						ab					a				a		a				a	a		
	Bluehead Wrasse						a					a						a				ab	a		
	French Grunt	a	a			a	ab						a		a			ab				b	a		
	Nassau Grouper															a		a				ab			
	Schoolmaster	ab	a			b	b						a		a			b				b			
	Yellowtail Snapper	b	a																						
Central Atlantic (SW)	Atlantic Menhaden	a	a	a			a					a						b	a			b			
	Spotted Seatrout	b		a			b					b						a	b			a			
	Striped Bass						ab					ab						b				b			
	Weakfish						b					b						ab				ab			
	White Perch	b	a															ab							
Mississippi Delta (SW)	Gulf Killifish										a	a						a				a			
	Red Drum						a				b														
	Spotted Seatrout						b					b						b				b			
Northeast GOM (SW)	Gag Grouper	a	a	a		a	a					a			a			a				a	a		
	Gulf Killifish										a	a						b				a		a	
	Largemouth Bass																	c							
	Red Drum						a									a									
	Red Snapper	a	b	b		b	a				b	a			b	a		c				b	b	a	
South Atlantic (SW)	Red Drum						a					a						a				a			
	Red Snapper						b					b						a				b			
West Florida (SW)	Common Snook								ab				a					ab	a						
	Gag Grouper	a	a	a		a	a		ab	a	a	a	a	a	a	a		a	b	a	a	a	a		
	Gray Snapper	a	a	a			a					b						b				b			
	Red Drum					a	a		a	a	a	b	a	a	b	a		ab				ab	b		
	Red Snapper			b			a		b		a	ab	a		b	a		b		a	b	ab	ab		
West GOM (SW)	Atlantic Croaker			a		a	a	a				a			a		a	a							
	Red Drum	a	a																						
	Red Snapper	a	a	b	a		b					b			b			b				a			
	Spotted Seatrout	a	a		b	b		a				a					b	b				b			
Central Atlantic (FW)	American Shad	a																c				a			a
	White Perch	a																				b			
	Blueback Herring																	a							a
	Striped Bass																	b							
	Alewife																	ab							a
North Atlantic (FW)	Alewife	a																b				a			a
	American Shad	b																a				b			a
	Tautog	c																ab				c			
	Blueback Herring																	b							a
South Atlantic (FW)	American Shad																	a							a
	Blueback Herring																	a							a

Table 3.5 Results of one-way permutation-based ANOVAs to test whether there are significant differences across regions for a species. Significant differences among regions for each constituent tested are shown using different letters. Cells without letters indicate that a test was not conducted for that constituent because there were not sufficient data.

Species (salinity)	Region	$\delta^{13}C$	$\delta^{18}O$	Li	B	Na	Mg	K	V	Cr	Fe	Mn	Co	Ni	Cu	Zn	Rb	Sr	Mo	Cd	Sn	Ba	Pb	Tl	Bi	U	Sr87/86
Gag Grouper	Northeast GOM	a	a	a		a	a	a				a			a			a				a	a				
(SW)	West Florida	a	a	b		a	a	a				a			a			b				a	a				
Gray Snapper	South Florida	a	a																								
(SW)	West Florida	b	b																								
Gulf Killifish (SW)	Mississippi Delta										a	a					a	a				a				a	
	Northeast GOM										b	a					a	a				b				a	
Red Drum (SW)	Mississippi Delta						a		a	a	a		a	a	a	a							a				
	Northeast GOM						a									a											
	South Atlantic						a					a				a		a				a					
	West Florida						a		a	a	a	a	a	a	a	a		a				a	a				
Red Snapper	Northeast GOM	a	ab	a	a		a		a		a	ab	a		a	a		a	a	a	a	ab	a	a	a		
(SW)	South Atlantic	a	a	a			ab					ab						a				c					
	West Florida						a		a		a	a	a		a	a		a		a	a	a	a				
	West GOM	a	b	a	a		b		a		a	b	a		a	a		a	a	a	a	b	a	a	a		
Spotted Seatrout	Central Atlantic	a		a			a					ab						a				a					
(SW)	Mississippi Delta	a	a	b			b					a						ab				a					
	West GOM	a	b									b						b				a					
Alewife (FW)	Central Atlantic																	a									a
	North Atlantic																	a									a
Blueback Herring	Central Atlantic																	a									a
(FW)	North Atlantic																	a									a
	South Atlantic																	a									a
American Shad	Central Atlantic		a															ab				a					a
(FW)	North Atlantic		a															a				a					a
	South Atlantic		b															b				a					a

Table 3.6 Results of two-way, permutation-based ANOVAs to determine if there is a significant difference in otolith constituent values among families and regions.

	$\delta^{13}C$	$\delta^{18}O$	Li	B	Na	Mg	Pb	K	Sc	V	Cr	Fe	Mn	Co	Ni	Cu	Zn	Ge	Rb	Sr	Y	Cd	Sn	Ba	Au	Pb	U
Family p-value	0.001	0.001	0.001	0.130	0.029	0.001	0.002	0.161	0.380	0.001	0.002	0.001	0.001	0.001	0.001	0.001	0.188	0.192	1.000	0.001	0.002	0.001	0.001	0.001	0.195	0.002	0.002
Region p-value	0.001	0.001	0.001	0.012	0.004	0.001	0.003	0.277	0.570	0.001	0.001	0.001	0.001	0.001	0.001	0.002	0.186	0.780	1.000	0.001	0.003	0.008	0.001	0.001	0.688	0.003	0.002
Family x region	0.366	1.000	0.995	0.161	1.000	0.011	1.000	1.000	0.496	1.000	0.434	1.000	0.008	0.997	0.369	0.309	1.000	0.910	1.000	0.001	0.008	1.000	1.000	1.000	0.997	1.000	1.000
Family effect	0.332	0.439	0.426	0.003	0.673	0.283	0.655	0.759	0.148	0.672	0.349	0.782	0.484	0.423	0.250	0.422	0.541	0.234	0.658	0.399	0.295	0.448	0.580	0.607	0.229	0.655	0.535
Region effect	0.255	0.442	0.364	0.090	0.884	0.419	0.306	0.637	0.012	0.343	0.316	0.267	0.156	0.414	0.433	0.153	0.419	0.004	0.698	0.067	0.137	0.141	0.375	0.409	0.009	0.306	0.226

3.6 Figures

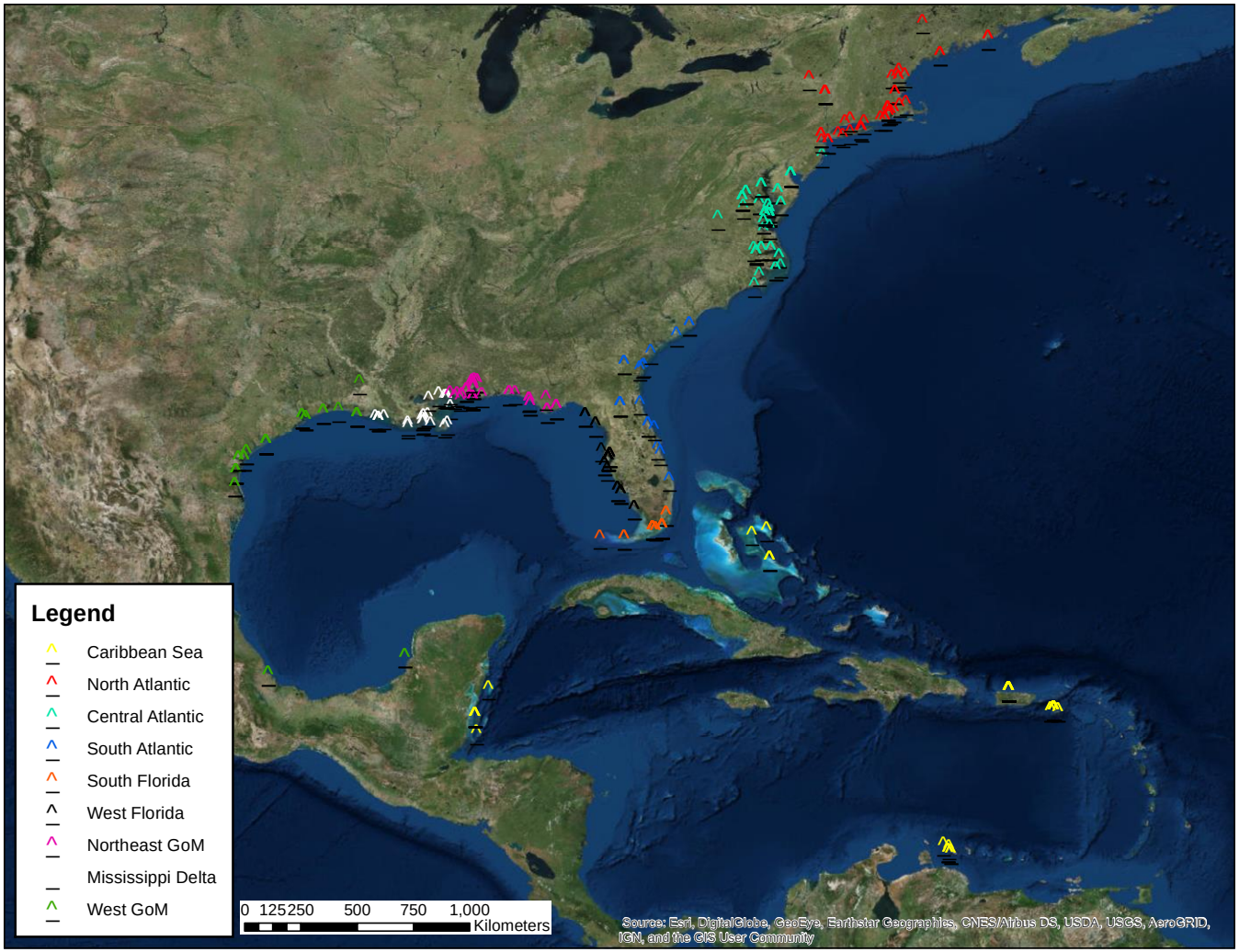

Fig. 3.1 Locations of sample collections from all studies used in this meta-analysis. Samples are sorted among 9 regions: Caribbean Sea, North Atlantic, Central Atlantic, South Atlantic, South Florida, West Florida, Northeast GoM, Mississippi Delta, and West GoM

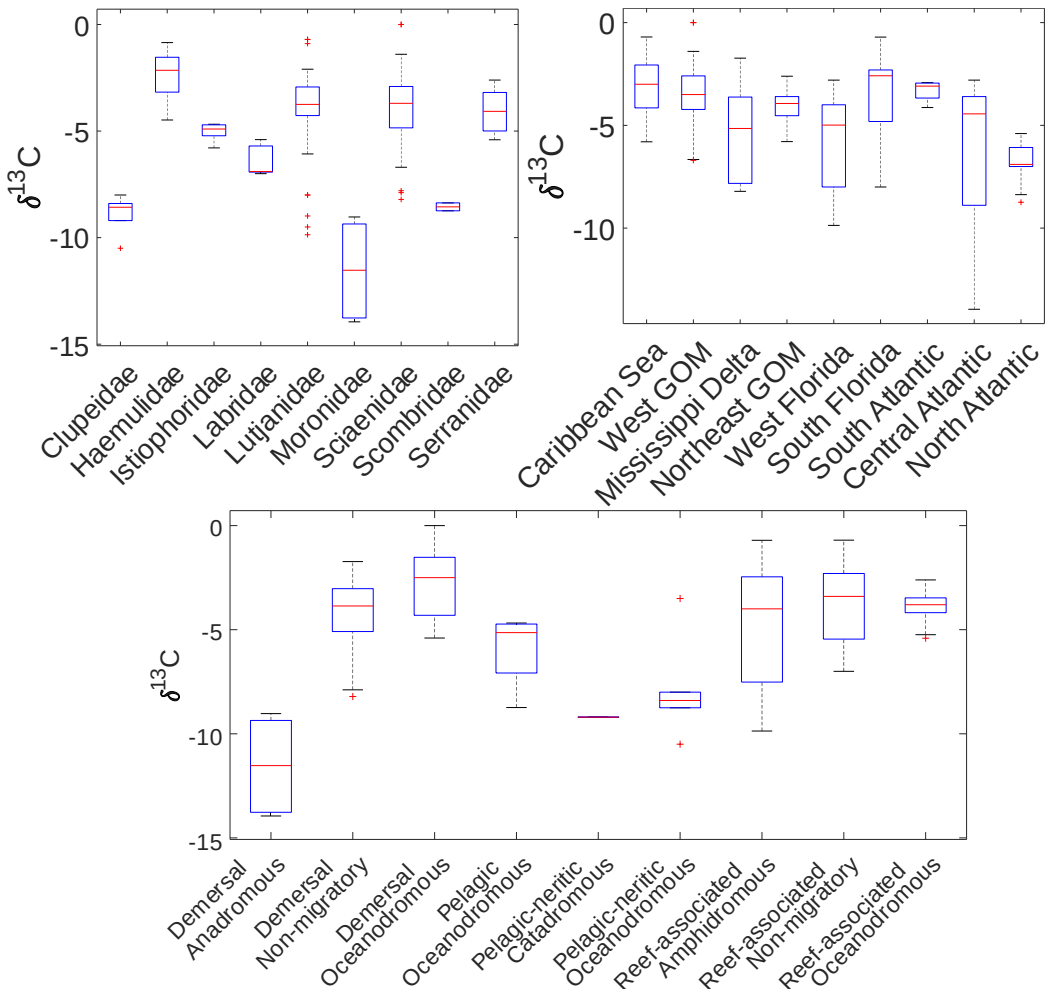

Fig. 3.2 Boxplots of $\delta^{13}C$ ratios (%, Air) in otoliths shown among regions (a), families (b), and ecological niches (c). The top and bottom of each box represent the 25th and 75th percentiles of the samples, respectively. The line in the middle of each box is the sample median. The whiskers incorporate the furthest observations that are not designated as outliers. Outliers are displayed with a red + sign and are values more than 1.5 times the interquartile range away from the top or bottom of the box. All the following boxplots follow these same rules.

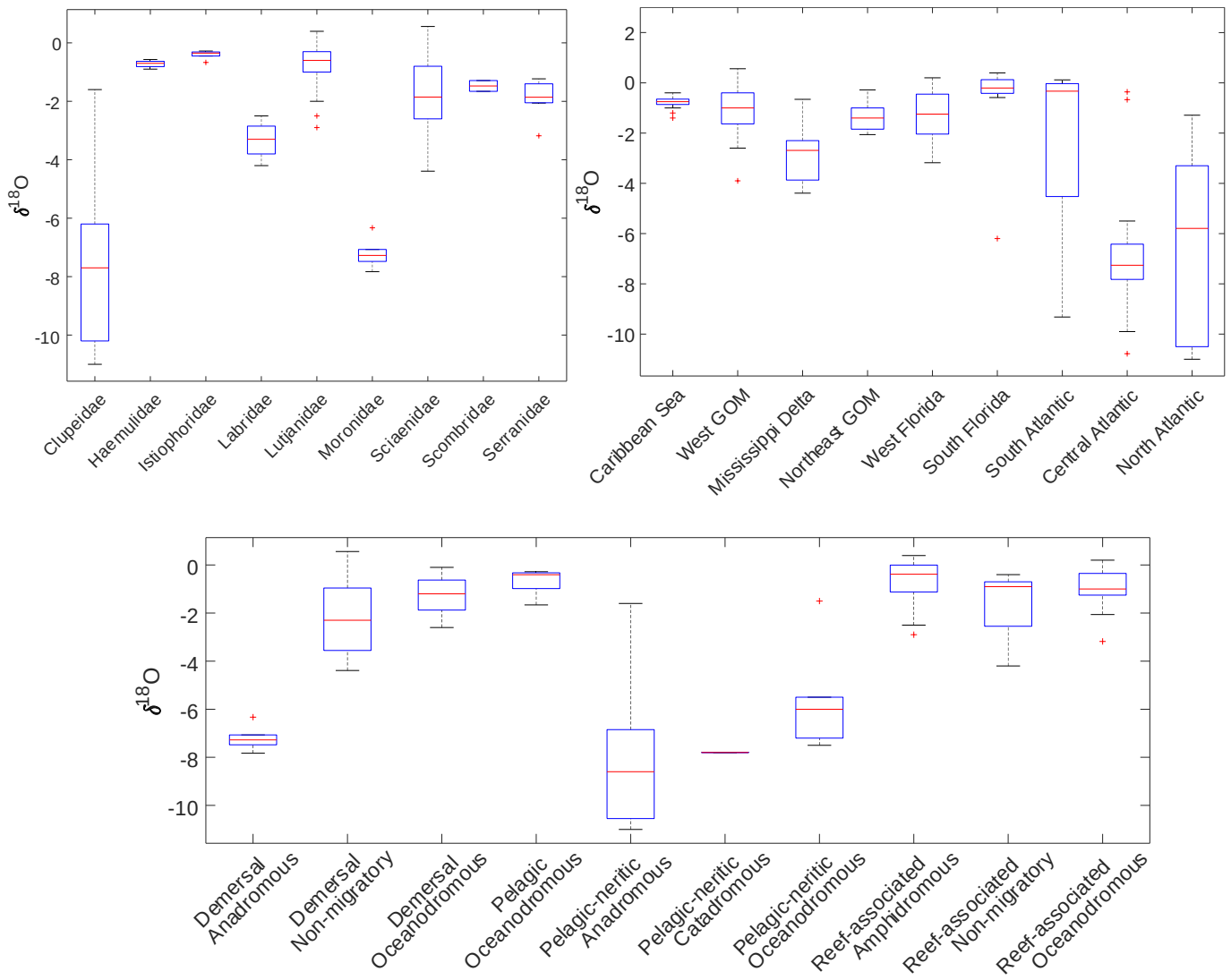

Fig. 3.3 Boxplots of $\delta^{18}O$ (‰, Air) ratios in otoliths shown among regions (a), families (b), and ecological niches (c).

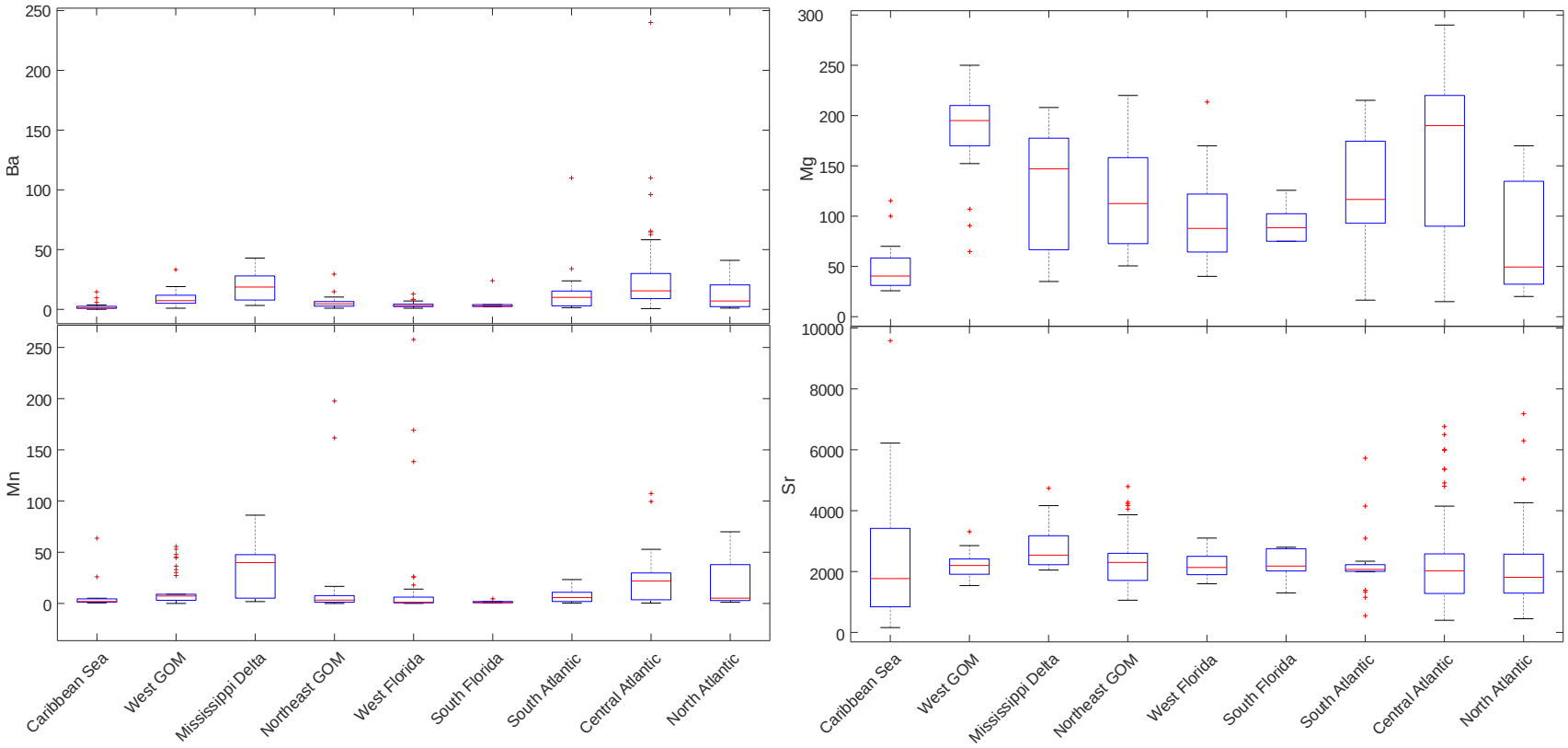

Fig. 3.4 Boxplot of element concentrations (ppm) shown among regions for Ba (a), Mg (b), Mn (c), and Sr (d).

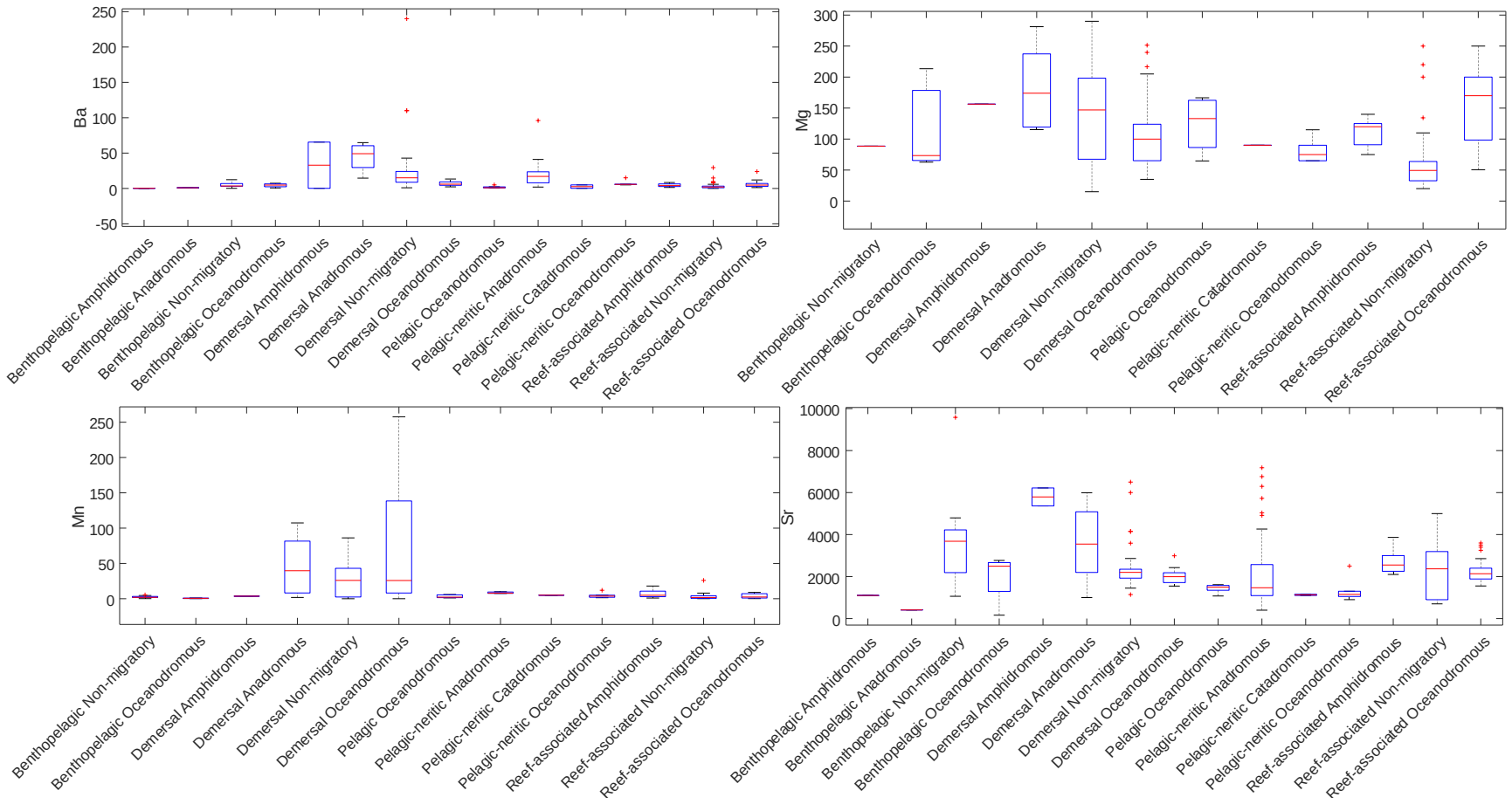

Fig. 3.5 Boxplot of element concentrations (ppm) shown among ecological niches for Ba (a), Mg (b), Mn (c), and Sr (d).

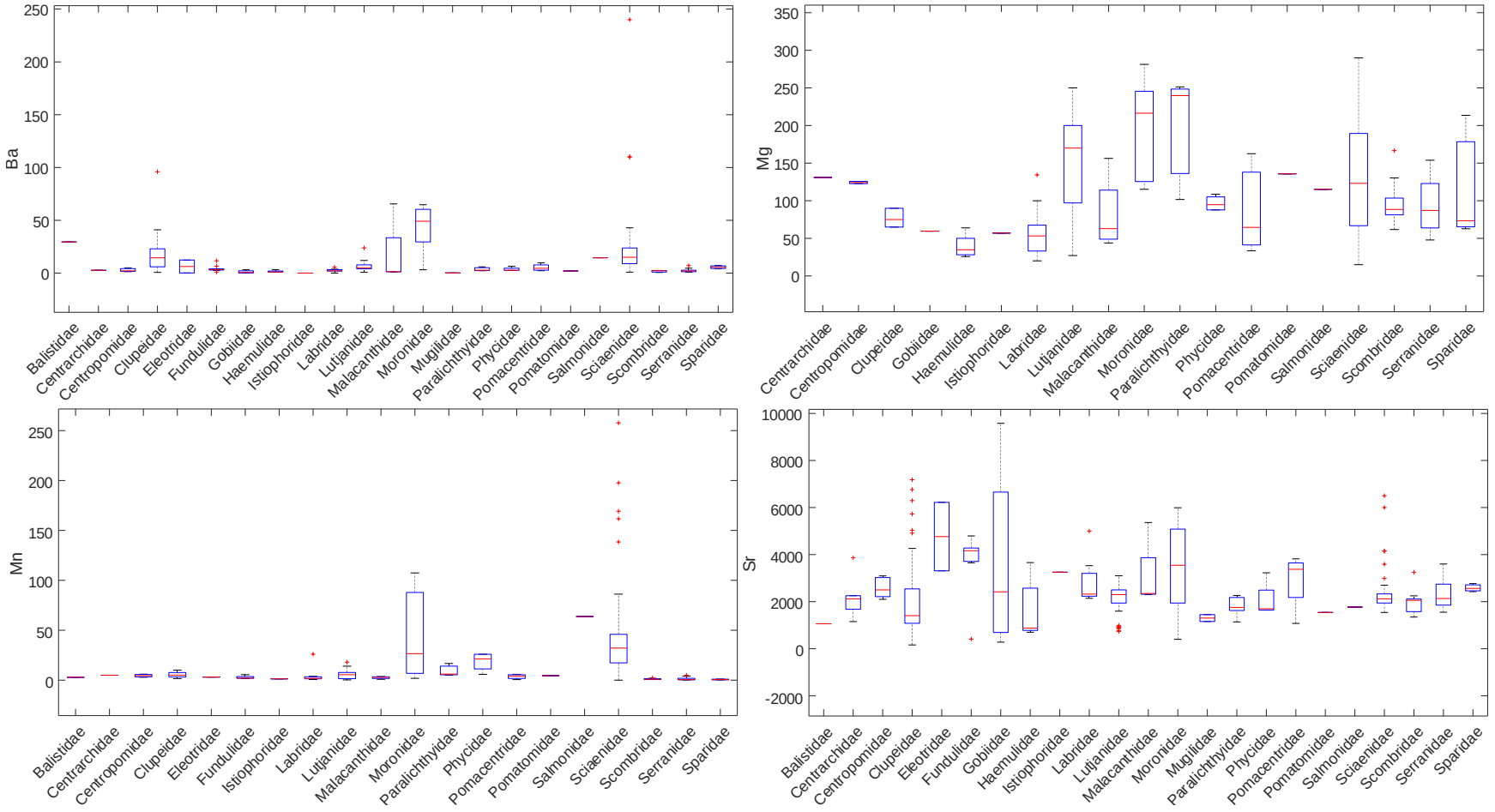

Fig. 3.6 Boxplot of element concentrations (ppm) shown among families for Ba (a), Mg (b), Mn (c), and Sr (d).

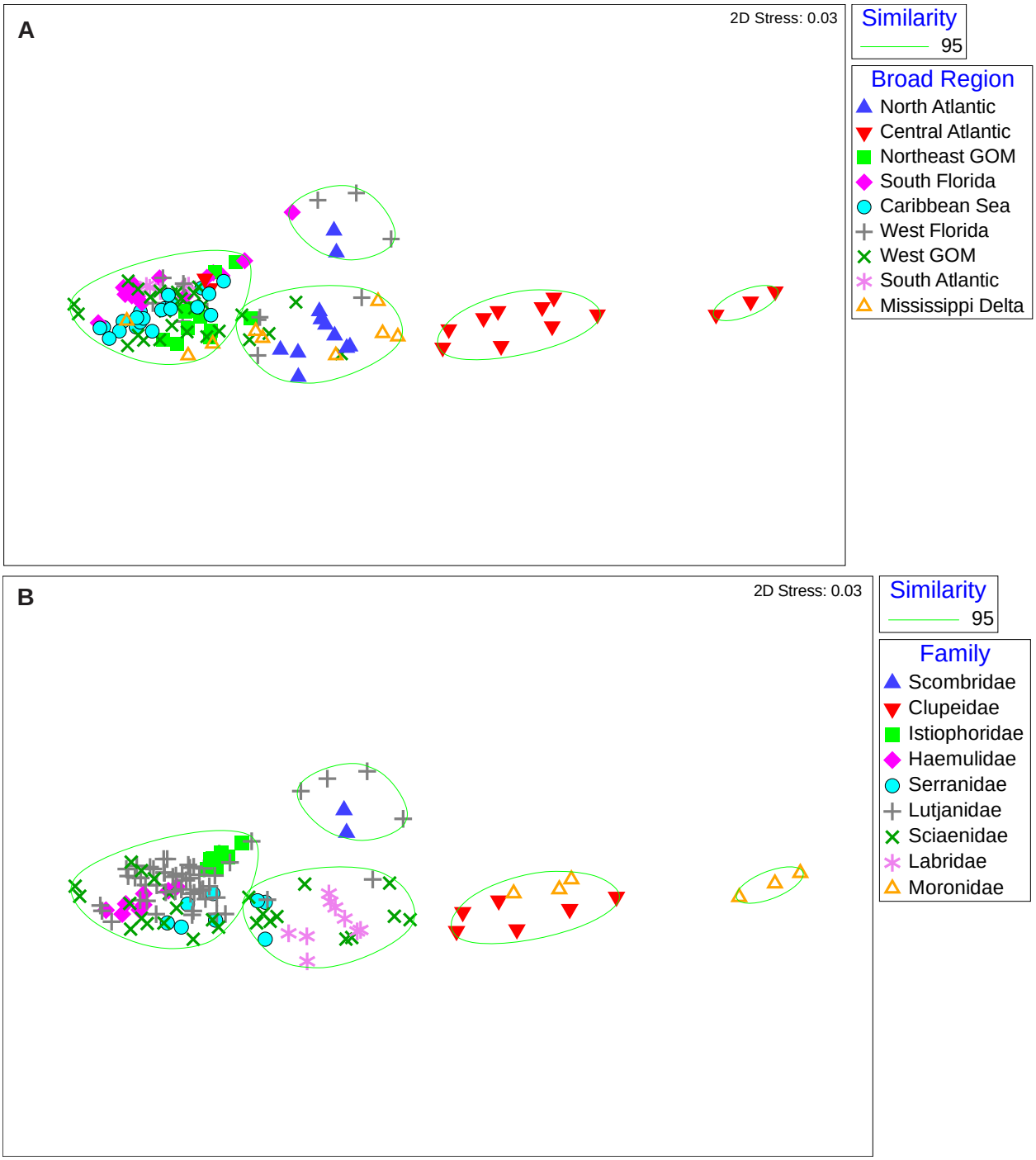

Fig. 3.7 Non-metric multi-dimensional scaling (nMDS) plot of $\delta^{13}C$ and $\delta^{18}O$ otolith isotope ratios (%, Air), with SIMPROF groupings outlined for regions (a) and families (b).

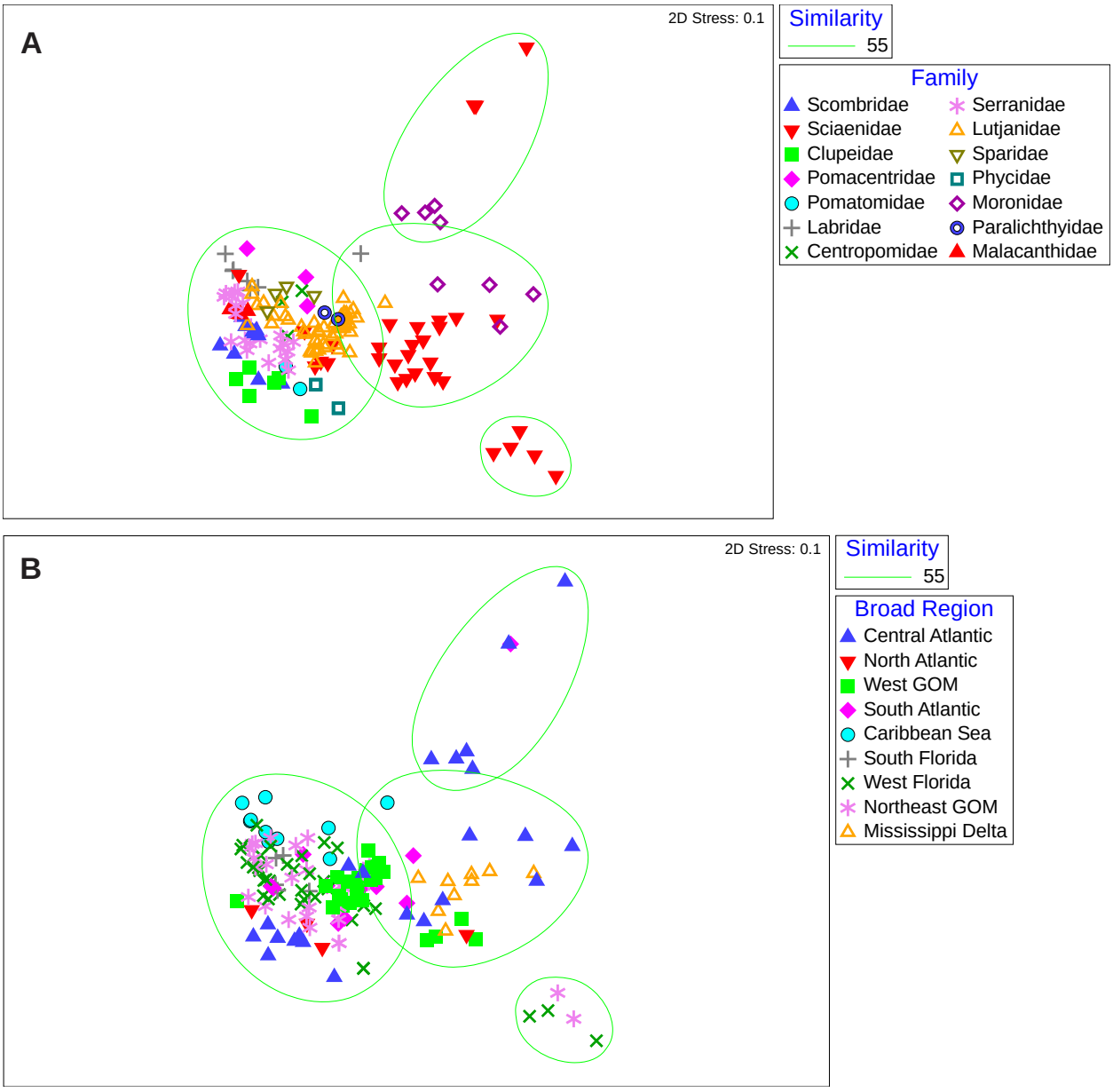

Fig. 3.8 Non-metric multi-dimensional scaling (nMDS) plot of Ba, Mg, Mn, and Sr otolith concentrations (ppm) with SIMPROF groupings outlined for regions (a) and families (b).

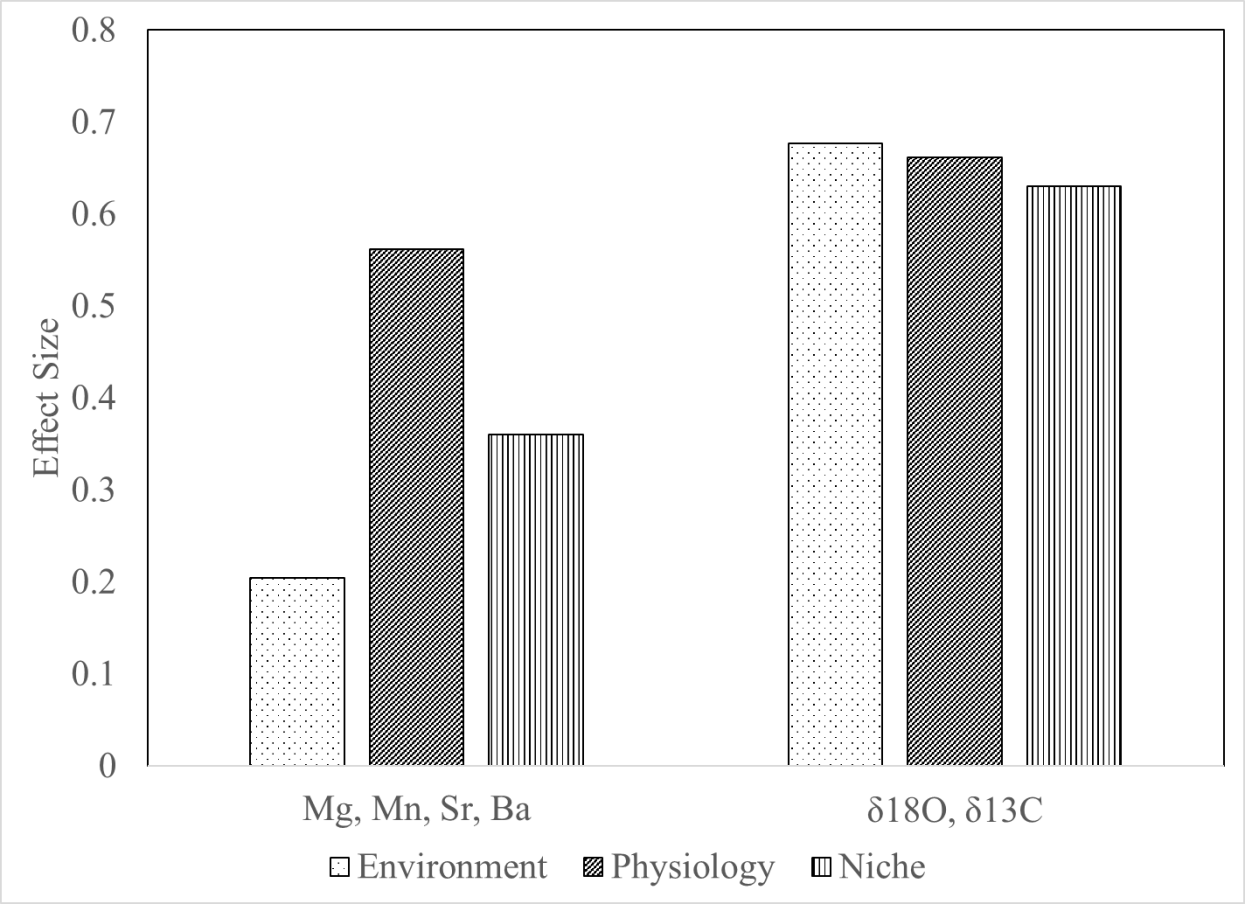

Fig. 3.9 Comparison of effect size of environment, physiology, and niche as determined using the partial eta-squared method.

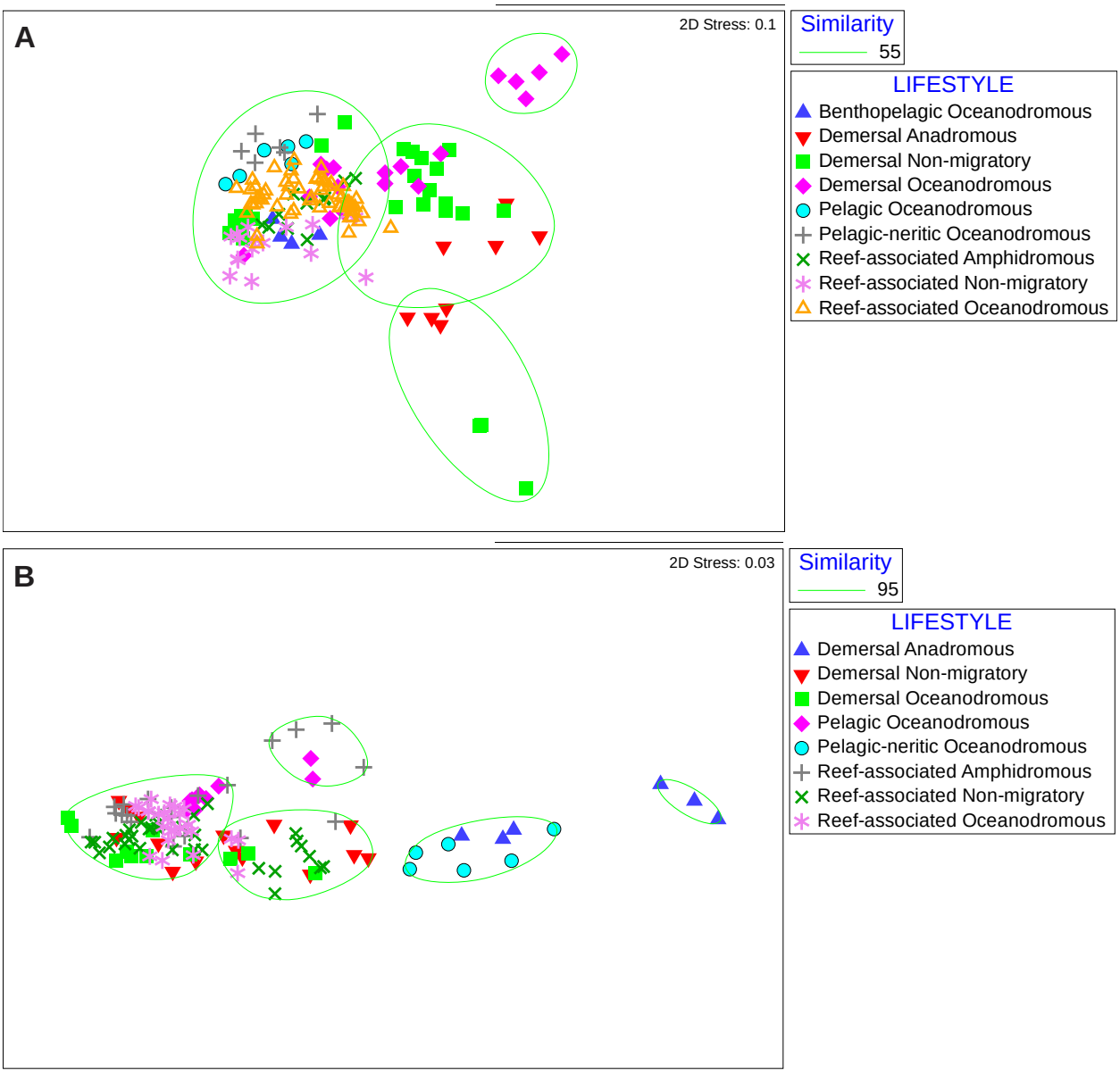

Fig. 3.10 Non-metric multi-dimensional scaling (nMDS) plot of (a) Ba, Mg, Mn, and Sr and (b) $\delta^{13}C$ and $\delta^{18}O$ otolith constituent values with SIMPROF groupings outlined for ecological niches.

Chapter 4. Fish eye-lens response to an experimental step-change in dietary $\delta^{15}N$

Abstract

The fish eye lens is composed of layers of lens fiber cells (LFCs) that form sequentially creating successive, concentric shells (laminae) that are similar to the layers of an onion. After LFCs form, they undergo an attenuated form of apoptosis, preventing new protein synthesis. This sequential cessation of new organic synthesis makes the eye lens a potential lifetime, isotopic recorder. To test the utility of fish eye lenses as recorders of isotopic history, I conducted an experimental step-change in dietary $\delta^{15}N$ and measured the $\delta^{15}N$ in eye lenses from fish exposed to the dietary change. Red Drum raised in captivity were switched from a diet depleted in $\delta^{15}N$ to a relatively enriched diet and sacrificed approximately 150 days after the diet switch. Additionally, juvenile Red Drum specimens (n = 145) spanning a broad range of body lengths were photographed, and standard length (SL) and lens (pupil) diameter were measured to convert measured eye lens diameter to age. Reductions in eye-lens $\delta^{15}N$ values occurred on average 15.7 d after the $\delta^{15}N$ of the feed was reduced by approximately 3.0‰, with residence times (τ) averaging 16.7 d after the change point. Mean 90% assimilation (τ_{90}) of the new feed isotopes occurred 38.5 d after the change point. In addition, the $\delta^{15}N$ discrimination factor for eye-lens tissue was 3.15 ± 0.06‰. These results support the use of fish eye lenses as recorders of isotopic history, although this record has a lag of approximately 16 days.

4.1 Introduction

Lifetime records of the carbon radioisotope ($\delta^{14}C$) stored within the vertebrate eye lens have been used to estimate the unknown ages of individual humans and sharks by matching lifelong trends in eye-lens $\delta^{14}C$ with decadal-scale trends in atmospheric $\delta^{14}C$ (Lynnerup et al. 2008, Stewart et al. 2013, Nielsen et al. 2016). The vertebrate eye lens grows by accreting new outer layers (laminae) with age, after which the new layers lose their ability to synthesize protein (via attenuated apoptosis, Greiling and Clark 2012), and thus conserve the isotopic characteristics that prevailed during lamina formation. These isotope-bearing laminae are retained internally while new, outer laminae are formed around them. Using forceps, successive laminae can be manually separated to produce time series of isotope data that extend backward throughout life. This approach has recently been applied to stable isotopes ($\delta^{13}C$ and $\delta^{15}N$) in the eye lenses of wild-caught bony fishes and sharks (Wallace et al. 2014, Quaeck 2017, Tzadik et al. 2017), yet the isotope-recording capability of the eye lens has not been experimentally confirmed.

The objective of the present study was to study the isotopic response, as indicated by fish eye-lens laminae, to an experimental step-change in dietary $\delta^{15}N$ that took place during an extended period of fish captivity (>200 d). The interest in $\delta^{15}N$ derives from its utility in recreating individual trophic and geographic histories (Wallace et al. 2014, Quaeck 2017), as it has been demonstrated that geographic variation in $\delta^{15}N$ often exists as predictable gradients (McMahon et al. 2013, Radabaugh et al. 2013, Radabaugh and Peebles 2014) that are potentially useful for reconstructing the geographic histories of individual animals. These $\delta^{15}N$ gradients exist between areas of the coastal ocean where the mass-balanced influences of surface runoff from land (and possibly denitrification) result in elevated $\delta^{15}N$, and oligotrophic areas where nitrogen fixation is dominant and $\delta^{15}N$ is low (e.g., oceanic gyres and other nitrogen-poor seas).

In fishes, individual histories for $\delta^{15}N$ are of particular interest because $\delta^{15}N$ is difficult to obtain from otoliths due to the otoliths' low nitrogen content, and thus the ability to obtain lifetime histories for $\delta^{15}N$ is particularly novel.

The general design of the present study was to cultivate a number of individual fish from the egg stage through a period of (isotopic) dietary transition, and then allow sufficient time in continued captivity to allow isotopic expression of the diet switch within the eye lens. Afterwards, the captive individuals were sacrificed and analyzed in the same manner as wild-caught specimens (e.g., Wallace et al. 2014). Note that the decision to sacrifice all individuals at the end of the experiment, rather than periodically sacrificing smaller numbers throughout the experiment, simplified the investigation of potential lags between diet switch and incorporation into eye lenses, and also simulated the procedures that have been used to investigate wild-caught specimens.

4.2. Methods

4.2.1 Experimental animals and feed

Fertilized red drum eggs were obtained from captive broodstock at the Stock Enhancement Research Facility (Manatee County, Florida, USA) of the Florida Fish and Wildlife Conservation Commission. The eggs were transported to Mote Aquaculture Park (Sarasota County, Florida, USA), where they hatched. Starting at age 3 d (posthatching), larvae were fed rotifers twice daily along with Otohime A (Marubeni Nisshin Feed Co., Ltd., Japan). Starting at age 7 d, *Artemia* (1-2 mL^{-1}) was added to the diet. Between ages 16 and 54 d, the fish were fed a variety of Otohime diets without rotifers or *Artemia* (Table 1). At age 54 d, the fish were switched from Otohime to extruded sinking steelhead (ESS) feed (Skretting, Tooele, UT,

USA). The top ingredients of the Otohime diet were krill, fish, and squid meal, whereas the top ESS feed ingredients were fish meal, whole wheat, and soybean meal. The ESS feed had approximately 3.0‰ lower δ^{15}N relative to the mixture of Otohime feeds at the time of the diet change on 12/2/15; the maximum difference in feed δ^{15}N was 4.0% (Table 4.1, isotope analysis methods are provided below). Eighteen fish were maintained for an additional 147-156 d after the switch to ESS feed. Water-quality conditions during the experiment are presented in Table 4.2.

4.2.2 Eye-lens isotope measurements

After a total period of 201-210 d in captivity, the fish were sacrificed using an overdose of the anesthetic MS-222 (tricaine methanesulfonate) and were weighed and measured (Table 4.3). After sacrifice, whole eyes were removed, wrapped with sample-identification labels in aluminum foil, and frozen at -20°C. Prior to dissection, one eye per specimen was thawed and processed individually while wearing nitrile gloves. The thawed lens was removed through a corneal incision and the elastic lens epithelium/capsule was removed from the lens. The lens was immersed in de-ionized water (Stewart et al. 2013) under a dissecting stereomicroscope, where successive layers of laminae were separated using two, fine-tipped forceps. Individual laminae were removed (delaminated) by starting near one lens pole and working towards the other. Note the term “delamination” may also refer to the embryonic lens separation from surface ectoderm. Prior to each delamination, the lens diameter at the equator was measured to the nearest 0.01 mm using an ocular micrometer, where “equator” was defined as the largest diameter that could be measured perpendicular to the polar axis (Wallace et al. 2014, Tzadik et al. 2017). Lamina position was defined as radial midpoint, $(r_1 + r_2)/2$, where r_1 and r_2 are lens radii before and after individual lamina removal, respectively. Dissected laminae were placed into a dessicator at 55°C

for 24 hours. Dried, homogenized samples from each lamina were stored in sealed plastic vials prior to isotope analysis.

4.2.3 Isotope analysis

After weighing with a Mettler-Toledo precision microbalance, duplicate 300-600 µg samples of dried, homogenized, lens or diet material were placed into separate tin capsules for measurement using a Carlo-Erba NA2500 Series II Elemental Analyzer (EA) combustion furnace coupled to a continuous-flow ThermoFinnigan Delta+XL isotope ratio mass spectrometer at the University of South Florida College of Marine Science in St. Petersburg, Florida, USA. Calibration standards were NIST 8573 and NIST 8574 L-glutamic acid. Results are presented in delta notation (δ, in ‰) relative to N_2 in air, which is the international standard for $\delta^{15}N$.

Eq. 1 $$\delta^{15}N = \left(\frac{(^{15}N/^{14}N)_{sample}}{(^{15}N/^{14}N)_{standard}} - 1\right) \times 1000$$

The analytical precision of the $\delta^{15}N$ measurements, which was estimated from replicate measurements of NIST 1577b bovine liver, was ±0.17 ‰ (mean of standard deviations of 210 replicates).

4.2.4 Lens-age relationship

Although the ages of the captive specimens were known, individuals were not sacrificed until the end of the experiment, necessitating assignment of ages to the internal lens laminae used to obtain isotope measurements, where radial midpoints correspond temporally to earlier points in life. Age and lens diameter at sacrifice were known for each specimen, and it was also known that initial values were zero for both age at fertilization and lens diameter at fertilization, yet a relationship was needed to describe the shape of the age-at-diameter curve between these two,

known endpoints (i.e., between fertilization and sacrifice). The first step was to establish a relationship between fish length and lamina position (radial midpoint). Because the pupils of most teleosts are immobile and have diameters that are similar to lens diameters, pupil diameter can be used as a proxy for lens diameter (Walls 1942, Jagger 1997, Dahm et al. 2007). Juvenile Red Drum specimens (n = 145) spanning a broad range of body lengths were photographed, and standard length (SL) and lens (pupil) diameter were measured from the photographs using calibrated ImageJ software. The specimens in this analysis were obtained from the fish collection at the Florida Fish and Wildlife Research Institute in St. Petersburg, FL (USA), and had been fixed in formalin for a period of days followed by preservation in alcohol for a period of years. When compared with measurements from the 18 recently frozen Red Drum from the experiment, the preserved Red Drum were found to have shorter lengths relative to their eye-lens (pupil) diameters, and thus a scaling factor was calculated to correct for shrinkage in the preserved specimens. Curve fitting of the corrected length data (preserved specimens only) was performed in MATLAB, producing regression-based conversions for length-at-diameter. Next, the length-at-age equation from Murphy and Taylor (1990) for Red Drum in Florida Gulf waters was rearranged to produce an age-at-length equation

Eq. 2
$$t = \left(\frac{1}{0.46}\right)\ x\ \left(Ln\left[\frac{934.1}{934.1-FL}\right]\right) + 0.029$$

where t is age in years and FL is fork length in mm. Correction from SL to FL was achieved using an equation specific to red drum from Fishbase (FL = 3.29 + 1.085SL, n = 1,075, R^2 = 1.00, p <0.0001; Froese and Pauly 2000). Finally, ages at measured laminar midpoints were calculated from the above series of equations, and the calculated ages of the outermost laminar diameters were verified using the known ages of the specimens.

4.2.5 Analysis of isotope data

After using the above procedure to convert radial midpoints to age, $\delta^{15}N$ values from individual laminae were plotted against lamina age, and the cubic-spline function in MATLAB was used to interpolate $\delta^{15}N$ values at a daily frequency. Note that splining interpolates between measured observations while preserving the measured values. For each Red Drum specimen, initial change points in the splines were identified using the 'findchangepts' function in MATLAB 2016b with the linear option to detect changes in mean and slope.

For each specimen, the calculated ages and corresponding $\delta^{15}N$ values (not interpolated data from splines) were trimmed to reset day one to the identified change point for that specimen. Isotopic residence time for $\delta^{15}N$ assimilation rate was calculated by fitting the Heady and Moore (2013) single-compartment equation for equilibrium tissue-turnover to trimmed data for each specimen, and also for all specimens combined. The Heady and Moore (2013) equation is

Eq. 3 $$\delta X_t = \delta X_{\text{Post}} - (\delta X_{\text{Post}} - \delta X_{\text{Pre}})\left(pe^{-\frac{t}{\tau_1}} + (1-p)e^{-\frac{t}{\tau_2}}\right)$$

where δX_{Pre} is the initial feed isotope value, δX_{Post} is the changed feed isotope value, t is time, and residence time (τ) is distributed as an exponential density function of time (del Rio and Anderson-Sprecher 2008)

Eq. 4 $$f(t) = \frac{1}{\tau}e^{\frac{-t}{\tau}}$$

A Pearson correlation matrix was used to identify potential relationships between residence time from the individual turnover regressions, change-point lag from time of feed change, and individual characteristics (age, weight, length, and eye-lens diameter at sacrifice). A

discrimination factor for $\delta^{15}N$ was calculated as the difference between (1) the mean $\delta^{15}N$ of the feed after the feed switch and (2) the predicted isotopic equilibrium, as modeled by regression, assuming Red Drum tissues reached isotopic equilibrium with the diet (Galvan et al. 2016). All error is reported as standard error (SE).

4.3 Results

Length had heterogeneous variance in its fit to eye-lens diameter, with residuals that otherwise appeared to be unbiased relative to predicted means (Fig. 4.1). The fitted model was curvilinear, although this curvature was subtle within the range of lens diameters (0.0–5.3 mm) that was relevant to the experimental specimens.

The final weights, lengths, eye diameters and ages of the 18 experimental specimens are presented in Table 4.3. During the experiment, each specimen experienced reductions in eye-lens $\delta^{15}N$ values at lens radii between 0.6 and 1.0 mm (Fig. 4.2). The change-point analysis indicated these reductions started, on average, 15.7 d after the $\delta^{15}N$ of the feed was reduced by about 3.0‰, with residence times (τ) averaging 16.7 d after the change point (Table 4.3, Fig. 4.3a). Note that the age scale in Figure 4.3 does not encompass the entire, known ages of the specimens (Table 4.3) because the scale extends from the radial midpoint of the lens nucleus to the radial midpoint of the outermost lamina; thus, the age scale does not include the entire radius (age range) of the lens. Mean 90% assimilation (τ_{90}) of the new feed isotopes occurred 38.5 d after the change point. The 18 regressions that produced these estimates had consistently good fit (all R^2 values >0.87; mean = 0.93), but yielded variable estimates for τ and τ_{90}. These two parameters were not significantly correlated (p >0.05, n = 18) with any of the variables in Table 4.3.

Describing isotopic assimilation with all fish combined produced a model (Fig. 4.4) that was used to calculate the new equilibrium after the feed switch, and this new equilibrium was used to calculate the $\delta^{15}N$ discrimination factor for eye-lens tissue as $3.15 \pm 0.06‰$. The residuals from this model had apparently biased distributions about predicted means; the residuals were mostly positive until about 15 d after the change point, then became mostly negative until about 60 d, and finally became mostly positive at >60 d.

4.4 Discussion

The development of the fish eye lens has been studied extensively, which allows a well-developed consideration of how laminae within the eye lens become isotopically isolated. This isolation can be examined at the molecular, cellular, and anatomical levels, with particular emphasis on vascular isolation, as vascular communication with tissues aids tissue turnover and contributes to the loss of isotopically conservative properties.

4.4.1 The pathway to isotopic conservation

The fish eye lens consists of layers of lens fiber cells (LFC) that arise from mitotic activity in the lens epithelium, a layer of cells that surrounds much of the lens in post-embryonic fish (Dahm et al. 2007, Greiling and Clark 2012). LFCs develop from precursor lens epithelial cells (LECs) that have migrated to the equatorial region of the epithelium (the transition zone), where the LFCs elongate towards both poles simultaneously, occupying space between the epithelium and the most recently formed LFC layer underneath. In fish, LFCs from the entire circumference of the equator meet at the poles at simple, unbranched sutures. This process forms successive, concentric shells (laminae) that are similar to the layers of an onion, with the oldest LFCs trapped in the interior (Zampighi et al. 2000).

Following the processes of (1) LEC replication, (2) LEC migration to the transition zone, and (3) pole-to-pole elongation of LFCs, LFCs degrade and remove their DNA and organelles (attenuated apoptosis), which improves the LFCs' optical properties, but also prevents new protein synthesis (Greiling and Clark 2012). In adult zebrafish (*Dania rerio*), LFC nuclei disappear abruptly at a depth of 75 µm from the epithelium, which equates to approximately 15% of the lens radius (Dahm et al. 2007). This sequential cessation of new organic synthesis is central to the explanation for eye lenses serving as isotopic recorders.

In the absence of new synthesis, lens material could still be isotopically altered by fluxes of materials into and out of the lens. LECs are nourished by the lens capsule, which is a membrane that exerts elastic pressure on the lens and lens epithelium (Danysh and Duncan 2009, Danysh et al. 2010). The lens capsule surrounds the lens/lens epithelium completely, and is the point of contact for the multipoint lens suspensorium, which consists of a system of ligaments and the tendon of the retractor lentis muscle (Khorramshahi et al. 2008). After initial embryonic development of the eye lens, there is no vascularization of the lens, the lens epithelium, the lens capsule, or the contacting tissues of the lens suspensorium (Khorramshahi et al. 2008, Greiling and Clark 2012, Hartsock et al. 2014). The falciform process vascularizes (and innervates) the retractor lentis muscle (Reckel and Melzer 2004), but this vascularization is separated from the lens capsule by the retractor lentis tendon. In short, the post-embryonic lens is completely isolated from direct contact with the vascular system, and so the vascular system cannot be a direct source of organic flux at the lens (Zampighi et al. 2000, Mathias et al. 2007).

However, in the absence of direct vascular communication, organic flux within the eye lens can still occur as diffusion and as the result of active transport of ions. Among its various functions, the lens capsule serves as a "molecular sieve" (Danysh et al. 2010), receiving

materials from the surrounding vitreous and aqueous humors (Zampighi et al. 2000, Mathias et al. 2007), including nitrogen-bearing nutrients used in cell formation, maturation, and maintenance. The vitreous and aqueous humors are viscous fluids that are supplied with nitrogen-bearing nutrients from adjacent, vascularized tissues, and are not isolated from each other due to the imperfect seal between the lens and iris and the transmissivity of the lens itself, which connects the two fluids (Mathias et al. 1997). Selective permeability at the vertebrate lens capsule, coupled with asymmetrical ion flux distributions within the lens (Mathias et al. 1997, Zampighi et al. 2000), allow circulation of water, O_2, CO_2, ions, glucose, and metabolic waste into and out of the lens, which is required for cellular maintenance, cell maturation, and regulation of the physical and biomechanical properties of the pre- and post-apoptotic LFCs (Mathias et al. 1997, 2007, Danysh and Duncan 2009). Zampighi et al. (2000) suggested the extracellular space at the polar sutures, which extends inward along the polar axis (i.e., along suture lines), facilitates movement of materials from the humors into the interior of the lens. Whether through diffusion or as the result of active transport (ion pumping), the general infusion of materials into the lens becomes more difficult with increasing distance into the lens, most notably at the lens nucleus. The mass-dominant proteins in the lens, crystallins, can undergo post-transcriptional modifications that render them more water-insoluble with age (Greiling and Clark 2012), and larger proportions of water-insoluble proteins in the older interior of the lens may impede water-based permeability and associated material transport. Diffusion of larger organic molecules (proteins) also exists within the vertebrate eye lens, yet this diffusion is primarily intra-laminar, and any centripetal diffusion (i.e., radial diffusion among laminae) is thought to produce only nominal isotopic deviations (Shi et al. 2009).

Thus, the post-embryonic isotopic communication of $\delta^{15}N$ to LFCs travels from the circulatory system to the humors, from the humors to the lens capsule, from the lens capsule to LECs, and finally from LECs to LFCs. LFCs contain organic nitrogen (and associated isotopic values) imparted to them at the lens epithelium. After LFC elongation and apoptosis, the LFCs become metabolically inert, or dead, in the same manner as hair, feathers, claws, hooves, fingernails, and chitinous exoskeletons (Dahm et al. 2007, Lynnerup et al. 2008, Auerswald 2010), yet may still be subjected to fluxes of materials into and out of the lens, as discussed above. Successive, concentric growth of the lens (i.e., the addition of new layers of LFCs) coincides with general somatic growth (Dahm et al. 2007; see also Fig. 4.1), creating the long-term isotopic records that have been used to quantify the ages of individuals according to their nuclear-bomb-related trends in radiocarbon (Lynnerup et al. 2010, Stewart et al. 2013, Nielsen et al. 2016). In the present experiment, the strong response of the lens to changing dietary $\delta^{15}N$ suggests that post-apoptotic fluxes of materials into or out of the lens did not have a strong isotopic effect. This observation is only possible because the fish were not sequentially sacrificed. Instead, older lens layers were subjected to several months of post-apoptotic conditions after the dietary shift, yet persisted in providing strong evidence of the dietary shift (Figures 4.2 and 4.3).

4.4.2 Model shape and isotopic lags

The Heady and Moore (2013) equation is a turnover equation, whereas the process that creates isotope records within eye lenses involves *de novo* protein synthesis prior to apoptosis (rather than directly engaging turnover), and this protein then becomes stored as metabolically inert (dead) tissue soon after its creation, as discussed above. While a diversity of potential isotopic compartments have been recognized within the vertebrate body [e.g., 21 compartments

modeled by Poupin et al. (2014)], the fundamental dynamics of isotopic exchange can be considered using just three body compartments: the metabolically dead pool, the metabolic pool, and the storage pool, the latter of which includes liver and collagen-rich tissues (Auerswald 2010). Increasing assimilation of altered dietary $\delta^{15}N$ contributes to the $\delta^{15}N$ of the metabolic pool, which then exchanges with $\delta^{15}N$ in the storage pool, creating the dynamic mass-balance (turnover) that contributes to negatively exponential isotopic turnover models such as the Heady and Moore (2013) model. The $\delta^{15}N$ in the metabolic pool becomes more integrated, or mixed together, by transamination, wherein new amino acids are synthesized by transferring amino groups from existing amino acids to alpha-keto carboxylic acid (Braun et al. 2014); the isotopic homogenization that results from transamination may be exchanged with the storage pool (Auerswald 2010, Braun et al. 2014). The metabolically dead pool, in contrast, derives its $\delta^{15}N$ solely from the metabolic pool, and does so while the metabolic pool is experiencing nitrogen turnover (Auerswald 2010). Thus, turnover in the source metabolic pool justifies the use of a turnover model for the metabolically dead pool (i.e., eye lenses). Despite this theoretical support, we found statistical irregularities in the fit of the Heady and Moore (2013) model. Each of the 18 fish experienced a substantial reduction in their eye-lens $\delta^{15}N$ following the large step change in dietary $\delta^{15}N$, yet some aspects of the transition were anomalous.

First, the apparent lag in lens isotope response was not expected, as the commonly used isotopic turnover models do not include lags. Yet visual inspection of the trends in Figure 4.3b suggests an overall lagged response. We used change-point analysis to accommodate this apparent lag, which identified an average change point of about 16 d (Table 4.4). As a statistical algorithm, change-point analysis is not exact, but attempts to balance Type I and Type II statistical errors by detecting meaningful change without including false changes; the

'findchangepts' function in MATLAB appeared to do a reasonable job of achieving this objective (Fig. 4.3a).

We are not aware of any well-established, process-based explanations for the observed temporal lag between the isotopic diet shift and its expression in the eye lens, except to note that in mouse embryos, one week may pass between the time when an LEC is labeled with BrdU (5-bromo-20-deoxyuridine) and the time of the cell's first appearance as a LFC within the lens cortex (Kallifatidis et al. 2011). The processes of LEC migration to the equatorial transition zone and LFC elongation towards the lens poles each require time; Greiling and Clark (2012) describe these processes in detail. Because both cell migration distances and poleward elongation distances increase geometrically with increasing lens radius length, the total time required for these processes would presumably also increase to some extent with increasing fish size (Fig. 4.1). In accordance with this explanation for the lagged response, the observed isotopic lag in lens $\delta^{15}N$ is somewhat analogous to the 6-15 d isotopic lag that has been observed in sheep wool, where new isotope values have been experimentally imparted to the wool at the follicle, but did not become expressed in external wool until the new hair-cell growth had had enough time to extend beyond the external surface of the sheep's skin (Zazzo et al. 2008). Finally, any isotopic lags that are associated with LEC formation, LEC migration, and LFC elongation are preceded by an unknown lag associated with isotopic turnover of humor secretions, as these connect the vascularized retina to the post-embryonic lens capsule and epithelium. We suspect that isotopic turnover in these fluids may be responsible for a substantial portion of the observed lag (Table 4.4, Figures 4.2 and 4.3).

A second anomaly involves the alternating bias in the signs of the residuals in Figure 4.4, which suggests the Heady and Moore (2013) turnover equation may not be the most appropriate

model for describing the isotopic replacement process. Moreover, the resulting (and possibly compromised) fit may have interfered with our calculation of trophic discrimination. One possible cause for this discrepancy is the irregularity in dietary $\delta^{15}N$ that occurred prior to the large step change in Figure 4.3. The slight increase in lens $\delta^{15}N$ that occurred between ages 35 and 60 d (Fig. 4.3b) may have reflected the lagged effect of an otherwise corresponding increase in dietary $\delta^{15}N$ that occurred between ages 10 and 24 (this increase was from 8.2 to 8.9‰, Table 4.1), causing an S-shaped response as lens $\delta^{15}N$ increased slightly, reversed, and then exponentially declined. The Heady and Moore (2013) equation may have been able to capture a simple exponential decline after the removal of the lag period, but was not able to accommodate any recurve that might have been created by the slight isotopic increase that preceded the large, stepped decrease.

4.4.3 Isotopic discrimination

The -3.0‰ difference in $\delta^{15}N$ of ESS feed relative to the Otohime feeds can be explained by its higher proportion of plant-derived protein. Specifically, soybean meal was a large component of the ESS feed, and because soybeans derive their organic N from the N_2 in air ($\delta^{15}N = 0$, by definition), soybeans have whole-plant $\delta^{15}N$ close to zero (Unkovich 2013). Likewise, wheat, which was an even larger component of the ESS feed, is likely to derive its organic N from Haber-Bosch fertilizer, which is also derived from the N_2 in air (Jenkinson 2001, Galloway et al. 2004).

The calculated trophic discrimination factor was near 3.2‰, which is identical to the value reported by McCutchan et al. (2003) for rainbow trout that were fed an ESS-type commercial feed (3.2 ± 0.20‰ standard error). Inspecting Figure 4.3b at day 140 (before the

isotopic fluctuation in feed) directly yields a similar estimate. The minimum value at 110 d is closer to 3.1‰, which is similar. However, McCutchan et al. (2003) reported a value of 3.8 ± 0.17‰ for brook trout fed an ESS-type feed, suggesting there may be interspecific variation in trophic discrimination.

McCutchan et al. (2003) also demonstrated various effects of food type (protein content, plant/algal content) and methodology (tissue-specific vs. whole body) on the trophic fractionations that were observed. Importantly, interpretations of eye-lens isotope histories from wild-caught specimens should not assume trophic-discrimination comparability with the results from the present study because the specimens in the present study were fed artificial diets.

4.4.4 Conclusions

The results of the present study support the use of fish eye lenses as recorders of isotopic history, except interpretation requires accommodation of an approximately 16 d lag between the diet switch and the observed isotopic transition within the eye lens. We suggest the lag results from the time required to complete all of the following processes: epithelial cell migration to the lens equator, lens-fiber cell elongation, lens fiber-cell apoptosis, and isotopic turnover of the aqueous and vitreous humors, which precedes the previous three processes. Unlike the post-embryonic eye lens, the humors have constant vascular communication with isotopic substrates in the diet, and we suspect that the relatively large mass of the humors and the associated length of time required for their isotopic turnover may contribute substantially to the overall lag. There are other molecular communications with the post-embryonic lens that persist after apoptosis, yet these post-transcriptional molecular communications were not influential enough to disrupt

incorporation of the diet-change signal into the lens, as the size of the isotopic transfer from the diet to the lens closely matched the size of the feed-based isotope shift.

4.5 Tables

Table 4.1 Feeding schedule of captive red drum. Hatching date was 10/8/15.

Dates (MM/DD/YY)	**Feed type**	**Crude Protein (%)**	**Crude Fat (%)**	**$\delta^{15}N$**
10/09/15 - 10/10/15	Rotifers			
10/11/15 - 10/14/15	Rotifers & Otohime A	52	12	10.235
10/15/15 - 10/17/15	Rotifers, *Artemia*, & Otohime A	52	12	10.235
10/18/15 - 10/20/15	*Artemia* & Otohime B1	51	11	8.173
10/21/15 - 10/23/15	*Artemia* & Otohime B1, B2	51	11	8.469
10/24/15 - 10/31/15	Otohime B1, B2	51	11	8.469
11/01/15 - 11/2/15	Otohime C1, S1	51.5	12.5	8.922
11/03/15 - 11/11/15	Otohime S2	52	14	8.74
11/12/15 - 11/22/15	Otohime EP1	48	14	9.589
11/23/15	Otohime EP1, EP2	48	14.3	9.566
11/24/15 - 12/1/15	Otohime EP2	48	14.5	9.543
12/02/15 - 02/28/16	Skretting ESS 3.0	45	16	6.554
02/29/16 - 03/02/16	Skretting ESS 4.5	45	16	6.604
03/03/16 - 03/09/16	Skretting ESS 3.0	45	16	6.554
03/10/16 - 03/18/16	Skretting ESS 4.0	45	16	6.243
03/19/16	Skretting ESS 3.0	45	16	6.554
03/20/16 - 05/05/16	Skretting ESS 4.0	45	16	6.243

Table 4.2 Summary of water quality data during the experiment.

	Dissolved Oxygen	pH	Salinity (ppm)	Temperature (°C)
Mean	7.60	7.96	23.52	24.34
Range	4.32-17.07	7.27-9.51	10.99-39.28	16.9-28.8

Table 4.3 Characteristics of each of the red drum individuals at the end of the experiment.

Specimen	Weight (kg)	Total length (mm)	Eye-lens diameter (mm)	Age (d)
1	0.101	208	4.48	201
2	0.083	192	4	203
3	0.101	214	4.48	204
4	0.103	221	3.6	206
5	0.082	212	5.28	208
6	0.093	214	4.68	210
7	0.212	268	4.46	201
8	0.112	215	5.01	202
9	0.141	236	5.08	203
10	0.045	168	4.36	204
11	0.103	219	4.5	206
12	0.075	202	4.6	208
13	0.098	220	4.78	202
14	0.087	208	4.01	203
15	0.11	229	4.3	204
16	0.106	224	4.84	206
17	0.112	227	4.12	208
18	0.09	215	4.62	210
Means	0.103	216	4.51	205

Table 4.4 Results of Heady and Moore (3013) regression models for individual red drum specimens (tissue turnover equation), including change-point lag, residence time (τ) with standard error (SE), time to 90% tissue turnover (t_{90}), and model fit, as R^2.

Specimen	Time to change point (d)	$\tau \pm$ SE (d)	t_{90}	R^2
1	14	11.94 ± 2.19	27.46	0.96
2	20	12.24 ± 3.44	28.16	0.94
3	12	15.43 ± 4.71	35.49	0.91
4	15	17.16 ± 5.18	39.46	0.93
5	19	8.32 ± 6.19	19.13	0.95
6	17	21.01 ± 8.58	48.31	0.88
7	14	24.99 ± 8.4	57.48	0.91
8	15	18.14 ± 5.78	41.72	0.9
9	8	21.67 ± 4.84	49.84	0.97
10	17	15.36 ± 6.97	35.33	0.88
11	17	15.24 ± 3.99	35.04	0.95
12	9	21.74 ± 6.3	50	0.94
13	14	16.25 ± 4.33	37.37	0.93
14	34	4.19 ± 0.7	9.63	0.99
15	11	24.08 ± 5.54	55.38	0.95
16	20	20.99 ± 8.31	48.27	0.91
17	10	8.74 ± 1.66	20.09	0.98
18	16	23.96 ± 8.56	55.1	0.88
Means	15.67	16.74 ± 5.32	38.51	0.93

4.6 Figures

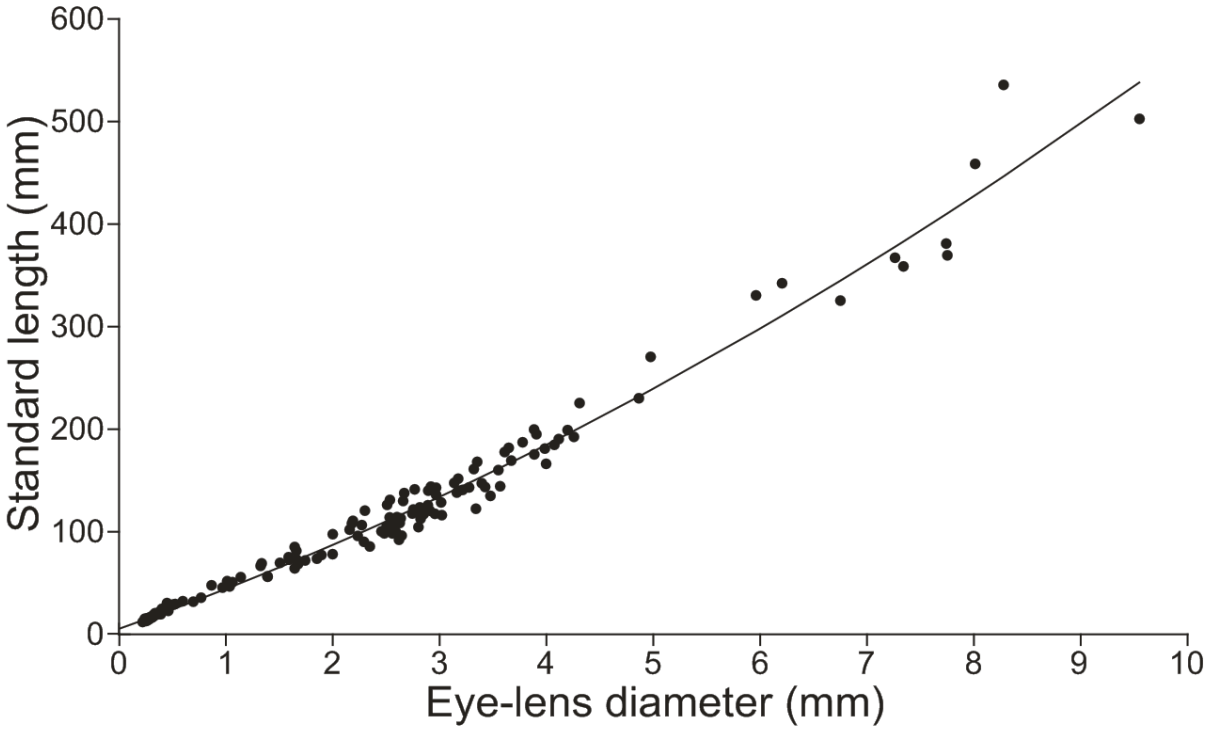

Figure 4.1 Regression describing the change in fish length (SL) with change in eye-lens diameter (d), where $SL = 5.404 + 1.97d^2 + 36.98d$ ($n = 145$, $R^2 = 0.98$, $p<0.0001$). Measurements were obtained from preserved specimens, which were corrected for shrinkage via comparison with recently frozen specimens.

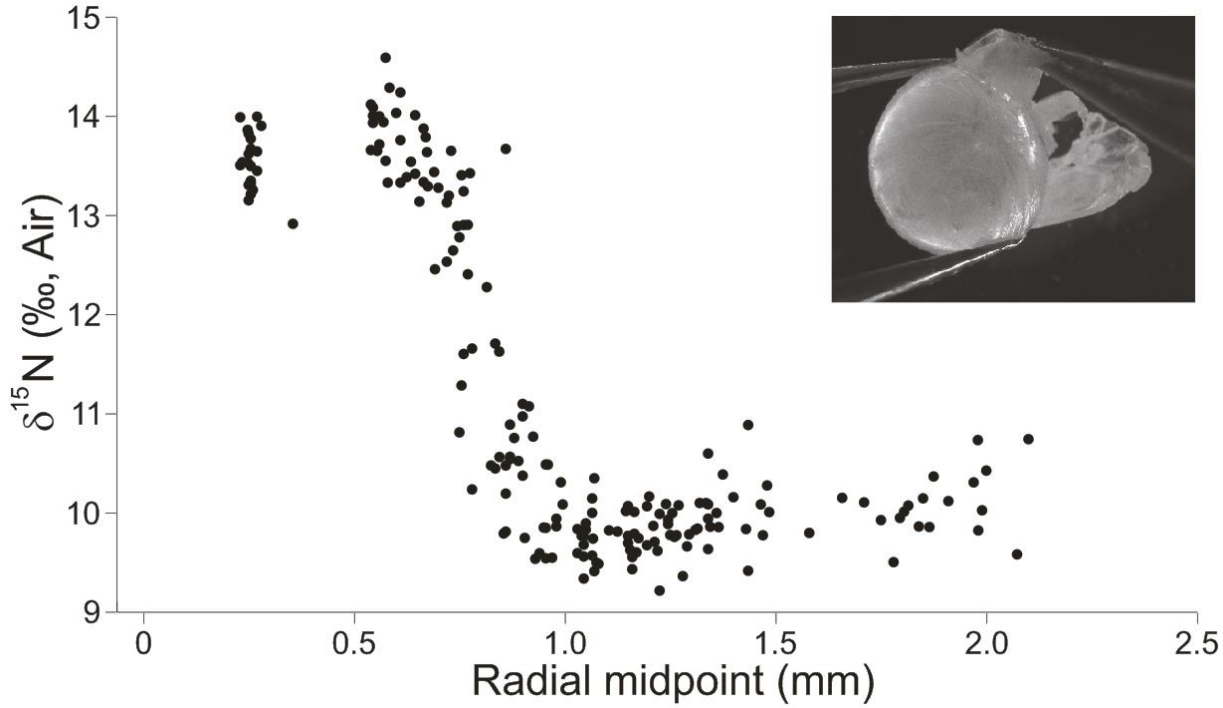

Figure 4.2 Eye-lens $\delta^{15}N$ values from 18 Red Drum raised in captivity from the egg stage to an age of 201-210 d. Each data point represents an average of replicate $\delta^{15}N$ measurements from individual eye-lens laminae. Radial midpoint is lamina position with the lens, as measured using an ocular micrometer, with low values being near the center of the lens and high values being near the outer margin (all lenses had diameters <5.3 mm). The inset photo depicts the delamination process (Amy Wallace photo credit).

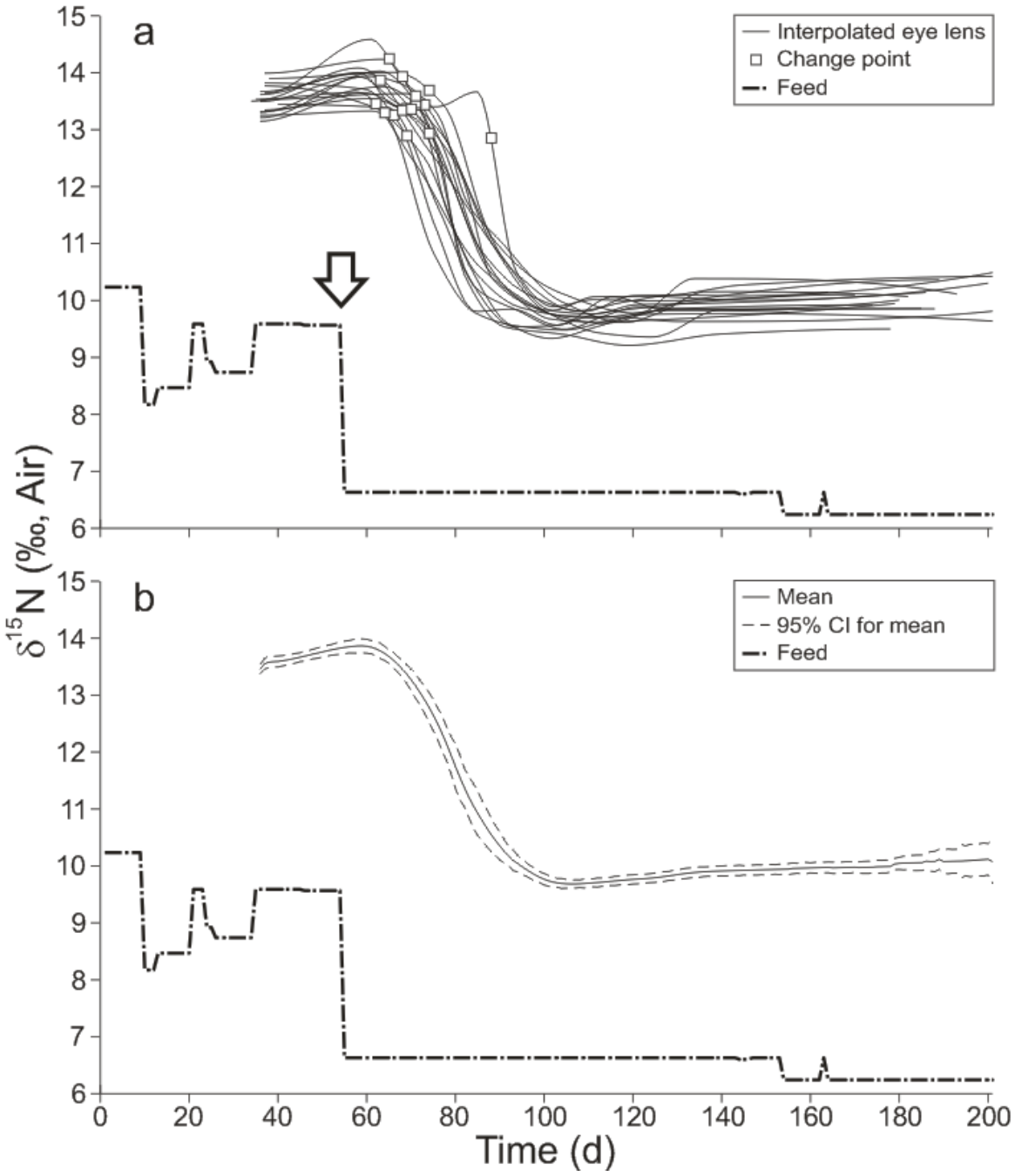

Figure 4.3 Variation in the $\delta^{15}N$ values of fish feed and red drum eye-lens laminae during time in captivity. Cubic splines were used to interpolate between the data in Figure 4.2 for each of the 18 fish in the experiment, with change points identified from the combination of measured data (Figure 4.2) and interpolated data (panel a). Change points ranged from 8 to 34d from the date when feed $\delta^{15}N$ was substantially reduced (arrow; Table 4.3). 95% confidence intervals (CI) for the means of the measured and interpolated data were calculated at daily intervals and are plotted in panel b without further modification (panel b).

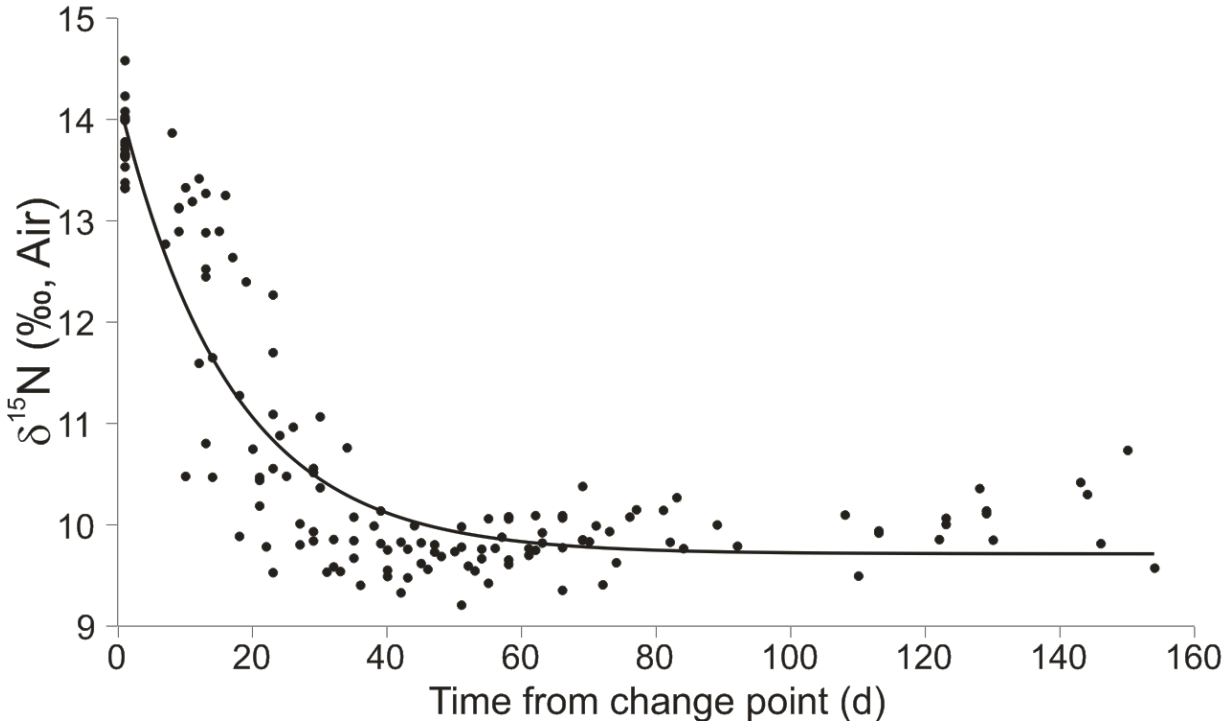

Figure 4.4 Fit of Heady and Moore (2013) single-compartment turnover model Y = b3 - (b3 - b2)(exp[-2(t/b1)]) to measured $\delta^{15}N$, where day 0 was set to the change points in Figure 3a and the regression was applied to data from all individuals combined. Parameter estimates are b1 = 16.57 ± 1.45, b2 = 14.23 ± 0.16, and b3 = 9.71 ± 0.09 (R^2 = 0.84).

Chapter 5: Examination of post-settlement movement patterns of Red Snapper (*Lutjanus campechanus*) in the Gulf of Mexico

Abstract

The purpose of this study was to use both eye lens $\delta^{15}N$ profiles and otolith microchemistry profiles from the same Red Snapper individuals to estimate movement of Red Snapper in the GoM. Numerous conventional and ultrasonic tagging studies have produced conflicting results on movement probability of Red Snapper in the Gulf of Mexico (GoM). Profiles of the Red Snapper eye lens stable isotopes were aligned with trace element profiles from the otoliths by ageing the Red Snapper. I quantified longitudinal gradients in Red Snapper otolith microchemistry from previous studies to compare to trace element profiles from Red Snapper in the current study. The concentrations of Ba, Mg, and Mn in Red Snapper otoliths all exhibited a similar geographic pattern with the lowest metal concentrations measured in Florida. Red Snapper otolith Ba, Mg, and Mn profiles and eye lens $\delta^{15}N$ profiles indicated that at least 8 of the 10 Red Snapper individuals used in this study moved from the northern GoM to the locations that they were captured on the east coast of the GoM. Although both methods indicated that Red Snapper moved from the northern GoM, the timing of this movement varied with the method used. This chapter presented a first step in using two complimentary methods for providing a potentially high-resolution, lifetime history of Red Snapper movement in the GoM.

5.1 Introduction

The recreational and commercial fisheries for Red Snapper, *Lutjanus campechanus*, are some of the more important and controversially managed finfish fisheries in the Gulf of Mexico (GOM). The first stock assessments of Red Snapper in the 1980s noted that Red Snapper were in decline and regulations have been introduced by the National Marine Fisheries Service (NMFS) since 1990 to help the stock recover (Nelson and Manooch III 1982; Goodyear 1988). Although the Red Snapper stock has experienced overfishing since at least the 1980s, the most recent assessment of Red Snapper indicated that overfishing ended, but the stock is still severely overfished (SEDAR 2013). Since management of Red Snapper began in the 1990s, the species has been managed as a unit stock with the management unit extending from the United States-Mexico border in the west through to west of the Dry Tortugas and the Florida Keys (SEDAR 2013). Evidence from genetic (Saillant et al. 2010), tagging (Patterson 2007), and morphometric studies (Fischer et al. 2004), however, suggests that Red Snapper in the GOM exhibit a metapopulation structure. Ignoring spatial population structure of Red Snapper could lead to depletion of localized subpopulations (Kell et al. 2009), thus adherence to "precautionary" management principles may require new management plans for separate Red Snapper stocks.

Early studies of Red Snapper genetic structure suggested that a single stock with considerable gene flow existed in the GOM (Camper et al. 1993; Gold 1994). A planktonic larval stage duration of approximately 4 weeks (Rooker et al. 2004) and protracted spawning season (Fitzhugh et al. 2012) was used to explain the lack of genetic divergence reported among GOM regions. Homogeneity in the distribution of selectively-neutral genetic markers, including both

mitochondrial and nuclear DNA microsatellites (Gold et al. 1997; Pruett et al. 2005; Saillant and Gold 2006), additionally implied a single, panmictic stock; however, these studies also identified different lines of evidence that suggested a metapopulation stock structure model for Red Snapper. For instance, Saillant and Gold (2006) found significant differences in genetic effective population size, or N_e, among southwest, northwest, and north-central regions of the GOM. Additionally, Pruett et al. (2005) discovered evidence for past range expansions and restricted gene flow with isolation by distance in Red Snapper, and suggested that a metapopulation structure would be difficult to detect with selectively neutral genetic markers. More recently, Saillant et al. (2010) observed non-random spatial distributions among young-of-the-year Red Snapper genotypes at small geographic scales, implying that Red Snapper are semi-isolated within regions. Thus, the most recent genetic evidence supports a metapopulation stock structure model for Red Snapper and suggests that self-recruitment of red Snapper occurs within a 50-100 km range. However, Pruett et al. (2005) indicated that more precise estimates of movement among regions are needed to determine if Red Snapper constitute a metapopulation.

Post-settlement movement of Red Snapper may be more important in facilitating gene flow among populations than previously thought (Addis et al. 2013). Red Snapper life history patterns of habitat use are well studied; as Red Snapper age, they generally recruit to habitats with increasing vertical relief (for review see Gallaway et al. 2009) . New settlers (16-19 mm TL) are attracted to low-relief shell habitat or to mud and sand habitat with little or no structure (Szedlmayer and Howe 1997; Szedlmayer and Conti 1999; Rooker et al. 2004; Szedlmayer and Lee 2004). Juvenile Red Snapper (>50 mm TL) are believed to move to more complex, inshore and low-relief habitat due to predation pressure (Workman and Foster 1994; Workman et al. 2002; Szedlmayer and Lee 2004; Piko and Szedlmayer 2007). Sub-adults (~20 cm TL) move to

mid- to high-relief structures, including reefs, shelf-edge banks, rock-outcroppings, and artificial structures such as oil platforms (Moseley 1966; Nieland and Wilson 2003). Finally, adults older than four years are found less often at these high-relief structures and may spend more time over soft bottoms (Render 1995; Gitschlag et al. 2003; Nieland and Wilson 2003; Szedlmayer 2007), perhaps due to lower site fidelity because they are largely invulnerable to predation, or because of high fishing mortality at these structures as they enter the directed fishery at age two.

Although ontogenetic patterns of habitat use are well-understood, the degree of site fidelity exhibited by Red Snapper at each of these habitats is a controversial topic. Numerous conventional and ultrasonic tagging studies have produced conflicting results on movement probability of Red Snapper in the GOM [summarized in Tables 5.1 and 5.2, respectively, reproduced from Patterson (2007) with additional recent studies]. This may be due, in part, to variability in the experimental designs of these studies, including differences in temporal and spatial scales, sample size, tagging and recapture methods, and study location, although most studies have been conducted on artificial reefs from the north-central GOM. For instance, acoustic studies may overestimate site fidelity because of the small spatial scale of these studies (0.02 km^2 to 8 km^2), which may bias estimates of movement by measuring 'stayers' versus 'movers' (Diamond et al. 2007). Conventional tagging studies suffer from low reporting rates of recapture by fishers, tag loss, tag-induced mortality, and the fact that movement can only be estimated as straight-line distances between release and recapture locations. Additionally, both types of studies have temporal scales much shorter than the lifespan of the Red Snapper, which can live as long as 55 years (Baker and Wilson 2001), and thus do not provide a complete picture of Red Snapper lifetime movement. Furthermore, Diamond et al. (2007) observed that time at liberty in a tag and recapture study was a significant factor predicting the movement probability

of Red Snapper. In a review of Red Snapper movement in the GOM, Patterson (2007) also suggested that the scale of Red Snapper movement increased with both the temporal scale and sample size of the tagging study.

Despite these caveats, tagging studies have revealed several factors predicting Red Snapper movement in the GOM. Red Snapper movement rates are positively correlated with age (Patterson et al. 2001b) and capture depth (Diamond et al. 2007). Seasonal patterns in Red Snapper movement have been observed (Topping and Szedlmayer 2011) and may be related to water temperature (Gallaway et al. 1999) or diet changes (McCawley and Cowan 2007). Finally, the degree of reef isolation and reef type (artificial vs. natural) have been shown to affect movement, as Red Snapper are more likely to move from isolated and/or natural reefs (Diamond et al. 2007). In general, most tagging studies suggest a metapopulation structure for Red Snapper in the GOM because most fish move only small distances (<10 km) rather than large distances (>50 km) (Tables 5.1 and 5.2). Yet, overall estimates of fish movement may be conservative because most studies of Red Snapper movement have used small, young fish (for an exception, see Topping and Szedlmayer 2011).

Wallace et al. (2014) documented the potential use of fish eye lenses to reveal the lifetime stable isotope ($\delta^{13}C$ and $\delta^{15}N$) history for an individual. Red Snapper eye lens laminae were observed to exhibit enough isotopic variation to detect broad-scale changes in the isotopic histories of Red Snapper individuals (Wallace et al. 2014). This approach was further validated by conducting an experimental step-change in dietary $\delta^{15}N$ in Red Drum and observing a corresponding change in eye lens laminae $\delta^{15}N$ (Chapter 3). Thus, it should be possible to use isoscape models developed for the GoM by Radabaugh et al. (2013) to examine lifetime

movement of Red Snapper using the isotopic histories generated from the analysis of eye lens laminae.

The objective of the present study was to use both eye lens $\delta^{15}N$ profiles and otolith microchemistry profiles from the same Red Snapper individuals to estimate movement of Red Snapper in the GoM. Longitudinal gradients in otolith microchemistry were documented in Chapter 2 and used in this chapter to estimate Red Snapper movement based on otolith microchemistry profiles. In addition, isoscape models were used to determine Red Snapper movement based on eye lens $\delta^{15}N$ profiles. This enabled me to estimate movement patterns for 10 Red Snapper individuals collected from the GoM and to determine if there were any patterns in otolith microchemistry that corresponded with $\delta^{15}N$ eye lens profiles.

5.2 Methods

5.2.1 Regional Otolith Microchemistry

The otolith element concentration database developed in Chapter 2 was used to select studies of Red Snapper in the GoM. Red Snapper otolith microchemistry from these studies was divided into the following five regions based on the states or countries from which the data were recorded: Mexico, Texas, Louisiana/Texas, Alabama/Mississippi, and Florida. Only elements with two or more data points for each region were selected for analysis.

5.2.2 Field collection (otoliths and eye lenses)

No fish were collected or killed for the purpose of this study. The Red Snapper used in this study were collected as part of a larger study funded by the C-IMAGE I consortium to examine the effects of the *Deepwater Horizon* (DWH) oil spill on fish in the GoM. Collections

were made in August 2014 using demersal longlines placed offshore of Pensacola, Florida (29.89255 N, -87.21297 W), and Tampa Bay, Florida (28.09967 N, -84.39887 W). Both sagittal otoliths were extracted from the Red Snapper and stored in envelopes for later processing. Red Snapper eyes were removed, wrapped in aluminum foil, placed in plastic bags on ice, and frozen at -40°C in the laboratory.

5.2.3 Eye lens analysis

Using the methods of Macko et al. (1997), Ellis (2012), and Wallace et al. (2014), Wallace et al. (2017) isolated the geographic component from lifetime, eye-lens isotopic records, and then classified 10 Red Snapper individuals as having low or high site fidelities. Individuals with high site fidelity appeared to have remained on the central West Florida Shelf throughout their lives, whereas individuals with low site fidelity appeared to have moved into the eastern Gulf of Mexico from the northern and northwest GoM. Wallace et al. (2017) reported an overall decline in $\delta^{15}N$ in 9 of the 10 Red Snapper examined; Red Snapper SL4-40-19 which was collected in Tampa Bay, was the exception. Comparisons with isoscapes suggested most Red Snapper moved from the northern and northwest GoM to the areas in which they were captured, near Panama City and Tampa Bay, Florida. Additionally, several individuals appeared to move between the northern/northwestern GoM and West Florida Shelf more than once.

5.2.4 Otolith analysis

Red Snapper otoliths were prepared for analysis using the preparation procedures described in Granneman et al. (2017). For each sample, a suite of 13 isotopes was measured: 7Li, 24Mg, 51V, 55Mn, 57Fe, 59Co, 63Cu, 64Zn, ^{88}Sr, ^{114}Cd, ^{118}Sn, ^{137}Ba, and ^{208}Pb. ^{43}Ca was measured for use as an internal standard. These isotopes were selected for analysis because they

less likely to have inter-elemental isobaric interferences during analysis and they have been measured in previous studies of Red Snapper otolith microchemistry in the GoM. Otoliths were ablated and mean metal concentrations were calculated following the methods described in Granneman et al. (2017).

Otolith element concentrations were converted from laser ablation path position to Red Snapper SL. The positions of Red Snapper annuli within laser ablation transects were determined using ImageJ software, thus translating laser ablation path position to Red Snapper age. Red Snapper age was converted to total length (TL) using the Von Bertalanffy growth functions for females and males developed by Patterson et al. (2001a):

$$\text{Eq. 3. Females: } TL = 976(1-e^{-0.191(t-0.051)})$$

$$\text{Eq. 4. Males: } TL = 956(1-e^{-0.194(t+0.054)})$$

Total length was converted to SL using the relationship described by Allen (1985):

$$\text{Eq. 5. } SL = 0.793 \times TL$$

Red Snapper standard length was linearly interpolated to match laser-ablation path position, which was recorded every 3.1µm.

5.2.5 Statistical Analyses

All statistical analyses were conducted with the Fathom toolbox for Matlab (Jones 2012). The underlying data distributions of Red Snapper otolith microchemistry from the database developed in Chapter 2 were often not reported and could not be assumed to be normal. Thus, these data were analyzed using non-parametric, permutation-based methods. One-way, permutation-based, ANOVAs were conducted among regions for each element for which there

was enough available data. For each element, concentrations were square-root transformed and a resemblance matrix was generated using Bray-Curtis similarity (Bray and Curtis 1957). If there was a significant difference in otolith element concentration among regions, *a posteriori*, multiple comparison (pair-wise) tests were performed to determine how regions differed. The distributions of element concentrations among regions were compared using boxplots for the elements that were found to be significantly different among regions.

Elements that were found to be significantly different among regions were used in the comparisons between otolith microchemistry and eye lens $\delta^{15}N$. For each Red Snapper individual, permutation-based linear regressions were conducted between SL with metal concentration to determine if there was a significant change over time. If a significant change in occurred over the lifetime of an individual, the direction of the slope was used to determine the potential direction of movement, based on the differences in element concentrations among regions.

5.3 Results

Of the 63 studies used to conduct a meta-analysis of otolith microchemistry in Chapter 2, 7 of these studies were on Red Snapper in the GoM (Table 5.3). The data for these studies were collected from individuals that lived anytime from 1996-2013. The only elements that were significantly different among the 5 regions examined were Ba, Mg, and Mn ($p < 0.05$). However, because Sr is frequently used an element to describe Red Snapper movement, it was included in some of the plots and analyses that follow. The concentrations of Ba, Mg, and Mn in Red Snapper otoliths all exhibited a similar geographic pattern (Fig. 5.1, Table 5.4). The lowest metal concentrations were measured in Florida, although the concentration of Ba was relatively

low in both Mexico and Florida. The concentration of Mg gradually increased moving counter-clockwise around the GoM. Finally, Mn concentrations were relatively higher, but not significantly different, in all regions of the GoM except Florida.

All otolith metals examined in this study, with the exception of Sr, exhibited a similar pattern over the lifetime of each Red Snapper individual (Figures 5.2 and 5.3). The highest metal concentrations observed for every individual were measured during the first year at a SL less than 100mm. This period of initial high metal concentration was followed by a rapid decrease in concentration and a relatively low concentration was maintained for the remainder of the individual's life. The otolith concentrations of Sr exhibited mixed patterns, with some Red Snapper experiencing an increase, decrease, or no apparent change in Sr throughout the lifetime of the individual.

There were significant, negative relationships between the concentrations of Ba, Mg, and Mn with SL for all the individuals measured ($p < 0.001$, Table 5.5), with the exception of individual SL8-40-23. The concentration of Ba appeared to gradually increase over time for Red Snapper SL8-40-23, although the R^2 value for this relationship was relatively low ($R^2 = 0.049$). The R^2 values for these relationships ranged between 0.02 and 0.75. The negative slope of these relationships indicates that movement of these Red Snapper, with the possible exception of SL8-40-23, may have occurred from the northwest GoM to the areas they were captured in the eastern GoM.

5.4 Discussion

Red Snapper otolith Ba, Mg, and Mn profiles and eye lens $\delta^{15}N$ profiles indicated that at least 8 of the 10 Red Snapper individuals used in this study moved from the northern GoM to the

locations that they were captured in the eastern GoM. Of the ten individuals examined using these techniques, two individuals had profiles exhibiting high site fidelity.

Both methods used in this study indicated that Red Snapper moved from the northern GoM; however, the timing of this movement varied with the method used. Otolith element profiles indicated that movement to the West Florida Shelf occurred during the first year, at a SL of less than 100mm. Eye lens $\delta^{15}N$ profiles indicated that Red Snapper movement from the northern GoM was more gradual and occurred over the lifetime of the individual. Additionally, for some individuals the $\delta^{15}N$ profiles appeared to indicate that movement between the northern GoM and WFS may have occurred repeatedly.

In Chapter 2, I provided evidence that physiology frequently is more important in controlling otolith element incorporation than the environment. The consistent pattern of otolith microchemistry observed in the Red Snapper profiles may suggest that a physiological or ontogenetic process is affecting otolith microchemistry. For instance, Red Snapper settlers are frequently observed in low-relief shell habitat, juveniles (>50 mm TL) are known to move to more complex, inshore habitat, and sub-adults (~20 cm TL) move to mid- to high-relief structures, such as oil platforms. This ontogenetic movement pattern, even if it occurs within the same region, may result in changes to Red Snapper otolith microchemistry profiles. Additionally, the variability in eye-lens profiles compared to the relatively consistent trends observed in otolith element profiles for the same individuals further suggests that a physiological process may be affecting otolith microchemistry. Controlled studies of captive Red Snapper would be needed to determine whether there is an innate physiological process that results in a decrease in otolith Mg, Mn, and Ba over time.

The eye lens profile from Red Snapper SL4-40-19 indicated that this individual remained near the capture location for the duration of its life. In addition, this individual exhibited atypical patterns in Mn, Ba, and Mg. Although there was a negative relationship between Mn, Ba, and Mg with SL, the R^2 values defining these relationships were comparatively lower for Mn and Ba than the R^2 values for other individuals. If Red Snapper SL4-40-19 resided near the Tampa Bay capture location for the duration of its life, then Mn and Ba may be indicative of Red Snapper movement and not physiological or ontogenetic processes. Additional sampling of Red Snapper along the WFS may help clarify whether these elements are reliable in determining Red Snapper movement in the GoM.

Red Snapper have been recorded to move in response to episodic events such as storms and hypoxic conditions (Patterson et al. 2001b; Stanley and Wilson 2004). For instance, the occurrence of hurricanes has repeatedly been documented as a significant factor predicting the likelihood and/or magnitude of Red Snapper movement in the GOM (Watterson et al. 1998; Patterson et al. 2001b; Addis et al. 2013). Since the 1970s, researchers have documented a hypoxic water mass that forms every summer from the mouth of the Mississippi River up to 125 km offshore and encompassing an area up to 20,700 km^2 (Rabalais et al. 2002). Stanley and Wilson (2004) documented that, when hypoxia was present, Red Snapper moved higher in the water column into zones of favorable dissolved oxygen levels.

Another episodic event that may influence movement of Red Snapper in the GOM is an oil spill. In 2010, the DWH oil rig exploded, releasing over 200 million gallons of crude oil into the GOM and making it the largest oil spill in US waters (Lehr 2010). Following the DWH oil disaster, Valentine and Benfield (2013) documented a significant decrease in benthic megafauna near the site of the spill, possibly as a result of increased mortality or emigration due to the event.

While movement of Red Snapper in response to an oil spill has not been explicitly examined, avoidance of oil is probably similar to hypoxia avoidance and may be dependent on species-specific physiological tolerances (Wannamaker and Rice 2000) weighed against predation risk (Froeschke and Stunz 2012). All of the Red Snapper used in this study were collected in 2014 and were at least 4 years old when they were collected. Thus, avoidance behavior due to the oil spill cannot be ruled out as a potential reason for the movement patterns recorded in this study.

Otolith microchemistry has previously been used to estimate Red Snapper movement and population connectivity in the GOM. Otolith microchemistry can serve as a natural tag for fish populations or nursery areas because ambient water chemistry is recorded in the structure of otoliths. To use this approach it is first necessary to verify that there are significant differences among regional otolith element signatures that can then be used as natural tags to estimate population connectivity. Several studies have reported significantly different otolith element signatures of age-0 Red Snapper among regions of the GOM (Fig. 5.1) (Patterson et al. 1998; Patterson et al. 2008; Patterson et al. 2010; Sluis et al. 2012; Sluis and Cowan 2013; Patterson et al. 2014). In most of these studies, classification accuracies of at least 70% were reported among regions; however, regional differences were lower in some years because otolith elemental signatures varied significantly among years, indicating that natural tags should be generated annually. Patterson et al. (2010) determined the source of Red Snapper recruits to regions in the GOM by assigning nursery origin to juvenile Red Snapper otolith elemental signatures using the natural regional tags of age-0 Red Snapper. Overall, Patterson et al. (2010) observed more mixing between the eastern and western GOM than has been previously found using conventional tagging studies. For instance, the northwest GOM was found to be a significant source of recruits to the northwest, north-central, and southwest GOM. Additionally, the source

of recruits to the eastern GOM was primarily from local recruitment and secondarily from the north-central GOM. Sluis and Cowan (2013) collected Red Snapper from 4 regions (LA, TX, AL, and FL) and 2 habitats (oil platforms and non-platform habitats) in order to determine both region and habitat of origin. Overall classification success in the Sluis and Cowan (2013) study was observed to be high among regions, but low among habitats, most likely because of Red Snapper movement within regions. They found that Red Snapper from Florida originated primarily from Louisiana and secondarily from Alabama, in contrast to the findings of Patterson et al. (2010). Yet, Sluis and Cowan (2013) did not collect baseline samples of Red Snapper from Florida; thus, their results should be interpreted with caution. Additionally, using maximum likelihood estimates (MLE), Sluis and Cowan (2013) found that Red Snapper from Louisiana and Texas consisted primarily of locally derived recruits. Thus, the current study supports these previous findings by suggesting that Red Snapper collected from Florida originated from the northern GoM.

The differences in otolith element concentrations among GoM regions observed in previous studies and in this study may be due to the influence of the Mississippi River on the GoM. In this study and in the meta-analysis conducted in Chapter 2, there was an increase in element concentrations from Florida to the northern GoM. The substantial flux of metals to the GoM from the Mississippi River (Trefry 1977) could explain the relatively high concentrations of these metals in the northern GoM. In addition, otolith Mn is more abundant in otoliths from fish exposed to hypoxia (Limburg et al. 2015). Thus, the relatively high Mn values recorded in Red Snapper otoliths taken from the northern GoM could be indicative of exposure to the northern Gulf of Mexico hypoxic zone.

Studies that have observed differences in Red Snapper size-at-age and age-frequency among GOM regions (Fischer et al. 2004; Saari 2011) provide additional support for the proposed metapopulation structure of Red Snapper in the GOM. Red Snapper from Texas and Florida have been observed to both grow more rapidly and reach smaller maximum sizes than fish from Alabama and Louisiana (Fischer et al. 2004; Saari 2011). Additionally, the percentage of females with spawning markers (i.e., mature females) was observed to be lower in the eastern GOM compared to the western GOM (Fitzhugh et al. 2012). Kulaw (2012) also found that Red Snapper reached maturity most rapidly in Texas, followed by the north-central GOM and, finally, Florida. Jackson et al. (2007) noted that Red Snapper from Alabama reached maturation more quickly than those sampled off Louisiana, and suggested this may be indicative of a density-dependent compensatory response to overfishing. These regional trends in reproductive biology may correlate with the spatial patterns of demographic variation in Red Snapper age and size. Nevertheless, these regional variations in life history suggest that management of Red Snapper as a unit stock may not be the most cautious approach.

Evidence from genetic, tagging, otolith microchemistry, and morphometric studies suggests that Red Snapper may constitute a metapopulation in the GOM; however, more precise estimates of Red Snapper movement are needed to reveal this metapopulation structure. Tagging studies have revealed that Red Snapper site fidelity may be affected by age, depth, habitat type, season, water temperature, reproductive condition, and large-scale weather and ocean phenomena. Previous studies of Red Snapper have presented short-term, and likely conservative, estimates of movement. The frequency and scale of movement of Red Snapper are indicators of stock structure and have important implications for management and conservation. For instance, Diamond et al. (2007) found that Red Snapper that moved between a tagging site

and a recapture site were in better condition than similarly sized fish that remained, indicating that movement may be beneficial for Red Snapper. Thus, there is a need for higher-resolution, lifetime histories of movement patterns of Red Snapper in the GOM to manage this species effectively.

The present study provides a first step in using two complimentary methods for providing a potentially high-resolution, lifetime history of Red Snapper movement in the GoM. These two approaches provided similar records of Red Snapper movement patterns in the GoM, with both methods indicating that majority of the individuals examined exhibited low site fidelity. The primary pattern of movement indicated from both methods was from the northern GoM to their capture locations on the West Florida Shelf. Future work should focus on increasing the sampling distribution and extent to determine if this movement pattern is widespread for Red Snapper in the GoM.

5.5 Tables

Table 5.1 Reproduced from Patterson 2007 with additional recent studies. Movement and site fidelity estimates from conventional tagging studies of Red Snapper in the northern GOM.

Study	Location and Habitat	Number Tagged	Mean TL at Tagging (mm)	Number Recaptured	Mean/Max Days Free	Mean/Max km moved	Site Fidelity
Beaumariage (1969)	West Florida; natural reefs	1,126	NA	384	113/ 2,049	NA/ 279	90% recaptured within 5 km of release site
Fable (1980)	Texas; natural reefs and oil platforms	299	286	17	112/ 253	0.3/ 5	94% recaptured at release site
Szedlmayer and Shipp (1994)	Alabama; artificial reefs	1,155	287	146	137/ 430	4.6/ 32	74% recaptured within 2 km of release site
Patterson and Cowan (2003)	Alabama; artificial reefs	2,932	335	599	404/ 1,501	30.9 / 558	25-27% per year
Strelcheck et al. (2007)	Alabama; artificial reefs	4,317	335	629	401/ 1,587	2.1/ 202	48-50% per year
Diamond et al. (2007) (TTU Tagging)	Texas; artificial and natural reefs	5,614	363	130	166/ 564	9.8/ 58.3	52.4% recaptured at release site
Addis et al. (2013)	West Florida; artificial reefs	2,114	358	232	313/ 395	37.1/ 1566	19% recaptured at release site

Table 5.2 Reproduced from Patterson 2007 with additional recent studies. Results from ultrasonic tagging studies of Red Snapper in the northern GOM.

Study	Location and Habitat	Area of Detection/ Hydrophone	Hydrophones/ site	Number Tagged	Mean TL at Tagging (mm)	Mean Days Detected in Study Area	Max Days Detected in Study Area	Mean Days Detected in Study Area
Szedlmayer (1997)	Alabama; artificial reefs	3.1 km^2	1; roving	23	349	150	597	150
Szedlmayer and Schroepfer (2005)	Alabama; artificial reefs	$\leq$ 8.0 km^2	3-4; fixed	54	589	212	595	212
Schroepfer and Szedlmayer (2006)	Alabama; artificial reefs	$\leq$ 8.0 km^2	3-4; fixed	77	542	179	597	179
Westmeyer et al. (2007)	Louisiana; petroleum platforms	0.02 km^2	7 within a 35 km^2 area	125	360	64	202	64
Piraino and Szedlmayer (2014)	Alabama; artificial reefs	0.4 km^2	5; fixed	46	460	325	694	325
Topping and Szedlmayer (2011)[a]	Alabama; artificial and natural reefs	0.8 km^2	5; fixed	102	639	411	1099	411
Topping and Szedlmayer (2011)[b]	Alabama; artificial reefs	0.6km2	5; fixed and 1; roving	12	631	448	958	448

Table 5.3 Summary of Red Snapper otolith microchemistry studies used to define regional otolith element concentrations.

Study	Collection Year(s)	Age	Region(s)	Technique	Sample Size	Elements
Granneman et al. 2017	2011-2013	Adult	Alabama/Mississippi and Florida	LA-ICPMS	89	All
Nowling et al. 2011	2002-2003	Adult	Louisiana/Texas and Alabama/Mississippi	SB-ICPMS	98	V, Co, Cu, Zn, Cd, Pb
Patterson et al. 2001	1996-1997	Juvenile	Texus and Alabama/Mississippi	SB-ICPMS	N/A	Mg, Sr, Cd, Ba
Patterson et al. 2008	1997-2000	Juvenile	Texas, Louisisana/Texas and Alabama/Mississippi	SB-ICPMS	750	Mg, Mn, Sr, Ba
Sluis 2011	2007-2009	Adult	Texas, Louisisana/Texas, Alabama/Mississippi, and Florida	SB-ICPMS	4043	Li, V, Mn, Fe, Co, Cu, Zn, Cd, Sn, Ba,
Sluis et al. 2012	2005-2007	Juvenile	All regions	SB-ICPMS and EA-IRMS	432	Li, Mg, Mn, Sr, Ba
Sturgeon et al. 2005	1999	Adult	Louisiana/Texas	SB-ICPMS	N/A	Li, Mg, Mn, Sr, Ba

Table 5.4 Average, otolith element concentrations (mean ± std) among regions in the GoM for Red Snapper.

Region	Mg	Mn	Sr	Ba
Alabama/Mississippi	182.99 ± 28.34	6.63 ± 2.31	2147.51 ± 394.48	5.97 ± 1.46
Florida	98.66 ± 51.24	1.31 ± 0.92	2342.63 ± 233.39	4.22 ± 1.32
Louisiana/Texas	160.05 ± 49.56	4.66 ± 3.06	2310.57 ± 360.47	5.94 ± 1.99
Mexico	197.50 ± 37.75	4.25 ± 2.40	2275.00 ± 95.74	6.75 ± 3.07
Texas	212.28 ± 27.89	5.69 ± 3.38	2242.99 ± 335.11	7.20 ± 2.25

Table 5.5 Results of permutation-based regression analyses of otolith element concentrations and $\delta^{15}N$ over the life of each Red Snapper analyzed in this study.

Element		SL4-40-2	SL4-40-3	SL4-40-6	SL4-40-19	SL4-40-21	SL8-40-3	SL8-40-8	SL8-40-12	SL8-40-19	SL8-40-23
Mg	Intercept	33.433	25.087	20.813	16.107	17.794	33.415	28.820	19.460	34.387	24.235
	Slope	-0.016	-0.011	-0.008	-0.009	-0.008	-0.018	-0.016	-0.010	-0.016	-0.013
	p-value	0.001	0.001	0.001	0.001	0.001	0.001	0.001	0.001	0.001	0.001
	R^2	0.535	0.591	0.640	0.714	0.465	0.752	0.687	0.741	0.616	0.723
	Direction Moved	South	South	South	South	South	South	South	South	South	South
Mn	Intercept	0.736	0.439	0.298	0.038	0.620	1.696	1.354	0.187	1.194	0.284
	Slope	-0.0005	-0.0003	-0.0002	-0.00001	-0.0005	-0.0012	-0.0010	-0.0001	-0.0007	-0.0002
	p-value	0.001	0.001	0.001	0.001	0.001	0.001	0.001	0.001	0.001	0.001
	R^2	0.150	0.145	0.236	0.021	0.118	0.322	0.229	0.258	0.370	0.299
	Direction Moved	South	South	South	South	South	South	South	South	South	South
Ba	Intercept	6.341	26.165	8.753	2.790	7.263	26.040	19.601	7.412	23.717	8.274
	Slope	-0.002	-0.014	-0.004	-0.001	-0.003	-0.014	-0.012	-0.003	-0.008	0.002
	p-value	0.001	0.001	0.001	0.001	0.001	0.001	0.001	0.001	0.001	0.001
	R^2	0.169	0.390	0.546	0.193	0.500	0.411	0.447	0.315	0.302	0.049
	Direction Moved	South	South	South	South	South	South	South	South	South	North

5.6 Figures

Fig 5.1 Boxplots of otolith element concentrations (ppm) among regions in the GoM for Red Snapper.

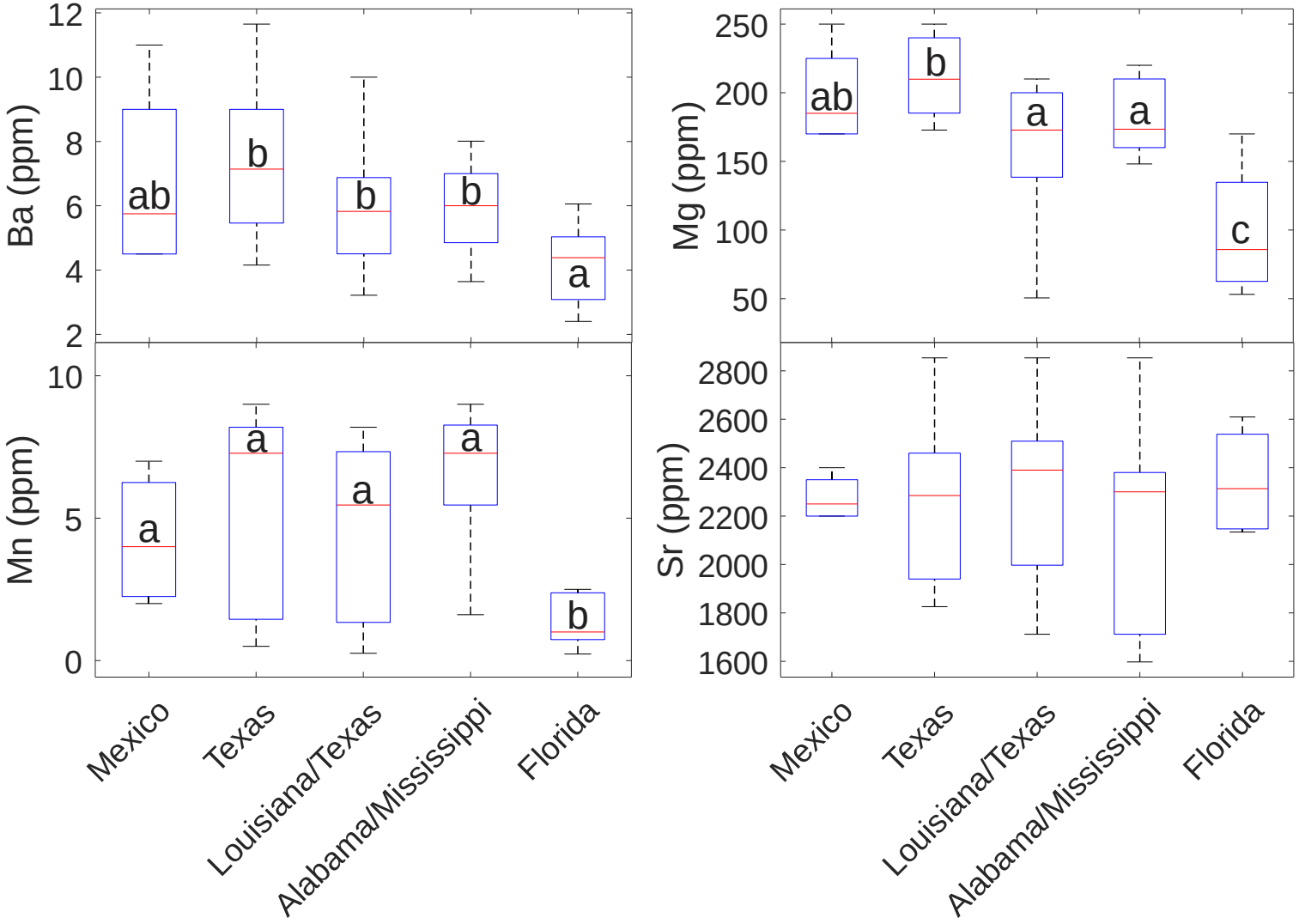

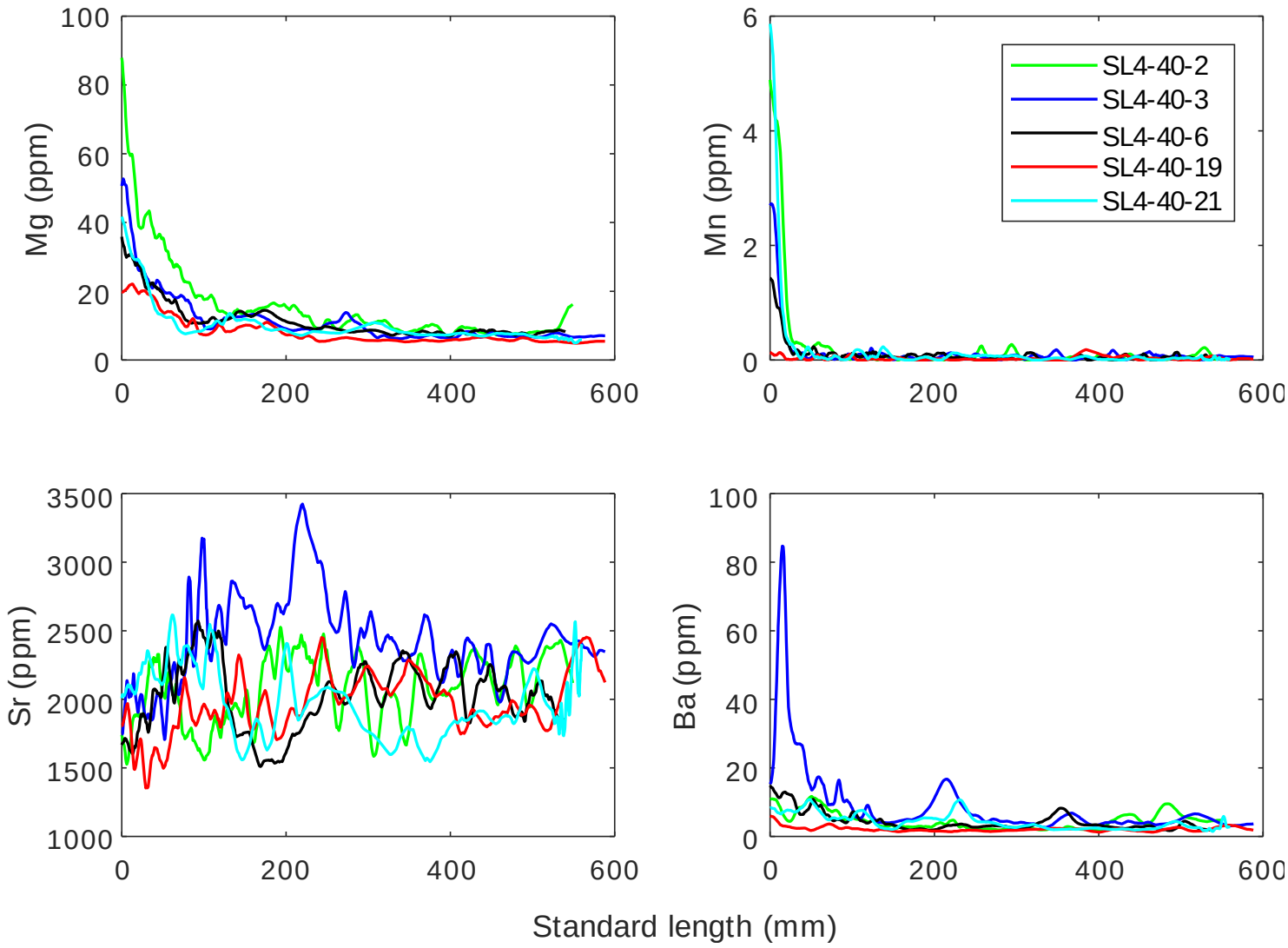

Fig 5.2 Otolith concentrations (ppm) of Mg, Mn, Sr, and Ba with each plotted line representing a different specimen captured in Tampa Bay.

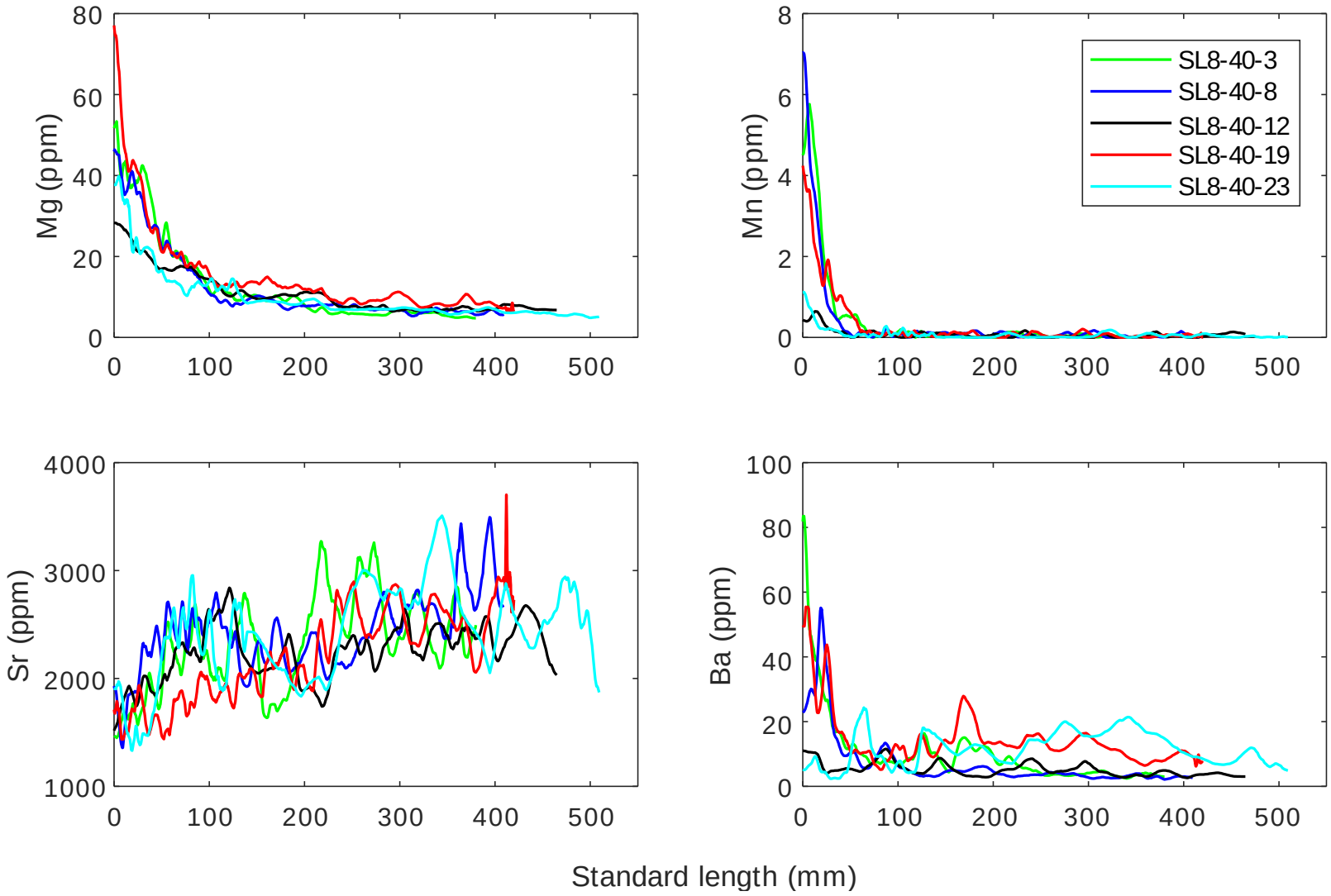

Fig 5.3 Otolith concentrations (ppm) of Mg, Mn, Sr, and Ba with each plotted line representing a different specimen captured at the Alabama/Mississippi border.

Chapter 6. Conclusions

The main objectives of this study were to explore the utility of otolith microchemistry and eye lens stable isotopes as techniques to examine fish movement and exposure to *Deepwater Horizon* (DWH) oil-associated metals. In the first chapter, we examined whether the unique, metal signatures recorded within fish otoliths could potentially serve as oil-exposure biomarkers that would not degrade over time. Several studies documented a substantial overlap of the known extent of surface oil from the DWH oil spill with the distributions of adult and larval fishes, suggesting the potential for oil exposure in many fish species. In Chapter 2, we took advantage of the chronological deposition of metals in otoliths in order to examine the metal-exposure histories and establish baseline conditions for offshore fish species collected after the DWH oil spill occurred. The objectives of this study were to: (1) examine patterns of short- and long-term metal exposure within the otoliths of six offshore fish species in varying states of health, as indicated by the presence of external skin lesions, and (2) determine if there was a change in otolith metal concentrations concurrent with the DWH oil spill. Otoliths collected from 2011 to 2013 in the Gulf of Mexico (GOM) were analyzed for a suite of trace-metals known to be associated with DWH oil. The short-term analysis of trends in otolith metal concentrations revealed no significant differences among the years prior to, during, or after the DWH oil spill for all of the species analyzed. We found that lesioned fish often had elevated levels of otolith ^{60}Ni and ^{64}Zn before, during, and after the DWH oil spill. In addition, metal exposure varied according to species-specific life history patterns. These findings indicate that

lesioned individuals were exposed to a persistent source of trace-metals in the GoM prior to the oil spill.

The results from Chapter 3 suggested that otolith chemistry is not a function of ambient water chemistry alone, but that physiology may play a larger role in regulating otolith element incorporation than has been previously recognized. This fact does not invalidate the use of otolith element fingerprints that can be studied as natural tags of habitat use; however, it does make interpretation of the results more complex. The purpose of Chapter 3 was to quantify otolith multi-consituent environmental, taxonomic, and ecological patterns of all fish species in the Gulf of Mexico (GoM), along the West Atlantic coast, and in the Caribbean Sea. A search of the relevant literature identified 63 studies of otolith microchemistry conducted on 45 species within 23 families within the Gulf of Mexico, Caribbean Sea, and West Atlantic. A total of 415 data points were extracted from these studies, including 36 elements. The following 8 constituents were found to potentially be indicative of ambient water chemistry in both the freshwater and marine environment: $\delta^{18}O$, Li, Mg, Ba, Mn, Sr, Fe, and $\delta^{13}C$. The only constituents that were found to be indicative of ambient water chemistry without being under some degree of physiological control were $\delta^{18}O$ and $\delta^{13}C$. In comparison, 70% of the constituents tested to determine the extent of physiological control on otolith constituent values indicated some degree of biological influence and the most important of these included: Ba, Sr, Cu, Li, Na, Mg, Mn, Fe, and Pb. Multiple tests demonstrated that taxonomic effects explained more of the variation in otolith chemical tags than regional effects. Although physiology apparently is frequently more important in controlling otolith element concentrations than the environment, regional patterns were observed in otolith element concentrations, and region was repeatedly observed to significantly affect otolith multi-constituent patterns.

The focus of Chapter 4 was the validation of a new and complimentary technique for tracking fish movement using fish eye lenses. The fish eye lens is composed of layers of lens fiber cells (LFCs) that form sequentially creating successive, concentric shells (laminae) that are similar to the layers of an onion. After LFCs form, they undergo an attenuated form of apoptosis, preventing new protein synthesis. This sequential cessation of new organic synthesis makes the eye lens a potential lifetime, isotopic recorder. To test the utility of fish eye lenses as recorders of isotopic history, I conducted an experimental step-change in dietary $\delta^{15}N$ and measured the $\delta^{15}N$ in eye lenses from fish exposed to the dietary change. Red Drum raised in captivity were switched from a $\delta^{15}N$-depleted diet to a relatively enriched diet and were sacrificed approximately 150 days after the diet switch. Additionally, juvenile Red Drum specimens (n = 145) spanning a broad range of body lengths were photographed, and standard length (SL) and lens (pupil) diameter were measured to convert measured eye lens diameter to age. Reductions in eye-lens $\delta^{15}N$ values occurred on average, 15.7 d after the $\delta^{15}N$ of the feed was reduced by about 3.0‰, with residence times (τ) averaging 16.7 d after the change point. Mean 90% assimilation (τ_{90}) of the new feed isotopes occurred 38.5 d after the change point. In addition, the $\delta^{15}N$ discrimination factor for eye-lens tissue was 3.15 ± 0.06‰. These results support the use of fish eye lenses as recorders of isotopic history, although this record has a lag of approximately 16 days.

After validating the use of fish eye lenses as isotopic recorders, this technique was applied to Red Snapper collected from the GoM. The objective of Chapter 5 was to use both eye lens $\delta^{15}N$ profiles and otolith microchemistry profiles from the same Red Snapper individuals to estimate movement of Red Snapper in the GoM. Numerous conventional and ultrasonic tagging studies have produced conflicting results on movement probability of Red Snapper in the Gulf of

Mexico (GoM). Profiles of the Red Snapper eye-lens stable isotopes were aligned with trace element profiles from the otoliths by ageing the Red Snapper. Longitudinal gradients in Red Snapper otolith microchemistry from previous studies were compared to trace element profiles from Red Snapper in the current study. The concentrations of Ba, Mg, and Mn in Red Snapper otoliths all exhibited a similar geographic pattern with the lowest metal concentrations measured in Florida. Red Snapper otolith Ba, Mg, and Mn profiles and eye lens $\delta^{15}N$ profiles indicated that at least 8 of the 10 Red Snapper individuals used in this study moved from the northern GoM to the locations that they were captured on the east coast of the GoM. Although both methods indicated that Red Snapper moved from the northern GoM, the timing of this movement varied with the method used. This chapter presented a first step in using two complimentary methods for providing a potentially high-resolution, lifetime history of Red Snapper movement in the GoM.

In conclusion, these chapters provide support for the use of otolith microchemistry and fish eye lens profiles to measure fish movement and provided indirect support for the use of otolith microchemistry to examine exposure to crude oil. The results from Chapter 2 did not suggest a change in oil-associated otolith metal concentrations coinciding with the timing of the DWH oil spill. This suggests that either the technique used is not sensitive enough to detect any transient changes that may have occurred because of exposure to the oil spill or that the fish examined were not exposed to the oil spill. However, lesioned fish in the study may have been exposed to a persistent source of trace-metals in the GoM prior to, during, and after the oil spill and metal-induced immunomodulation may have occurred in these fish. These interactions between the physiological and environmental modulation of otolith element incorporation were explored further in Chapter 3, in which multiple tests demonstrated that physiology explained

more of the variation in otolith chemical tags than ambient water chemistry. These findings suggest that the use of otolith microchemistry alone to track fish movement and potential exposure to harmful metals may be complicated by physiological control of otolith microchemistry. In Chapter 4 the use of fish eye lenses as potential lifetime recorders of isotopic histories was validated. Chapter 5 compared the use of fish eye lens $\delta^{15}N$ profiles to otolith microchemistry profiles to examine fish movement. Both techniques suggested similar patterns of movement in Red Snapper from the northern GoM to the West Florida Shelf. This is the first study to use these complimentary techniques to track fish movement.

References

Addis, D. T., W. F. Patterson, M. A. Dance, and G. W. Ingram. 2013. Implications of reef fish movement from unreported artificial reef sites in the northern Gulf of Mexico. Fisheries Research 147:349-358.

Allen, G. R. 1985. FAO species catalogue. v.6: Snappers of the world. An annotated and illustrated catalogue of Lutjanid species known to date. FAO.

Anderson, M. J. 2001. A new method for non-parametric multivariate analysis of variance. Austral Ecology 26(1):32-46.

Ashford, J., M. La Mesa, B. A. Fach, C. Jones, and I. Everson. 2010. Testing early life connectivity using otolith chemistry and particle-tracking simulations. Canadian Journal of Fisheries and Aquatic Sciences 67(8):1303-1315.

Auerswald, K., M.H.O.M. Wittmer, A. Zazzo, R. Schäufele, and H. Schnyder. 2010. Biases in the analysis of stable isotope discrimination in food webs. Journal of Applied Ecology 47: 936–941.

Baker, M. S., and C. A. Wilson. 2001. Use of bomb radiocarbon to validate otolith section ages of red snapper Lutjanus campechanus from the northern Gulf of Mexico. Limnology and Oceanography 46(7):1819-1824.

Begg, G. A. C., M.; Cameron, D.S.; Boyle, S.; Sellin, M.J. 1998. Stock discrimination of school mackerel, *Scomberomorus queenslandicus*, and spotted mackerel, *Scomberomous munroi*, in coastal waters of eastern Australia by analysis of minor and trace elements in whole otoliths. Fishery Bulletin 96(4):653-666.

Braun, A., A. Vikari, W. Windisch, and K. Auerswald. 2014. Transamination governs nitrogen isotope heterogeneity of amino acids in rats. J. Agric. Food Chem. 62: 8008−8013.

Bray, J. R., and J. T. Curtis. 1957. An Ordination of the Upland Forest Communities of Southern Wisconsin. Ecological Monographs 27(4):326-349.

Brown, J. A. 2006. Classification of juvenile flatfishes to estuarine and coastal habitats based on the elemental composition of otoliths. Estuarine Coastal and Shelf Science 66(3-4):594-611.

Buckel, J. A., B. L. Sharack, and V. S. Zdanowicz. 2004. Effect of diet on otolith composition in Pomatomus saltatrix, an estuarine piscivore. Journal of Fish Biology 64(6):1469-1484.

Campana, S. E. 1999. Chemistry and composition of fish otoliths: pathways, mechanisms and applications. Marine Ecology-Progress Series 188:263-297.

Campana, S. E. 2005. Otolith science entering the 21st century. Marine and Freshwater Research 56(5):485-495.

Campana, S. E., and S. R. Thorrold. 2001. Otoliths, increments, and elements: keys to a comprehensive understanding of fish populations? Canadian Journal of Fisheries and Aquatic Sciences 58(1):30-38.

Camper, J., R. Barber, L. Richardson, and J. Gold. 1993. Mitochondrial DNA variation among red snapper (*Lutjanus campechanus*) from the Gulf of Mexico. Molecular Marine Biology and Biotechnology 2(3):154-161.

Chang, M., and A. Geffen. 2012. Taxonomic and geographic influences on fish otolith microchemistry. Fish and Fisheries.
Chang, M., and A. Geffen. 2013. Taxonomic and geographic influences on fish otolith microchemistry. Fish and Fisheries 14(4):458-492.
Clarke, K. R., and R. N. Gorley. 2006. PRIMER v6: User Manual/Tutorial. PRIMER-E, Plymouth.
Clarke, K. R., P. J. Somerfield, and R. N. Gorley. 2008. Testing of null hypotheses in exploratory community analyses: similarity profiles and biota-environment linkage. Journal of Experimental Marine Biology and Ecology 366(1-2):56-69.
Coffey, M., F. Dehairs, O. Collette, G. Luther, T. Church, and T. Jickells. 1997. The behaviour of dissolved barium in estuaries. Estuarine Coastal and Shelf Science 45(1):113-121.
Dahm, R., H. B. Schonthaler , A. S. Soehn, J. van Marle, and G. F.J.M. Vrensen. 2007. Development and adult morphology of the eye lens in the zebrafish. Experimental Eye Research 85: 74-89.
Danysh, B.P. and M.K. Duncan. 2009. The lens capsule. Experimental Eye Research 88: 151–164.
Degens, E. T., W. G. Deuser, and R. L. Haedrich. 1969. Molecular structure and composition of fish otoliths. Marine Biology 2(2):105-109.
del Rio, C.M. and R. Anderson-Sprecher. 2008. Beyond the reaction progress variable: the meaning and significance of isotopic incorporation data. Oecologia 156: 765-772.
Diamond, S. L., M. D. Campbell, D. Olson, and Y. Wang. 2007. Movers and stayers: Individual variability in site fidelity and movements of red snapper off Texas. Pages 149-170 *in* American Fisheries Society Symposium. American Fisheries Society.
Dorval, E., C. M. Jones, R. Hannigan, and J. van Montfrans. 2005. Can otolith chemistry be used for identifying essential seagrass habitats for juvenile spotted seatrout, *Cynoscion nebulosus*, in Chesapeake Bay? Marine and Freshwater Research 56(5):645-653.
Dorval, E., C. M. Jones, R. Hannigan, and J. van Montfrans. 2007. Relating otolith chemistry to surface water chemistry in a coastal plain estuary. Canadian Journal of Fisheries and Aquatic Sciences 64(3):411-424.
Edmonds, J. S., N. Caputi, and M. Morita. 1991. Stock Discrimination by Trace-Element Analysis of Otoliths of Orange Roughy (*Hoplostethus atlanticus*), a Deep-Water Marine Teleost. Australian Journal of Marine and Freshwater Research 42(4):383-389.
Ellis, G. S. 2012. Compound-specific stable isotopic analysis of protein amino acids: Ecological applications in modern and ancient systems. Dissertation. University of South Florida, Graduate Theses and Dissertations.
Elsdon, T. S., and B. M. Gillanders. 2002. Interactive effects of temperature and salinity on otolith chemistry: challenges for determining environmental histories of fish. Canadian Journal of Fisheries and Aquatic Sciences 59(11):1796-1808.
Elsdon, T. S., and B. M. Gillanders. 2006. Temporal variability in strontium, calcium, barium, and manganese in estuaries: Implications for reconstructing environmental histories of fish from chemicals in calcified structures. Estuarine Coastal and Shelf Science 66(1-2):147-156.
Elsdon, T. S., B. K. Wells, S. E. Campana, B. M. Gillanders, C. M. Jones, K. E. Limburg, D. H. Secor, S. R. Thorrold, and B. D. Walther. 2008. Otolith chemistry to describe movements and life-history parameters of fishes: Hypotheses, assumptions, limitations and inferences. Oceanography and Marine Biology: An Annual Review, Vol 46 46:297-302.

Fischer, A. J., M. S. Baker, and C. A. Wilson. 2004. Red snapper (*Lutjanus campechanus*) demographic structure in the northern Gulf of Mexico based on spatial patterns in growth rates and morphometrics. Fishery Bulletin 102(4):593-603.

Fitzhugh, G. R., E. T. Lang, and H. Lyon. 2012. Expanded Annual Stock Assessment Survey 2011: Red Snapper Reproduction. SEDAR31-DW07, Pensacola, Florida.

Froeschke, J. T., and G. W. Stunz. 2012. Hierarchical and interactive habitat selection in response to abiotic and biotic factors: The effect of hypoxia on habitat selection of juvenile estuarine fishes. Environmental Biology of Fishes 93(1):31-41.

Gallaway, B. J., J. G. Cole, R. Meyer, and P. Roscigno. 1999. Delineation of essential habitat for juvenile red snapper in the northwestern Gulf of Mexico. Transactions of the American Fisheries Society 128(4):713-726.

Gallaway, B. J., S. T. Szedlmayer, and W. J. Gazey. 2009. A Life History Review for Red Snapper in the Gulf of Mexico with an Evaluation of the Importance of Offshore Petroleum Platforms and Other Artificial Reefs. Reviews in Fisheries Science 17(1):48-67.

Galloway, J.N., F.J. Dentener, D.G. Capone, E.W. Boyer, R.W. Howarth, S.P. Seitzinger, G.P. Asner, C.C. Cleveland, P.A. Green, E.A. Holland, D.M. Karl, A.F. Michaels, J.H. Porter, A.R. Townsend, and C.J. Vorosmarty. 2004. Nitrogen cycles: past, present, and future. Biogeochemistry 70: 153-226.

Galvan, D.E., J. Janez, and A.J. Irigoyen. 2016. Estimating tissue-specific discrimination factors and turnover rates of stable isotopes of nitrogen and carbon in the smallnose fanskate *Sympterygia bonapartii* (Rajidae). Journal of Fish Biology 89(2): 1258-1270.

Gitschlag, G. R., M. J. Schirripa, and J. E. Powers. 2003. Impacts of red snapper mortality associated with the explosive removal of oil and gas structures on stock assessments of red snapper in the Gulf of Mexico. Pages 83-94 *in* American Fisheries Society Symposium.

Gold, J. R., L.R. Richardson, C. Furman, and F. Sun. 1994. Mitochondrial DNA Diversity and Population Structure in Marine Fish Species from the Gulf of Mexico. Canadian Journal of Fisheries and Aquatic Sciences 51(1):205-214.

Gold, J. R., F. Sun, and L. R. Richardson. 1997. Population structure of red snapper from the Gulf of Mexico as inferred from analysis of mitochondrial DNA. Transactions of the American Fisheries Society 126(3):386-396.

Goodyear, C. P. 1988. Recent trends in the red snapper fishery of the Gulf of Mexico. Southeast Fisheries Center, Miami Laboratory, Coastal Reources Division, Southeast Fisheries Center.

Greiling, T. M. S., and J. I. Clark. 2012. New Insights into the Mechanism of Lens Development Using Zebra Fish. International Review of Cell and Molecular Biology, Vol 296:1-61.

Hamer, P. A., and G. P. Jenkins. 2007. Comparison of spatial variation in otolith chemistry of two fish species and relationships with water chemistry and otolith growth. Journal of Fish Biology 71(4):1035-1055.

Hartsock, A., C. Lee, V. Arnold, and J.M. Gross. 2014. *In vivo* analysis of hyaloid vasculature morphogenesis in zebrafish: A role for the lens in maturation and maintenance of the hyaloid. Developmental Biology 394: 327–339.

Heady, W.N. and J.W. Moore. 2013. Tissue turnover and stable isotope clocks to quantify resource shifts in anadromous rainbow trout. Oecologia 172: 21-34.

Heidemann, F., L. Marohn, H. H. Hinrichsen, B. Huwer, K. Hussy, A. Klugel, U. Bottcher, and R. Hanel. 2012. Suitability of otolith microchemistry for stock separation of Baltic cod. Marine Ecology Progress Series 465:217-226.

Hoover, R. R., C. M. Jones, and C. E. Grosch. 2012. Estuarine ingress timing as revealed by spectral analysis of otolith life history scans. Canadian Journal of Fisheries and Aquatic Sciences 69(8):1266-1277.

Horwitz, J. 2003. Alpha-crystallin. Experimental Eye Research 76(2):145-153.

Jackson, M. W., J. H. Cowan Jr, D. L. Nieland, W. Patterson, J. Cowan, G. Fitzhugh, and D. Nieland. 2007. Demographic differences in northern Gulf of Mexico red snapper reproductive maturation: implications for the unit stock hypothesis. Pages 197-206 *in* American Fisheries Society Symposium. American Fisheries Society.

Jagger, W.S. 1997. Chromatic and monochromatic optical resolution in the rainbow trout. Vision Research 37: 1249-1254.

Jenkinson, D.S. 2001. The impact of humans on the nitrogen cycle, with focus on temperate arable agriculture. Plant and Soil 228: 3-15.

Jones, D. 2012. Processing LA-ICP-MS otolith microchemistry data using the Fathom Toolbox for Matlab. College of Marine Science, University of South Florida, St. Petersburg, FL.

Kallifatidis, G., J. Boros, E.H.H. Shin, J.W. McAvoy, and F.J. Lovicu. 2011. The fate of dividing cells during lens morphogenesis, differentiation and growth. Experimental Eye Research 92: 502-511.

Kell, L. T., M. Dickey-Collas, N. T. Hintzen, R. D. Nash, G. M. Pilling, and B. A. Roel. 2009. Lumpers or splitters? Evaluating recovery and management plans for metapopulations of herring. ICES Journal of Marine Science:181.

Khorramshahi, O., J.M. Schartau, and R.H.H. Kröger. 2008. A complex system of ligaments and a muscle keep the crystalline lens in place in the eyes of bony fishes (teleosts). Vision Research 48: 1503–1508.

2012. Habitat-and region-specific reproductive biology of female red snapper (Lutjanus campechanus) in the Gulf of Mexico. Louisiana State University

Lehr, B., Bristol S., and A. Possolo. 2010. Oil budget calculator: Deepwater Horizon, Washington, D.C.

Limburg, K. E., B. D. Walther, Z. L. Lu, G. Jackman, J. Mohan, Y. Walther, A. Nissling, P. K. Weber, and A. K. Schmitt. 2015. In search of the dead zone: Use of otoliths for tracking fish exposure to hypoxia. Journal of Marine Systems 141:167-178.

Lynnerup, N., Kjeldsen, H., Heegaard, S., Jacobsen, C. & Heinemeier, J. 2008. Radiocarbon dating of the human eye lens crystallines reveal proteins without carbon turnover throughout life. PLoS One.

Lynnerup, N., Kjeldsen, H., Zweihoff, R., Heegaard, S., Jacobsen, C. & Heinemeier, J. 2010. Ascertaining year of birth/age at death in forensic cases: A review of conventional methods and methods allowing for absolute chronology. Forensic Science International 201:74-78.

Macko, S. A., M. E. Uhle, M. H. Engel, and V. Andrusevich. 1997. Stable nitrogen isotope analysis of amino acid enantiomers by gas chromatography combustion/isotope ratio mass spectrometry. Analytical Chemistry 69(5):926-929.

Martin, G. B., and M. J. Wuenschel. 2006. Effect of temperature and salinity on otolith element incorporation in juvenile gray snapper *Lutjanus griseus*. Marine Ecology Progress Series 324:229-239.

Martinec, C. C., J. M. Miller, N. K. Barron, R. Tao, K. Yu, P. M. Stewart, A. C. Nichols, D. A. Steffy, and S. C. Landers. 2014. Sediment chemistry and meiofauna from the northern Gulf of Mexico continental shelf. International Journal of Oceanography 2014.

Mathias, R.T., J. Kistler, and P. Donaldson. 2007. The lens circulation. Journal of Membrane Biology 216: 1-16.

Mathias, R.T., J.L. Rae, and G.J. Baldo. 1997. Physiological properties of the normal lens. Physiological Reviews 77: 21-50.

McCawley, J. R., and J. H. Cowan. 2007. Seasonal and size specific diet and prey demand of red snapper on Alabama artificial reefs: Implications for management. American Fisheries Society Symposium. American Fisheries Society.

McCutchan, J. H. Jr, Lewis, W. M., Kendall, C. and McGrath, C. C. 2003. Variation in trophic shift for stable isotope ratios of carbon, nitrogen, and sulfur. Oikos 102: 378–390.

Morales-Nin, B., S. C. Swan, J. D. M. Gordon, M. Palmer, A. J. Geffen, T. Shimmield, and T. Sawyer. 2005. Age-related trends in otolith chemistry of Merluccius merluccius from the north-eastern Atlantic Ocean and the western Mediterranean Sea. Marine and Freshwater Research 56(5):599-607.

Moseley, F. N. 1966. Biology of the red snapper, Lutjanus aya Bloch, of the northwestern Gulf of Mexico. Publications of the Institute of Marine Science 11:90-101.

Murphy, M.D. and R.G. Taylor. 1990. Reproduction, growth, and mortality of red drum *Sciaenops ocellatus* in Florida waters. Fishery Bulletin 88: 531-542.

Nelson, R. S., and C. S. Manooch III. 1982. Growth and mortality of red snappers in the west-central Atlantic Ocean and northern Gulf of Mexico. Transactions of the American Fisheries Society 111(4):465-475.

Nieland, D. L., and C. A. Wilson. 2003. Red snapper recruitment to and disappearance from oil and gas platforms in the Northern Gulf of Mexico. Pages 73-82 *in* American Fisheries Society Symposium. American Fisheries Society.

Nielsen, J., R. B. Hedeholm, J. Heinemeier, P.G. Bushnell, J.S. Christiansen, J. Olsen, C.B. Ramsey, R.W. Brill, M. Simon, K.F. Steffensen, and J.F. Steffensen. 2016. Eye lens radiocarbon reveals centuries of longevity in the Greenland shark (*Somniosus microcephalus*). Science 353: 702-704.

Panfili, J., H. Pontual, H. Troadec, and P. J. Wright. 2002. Manual of Fish Sclerochronology. Ifremer-IRD coedition, Brest, France.

Pannella, G. 1971. Fish otoliths - daily growth layers and periodical patterns. Science 173(4002):1124-1131.

Patterson, W. F., J. H. Cowan, C. A. Wilson, and Z. X. Chen. 2008. Temporal and spatial variability in juvenile red snapper otolith elemental signatures in the northern Gulf of Mexico. Transactions of the American Fisheries Society 137(2):521-532.

Patterson, W. F., III. 2007. A Review of Movement in Gulf of Mexico Red Snapper: Implications for Population Structure. Pages 245-261 *in* W. F. Patterson III, J.H. Cowan, Jr., G.R. Fitzhugh, and D.L. Nieland, editor. Red Snapper Ecology and Fisheries in the U.S. Gulf of Mexico. American FIsheries Society, Symposium 60, Bethesda, Maryland.

Patterson, W. F., III, B. K. Barnett, M. Z. Sluis, J. H. Cowan, Jr., and A. M. Shiller. 2014. Interspecific variation in juvenile snapper otolith chemical signatures in the northern Gulf of Mexico. Aquatic Biology 21(1):1-10.

Patterson, W. F., III, J. H. Cowan, B. K. Barnett, and M. Z. Sluis. 2010. Estimation of the source of red snapper recruits to west Florida and south Texas with otolith chemistry: implications for stock structure and management. SEDAR31-RD14. Final Report MARFIN grant no. NA05NMF4331072, Pensacola, Florida.

Patterson, W. F., III, J. H. Cowan, Jr., E. Y. Graham, and W. B. Lyons. 1998. Otolith Microchemical Fingerprints of Age-0 Red Snapper, *Lutjanus campechanus*, from the Northern Gulf of Mexico. Gulf of Mexico Science 16(1):83-91.

Patterson, W. F., III, J. H. Cowan, C. A. Wilson, and R. L. Shipp. 2001a. Age and growth of red snapper, *Lutjanus campechanus*, from an artificial reef area off Alabama in the northern Gulf of Mexico. Fishery Bulletin 99(4):617-627.

Patterson, W. F., III, J. C. Watterson, R. L. Shipp, and J. H. Cowan. 2001b. Movement of tagged red snapper in the northern Gulf of Mexico. Transactions of the American Fisheries Society 130(4):533-545.

Piko, A. A., and S. T. Szedlmayer. 2007. Effects of habitat complexity and predator exclusion on the abundance of juvenile red snapper. Journal of Fish Biology 70(3):758-769.

Popper, A. N., and R. R. Fay. 1973. Sound detection and processing by teleost fishes: a critical review. Brain Behavior and Evolution 41(1):14-38.

Poupin, N., F. Mariotti, J. Huneau, D. Mermier, & H. Fouillet. 2014. Natural isotopic signatures of variations in body nitrogen fluxes: a compartmental model analysis. PLoS Computational Biology 10, 1-17.

Quaeck, K. 2017. Stable isotope analysis of fish eye lenses: reconstruction of ontogenetic trends in spatial and trophic ecology of elasmobranchs and deep-water teleosts. Doctoral dissertation, University of Southampton, Southhampton, UK, 209pp.

Pruett, C., E. Saillant, and J. Gold. 2005. Historical population demography of red snapper (*Lutjanus campechanus*) from the northern Gulf of Mexico based on analysis of sequences of mitochondrial DNA. Marine Biology 147(3):593-602.

Rabalais, N. N., R. E. Turner, and W. J. Wiseman. 2002. Gulf of Mexico hypoxia, aka "The dead zone". Annual Review of Ecology and Systematics 33:235-263.

Radabaugh, K. R., D. J. Hollander, and E. B. Peebles. 2013. Seasonal delta C-13 and delta N-15 isoscapes of fish populations along a continental shelf trophic gradient. Continental Shelf Research 68:112-122.

Radabaugh, K.R. and E.B. Peebles. 2014. Multiple regression models of $\delta^{13}C$ and $\delta^{15}N$ for fish populations in the eastern Gulf of Mexico. Continental Shelf Research 84:158-168.

Radabaugh, K.R., D.J. Hollander and E.B. Peebles. 2013. Seasonal $d^{13}C$ and $d^{15}N$ isoscapes of fish populations along a continental shelf trophic gradient. Continental Shelf Research 68: 112-122.

Reckel, F. and R.R. Melzer. Modifications of the falciform process in the eye of Beloniformes (Teleostei: Atherinomorpha): Evolution of a curtain-like septum in the eye. Journal of Morphology 260: 13–20.

Reis-Santos, P., B. M. Gillanders, S. E. Tanner, R. P. Vasconcelos, T. S. Elsdon, and H. N. Cabral. 2012. Temporal variability in estuarine fish otolith elemental fingerprints: Implications for connectivity assessments. Estuarine Coastal and Shelf Science 112:216-224.

Reis-Santos, P., R. P. Vasconcelos, M. Ruano, C. Latkoczy, D. Gunther, M. J. Costa, and H. Cabral. 2008. Interspecific variations of otolith chemistry in estuarine fish nurseries. Journal of Fish Biology 72(10):2595-2614.

Render, J. H. 1995. The life history (age, growth and reproduction) of red snapper (*Lutjanus campechanus*) and its affinity for oil and gas platforms. Louisiana State University, Baton Rouge.

Rooker, J., A. Landry, B. Geary, and J. Harper. 2004. Assessment of a shell bank and associated substrates as nursery habitat of postsettlement red snapper. Estuarine, Coastal and Shelf Science 59(4):653-661.

Saari, C. R. 2011. Comparison of the age and growth of red snapper (*Lutjanus campechanus*) amongst habitats and regions in the Gulf of Mexico. Louisiana State University.

Saillant, E., S. C. Bradfield, and J. R. Gold. 2010. Genetic variation and spatial autocorrelation among young-of-the-year red snapper (*Lutjanus campechanus*) in the northern Gulf of Mexico. ICES Journal of Marine Science 67(6):1240-1250.

Saillant, E., and J. R. Gold. 2006. Population structure and variance effective size of red snapper (Lutjanus campechanus) in the northern Gulf of Mexico. Fishery Bulletin 104(1):136-148.

SEDAR. 2013. SEDAR 31 - Gulf of Mexico Red Snapper Stock Assessment Report, North Charleston, SC.

Shi, Y., Barton, K., De Maria, A., Petrash, J.M., Shiels, A. & Bassnett, S. 2009. The stratified syncytium of the vertebrate lens. Journal of Cell Science 122, 1607-1615.

Sluis, M., and J. H. Cowan. 2013. Platform recruited reef fish, phase II: Do platforms provide habitat that increases the survival of reef fishes? Department of Interior, editor, New Orleans, LA.

Sluis, M. Z., B. K. Barnett, W. F. Patterson, J. H. Cowan, and A. M. Shiller. 2012. Discrimination of Juvenile Red Snapper Otolith Chemical Signatures from Gulf of Mexico Nursery Regions. Marine and Coastal Fisheries 4(1):587-598.

Stanley, D. R., and C. A. Wilson. 2004. Effect of hypoxia on the distribution of fishes associated with a petroleum platform off coastal Louisiana. North American Journal of Fisheries Management 24(2):662-671.

Stewart, D.N., J. Lango, K.P. Nambiar, M.J.S. Falso, P.G. FitzGerald, D.M. Rocke, B.D. Hammock and B.A. Buchholz. 2013. Carbon turnover in the water-soluble protein of the adult human lens. Molecular Vision 19: 463-475.

Sturrock, A. M., C. N. Trueman, J. A. Milton, C. P. Waring, M. J. Cooper, and E. Hunter. 2014. Physiological influences can outweigh environmental signals in otolith microchemistry research. Marine Ecology Progress Series 500:245-264.

Swearer, S. E., G. E. Forrester, M. A. Steele, A. J. Brooks, and D. W. Lea. 2003. Spatio-temporal and interspecific variation in otolith trace-elemental fingerprints in a temperate estuarine fish assemblage. Estuarine Coastal and Shelf Science 56(5-6):1111-1123.

Syedang, H., C. Andre, P. Jonsson, M. Elfman, and K. E. Limburg. 2010. Migratory behaviour and otolith chemistry suggest fine-scale sub-population structure within a genetically homogenous Atlantic Cod population. Environmental Biology of Fishes 89(3-4):383-397.

Szedlmayer, S. 2007. An evaluation of the benefits of artificial habitats for red snapper, *Lutjanus campechanus*, in the northeast Gulf of Mexico. Pages 223-230 *in* Proceedings of the Gulf and Caribbean Fisheries Institute.

Szedlmayer, S., and J. Conti. 1999. Nursery habitats, growth rates, and seasonality of age-0 red snapper, Lutjanus campechanus, in the northeast Gulf of Mexico. Fishery Bulletin 97(3):626-635.

Szedlmayer, S., and J. Lee. 2004. Diet shifts of juvenile red snapper (*Lutjanus compechanus*) with changes in habitat and fish size. Fishery Bulletin 102(2):366-375.
Szedlmayer, S. T., and J. C. Howe. 1997. Substrate preference in age-0 red snapper, *Lutjanus campechanus*. Environmental Biology of Fishes 50(2):203-207.
Taft, W. H., and J. W. Harbaugh. 1964. Modern Carbonate Sediments of Southern Florida, Bahamas, and EspÃritu Santo Island, Baja California: A Comparison of Their Mineralogy and Chemistry, volume 8. Stanford University Press.
Thorrold, S. R., G. P. Jones, S. Planes, and J. A. Hare. 2006. Transgenerational marking of embryonic otoliths in marine fishes using barium stable isotopes. Canadian Journal of Fisheries and Aquatic Sciences 63(6):1193-1197.
Topping, D. T., and S. T. Szedlmayer. 2011. Site fidelity, residence time and movements of red snapper *Lutjanus campechanus* estimated with long-term acoustic monitoring. Marine Ecology Progress Series 437:183-200.
Trefry, J., III. 1977. The transport of heavy metals by the Mississippi River and their fate in the Gulf of Mexico. Texas A&M University.
Tzadik, O. E., J. S. Curtis, J. E. Granneman, B. N. Kurth, T. J. Pusack, A. A. Wallace, D. J. Hollander, E. B. Peebles, and C. D. Stallings. 2017. Chemical archives in fishes beyond otoliths: A review on the use of other body parts as chronological recorders of microchemical constituents for expanding interpretations of environmental, ecological, and life-history changes. Limnology and Oceanography-Methods 15(3):238-263.
Unkovich, M. 2013. Isotope discrimination provides new insight into biological nitrogen fixation. New Phytologist 198: 643-646. DOI: 10.1111/nph.12227
Valentine, M. M., and M. C. Benfield. 2013. Characterization of epibenthic and demersal megafauna at Mississippi Canyon 252 shortly after the Deepwater Horizon Oil Spill. Marine Pollution Bulletin 77(1-2):196-209.
Wallace, A. A., G. S. Ellis, D. J. Hollander, and E. B. Peebles. 2017. Lifetime changes in trophic level, as determined from compound-specific amino acid analysis of $\delta^{13}C$ and $\delta^{15}N$ within isolated eye-lens layers 147th Annual Meeting of the American Fisheries Society, Tampa, FL.
Wallace, A. A., D. J. Hollander, and E. B. Peebles. 2014. Stable Isotopes in Fish Eye Lenses as Potential Recorders of Trophic and Geographic History. Plos One 9(10).
Walls, G.L. 1942. *The vertebrate eye and its adaptive radiation.* New York: Hafner.
Walther, B. D., and K. E. Limburg. 2012. The use of otolith chemistry to characterize diadromous migrations. Journal of Fish Biology 81(2):796-825.
Wannamaker, C. M., and J. A. Rice. 2000. Effects of hypoxia on movements and behavior of selected estuarine organisms from the southeastern United States. Journal of Experimental Marine Biology and Ecology 249(2):145-163.
Watterson, J. C., W. F. Patterson, III, R. L. Shipp, and J. H. Cowan, Jr. 1998. Movement of red snapper, Lutjanus campechanus, in the North Central Gulf of Mexico: potential effects of hurricanes. Gulf of Mexico Science 16(1):92-104.
Workman, I., A. Shah, D. Foster, and B. Hataway. 2002. Habitat preferences and site fidelity of juvenile red snapper (*Lutjanus campechanus*). ICES Journal of Marine Science 59:S43-S50.
Workman, I. K., and D. G. Foster. 1994. Occurrence and behavior of juvenile red snapper, Lutjanus campechanus, on commercial shrimp fishing grounds in the northeastern Gulf of Mexico. Marine Fisheries Review 56(2):9-11.

Wride, M. A. 2011. Lens fibre cell differentiation and organelle loss: many paths lead to clarity. Philosophical Transactions of the Royal Society B-Biological Sciences 366(1568):1219-1233.

Zampighi, G. A., S. Eskandari, and M. Kreman. 2000. Epithelial organization of the mammalian lens. Experimental Eye Research 71(4):415-435.

Zazzo, A., A.P. Moloney, F.J. Monahan, C.M. Scrimgeour, and O. Schmidt. 2008. Effect of age and food intake on dietary carbon turnover recorded in sheep wool. Rapid Commun. Mass Spectrom. 22: 2937–2945.

Addis, D. T., W. F. Patterson, M. A. Dance, and G. W. Ingram. 2013. Implications of reef fish movement from unreported artificial reef sites in the northern Gulf of Mexico. Fisheries Research 147:349-358.

Appendix A:

Author contributions and copyright permissions

Associations between metal exposure and lesion formation in offshore Gulf of Mexico fishes collected after the Deepwater Horizon oil spill

J.E. Granneman conceived the research design, led the data collection and analysis, and wrote the manuscript.
E.B. Peebles secured funding, assisted with the research design, and edited the manuscript.
D. Jones assisted with data collection and analysis and edited the manuscript.

From: Norman, Dan (ELS-EXE) [mailto:d.norman@elsevier.com]
Sent: Monday, 9 July 2018 10:07 PM
To: Victor Quintino <victor.quintino@ua.pt>; Pat Hutchings <Pat.Hutchings@austmus.gov.au>; Francois Galgani <Francois.Galgani@ifremer.fr>
Cc: Sylvester, Harriet (ELS-EXE) <h.sylvester@elsevier.com>
Subject: RE: Enquiry: reprint permission

Dear all,

Thank you for your comments, you are correct that this reuse is permitted and will cause no violation.

Kind regards,

Dan Norman (on behalf of Harriet Sylvester)

From: jgranneman@mail.usf.edu <jgranneman@mail.usf.edu>
Sent: Saturday, 7 July 2018 11:35 AM
To: Pat Hutchings
Subject: Enquiry: reprint permission

Dr. Hutchings,
I am the first author of the following article published in Marine Pollution Bulletin: Associations between metal exposure and lesion formation in offshore Gulf of Mexico fishes collected after the Deepwater Horizon oil spill. Can you please give me permission to reprint this article as a chapter of dissertation research to fulfill the requirements of my PhD program?
Thanks,
Jen

Appendix B Published chapter

Marine Pollution Bulletin 117 (2017) 462–477

Contents lists available at ScienceDirect

Marine Pollution Bulletin

journal homepage: www.elsevier.com/locate/marpolbul

Associations between metal exposure and lesion formation in offshore Gulf of Mexico fishes collected after the Deepwater Horizon oil spill

Jennifer E. Granneman *, David L. Jones, Ernst B. Peebles

College of Marine Science, University of South Florida, 140 7th Ave. South, St. Petersburg, FL 33701, USA

ARTICLE INFO

Article history:
Received 13 July 2016
Received in revised form 24 January 2017
Accepted 26 January 2017
Available online 14 February 2017

Keywords:
Metal
Otolith
Microchemistry
Red Snapper
Red Grouper
Tilefish

ABSTRACT

The objectives of this study were to: (1) examine patterns of short- and long-term metal exposure within the otoliths of six offshore fish species in varying states of health, as indicated by the presence of external skin lesions, and (2) determine if there was a change in otolith metal concentrations concurrent with the Deepwater Horizon (DWH) oil spill. Otoliths collected from 2011 to 2013 in the Gulf of Mexico (GOM) were analyzed for a suite of trace metals known to be associated with DWH oil. We found that lesioned fish often had elevated levels of otolith ^{60}Ni and ^{64}Zn before, during, and after the DWH oil spill. In addition, metal exposure varied according to species-specific life history patterns. These findings indicate that lesioned individuals were exposed to a persistent source of trace-metals in the GoM prior to the oil spill.

1. Introduction

After the *Deepwater Horizon* drilling platform exploded on April 20, 2010, approximately 4.9 million barrels of crude oil were released into the Gulf of Mexico (GoM) at a depth of 1500 m before the Macondo well could be capped (Camilli et al., 2010). The *Deepwater Horizon* (DWH) oil spill was not only the largest oil spill in US history, it was also the first to release oil at the deep seafloor and to involve extensive use of chemical dispersants at depth (Lubchenco et al., 2012). Due to the depth of the Macondo wellhead and its distance offshore, subsurface and benthic oil from the DWH oil spill may have directly impacted marine fishes over an unprecedented depth range (0–1500 m) and spatial distribution (3200 km^2) (Valentine et al., 2014). Several studies have documented substantial overlap of the known extent of surface oil with the distributions of adult and larval fishes, suggesting the potential for oil exposure in many fish species (Chakrabarty et al., 2012; Muhling et al., 2012; Rooker et al., 2013). Physiological biomarkers of sub-lethal oil exposure have been detected in several fish species since the spill occurred; the prevalence of external skin lesions on fish and concentrations of biliary polycyclic aromatic hydrocarbons (PAHs) were higher in the vicinity of the spill site compared to the West Florida Shelf, and have decreased since the oil spill occurred, suggesting exposure to PAH pollution from an episodic event (Murawski et al., 2014). Alterations of genome expression in liver and gill tissue have been observed in resident fish from Louisiana marshes that were likely exposed to weathered crude oil from the spill (Dubansky et al., 2013). Yet, establishing a causal link between the spill and any of the sub-lethal effects of oil exposure (e.g., disease prevalence) measured in fishes is problematic due to a lack of baseline data and the rapid deterioration of oil-exposure biomarkers as a result of the efficient metabolization of PAHs by the fishes themselves (Varanasi et al., 1989).

The unique, metal signatures recorded within fish otoliths could potentially serve as oil-exposure biomarkers that would not degrade over time. Fish otoliths are metabolically inert stones (primarily consisting of aragonitic $CaCO_3$) located within teleost ears that incorporate trace elements from the surrounding water and diet (Campana et al., 1995). Previous studies have demonstrated that trace metals, particularly Ni and V, can be highly enriched in crude oil and are characteristic of the geographic origin of the oil (Fingas, 2011). In a review of oil-spill literature, Gohlke et al. (2011) concluded that trace metals in oil can accumulate in marine organisms at levels above the baseline. For instance, concentrations of Ni and V in mollusks have been used as tracers of exposure to past oil spills (Amiard et al., 2004). Thus, the detection of crude-oil-associated metals in fish otoliths could indicate exposure to spilled oil. A laboratory-based study by Morales-Nin et al. (2007) demonstrated that some of the trace metals in fuel oil (e.g., Na, Mg, Sr, Cr, Ni, and Cu) were incorporated through the diet into the otoliths of juvenile Turbot (*Scophthalmus maximus*).

The metal content of the DWH crude oil, as identified by Liu et al. (2012), includes Mg, Al, V, Cr, Fe, Ni, Co, Cu, Zn, and Pb. Additionally,

* Corresponding author.
E-mail address: jgranneman@mail.usf.edu (J.E. Granneman).

http://dx.doi.org/10.1016/j.marpolbul.2017.01.066
0025-326X/

the 1.84 million gallons of chemical dispersants (Corexit 9500A) applied by BP to dissipate the oil also contain trace amounts of As, Cr, and Cu (USEPA, 1995). Steffy et al. (2013) identified a significant increase from 2009 to 2010 in the concentrations of Ni, Cr, and Pb in northern GoM (NGoM) sediments, suggesting the spilled oil and dispersants contributed a new source of trace metals to the GoM. Elevated concentrations of Co identified within a subsurface intrusion of natural oil and gas (1000–1400 m depth) (Joye et al., 2011) were also attributed to the DWH oil (Joung and Shiller, 2013).

Studies of coastal marine organisms in the GoM have thus far not suggested a significant change in trace-metal tissue concentrations due to the DWH oil spill (Carmichael et al., 2012; Apeti et al., 2013). In coastal saltmarshes of the northern GoM, researchers collected Gulf Killifish (*Fundulus grandis*) after the oil spill at oiled and non-oiled reference sites to determine if oil exposure could be detected in Gulf Killifish otoliths (Nelson et al., 2014). The authors found no consistent differences in the metal signatures of otoliths from fish collected at oiled versus non-oiled sites. However, this result may be misleading because most of the fish analyzed by Nelson et al. (2014) were spawned after the DWH oil spill occurred. Additionally, these authors did not use Gulf Killifish otoliths to establish baseline conditions prior to exposure, but instead relied on comparisons between presumptive oiled versus non-oiled sites.

In the present study, we took advantage of the chronological deposition of metals in otoliths in order to examine the metal-exposure histories and establish baseline conditions for offshore fish species collected after the DWH oil spill occurred. Otoliths grow continually by the concentric deposition of calcium carbonate layers, resulting in identifiable daily and annual increments (Pannella, 1971) that can be used to determine fish age and growth rates (Campana and Neilson, 1985). Additionally, otoliths are useful because no resorption or alteration of an otolith occurs under stressful conditions (Campana and Neilson, 1985), although stress has been observed to affect the incorporation of some metals into fish otoliths (Kalish, 1992). Thus, the dual function of an otolith as a recorder of both fish age and trace elements provides a history of the annual element exposure through the environment and the diet of an individual fish throughout its lifetime.

In the aftermath of the DWH oil spill, federal and state agencies conducted post-spill sampling of nearshore fish more frequently than deepwater fish (Fitzgerald and Gohlke, 2014), despite the substantial overlap of oil with the distributions of offshore fish species (Chakrabarty et al., 2012). The only studies of metal exposure in marine organisms from the offshore environment of the GoM alternately suggested an increase in metal exposure (Lu et al., 2012; Wise et al., 2014) or no change (Fitzgerald and Gohlke, 2014) due to the DWH oil spill. In either case, these studies were confounded by an important lack of baseline data. The ability to establish baseline metal concentration in fish immediately prior to the DWH oil spill is invaluable, considering the only comprehensive dataset for comparison in the GoM is from fish tissue collected in 1978 (Hall et al., 1978).

The objectives of the present study were to (1) examine patterns of short- and long-term metal exposure within the otoliths of several offshore fish species in varying states of health, as indicated by the presence of external skin lesions, and (2) determine if there was a change in otolith metal concentrations concurrent with the DWH oil spill. These objectives were addressed by analyzing the lifetime otolith chemistries of six offshore fish species collected in the GoM following the DWH oil spill. This approach is unique because it allowed us to establish baseline conditions immediately preceding the DWH oil spill for individuals that were collected after the spill. Unlike previous approaches, which relied on collection of individuals prior to the oil spill in order to establish baseline conditions, this novel approach does not require any a priori information on fish location during the time period of the oil spill or the extent of the oil spill, and can be applied to a wide array of species.

2. Methods

2.1. Study site and specimen collection

Longline surveys were conducted during the summer months (June–August) of the three years that followed the DWH oil spill (2011 − 2013). Fish were collected at stations along transects in the region of the DWH oil spill and off the West Florida Shelf (Fig. 1). Each station was fished for 2 h using baited demersal long lines in an 8 km string at a depth of approximately 10–150 m. For additional details on field collection methods refer to Snyder et al. (2015). Total length, weight, and sex were recorded for the target fish species. Both sagittal otoliths were extracted from a subsample of the target species at the time of capture and stored for later processing.

Otoliths from the following species collected in the field were selected for analysis using a stratified-random design across transects: Red Grouper, *Epinephelus morio*; Red Porgy, *Pagrus pagrus*; Red Snapper, *Lutjanus campechanus*; Southern Hake, *Urophycis floridana*; Tilefish, *Lopholatilus chamaeleonticeps*; and Yellowedge Grouper, *Hyporthodus flavolimbatus*. These species were selected for analysis because there is the potential for overlap of the oil spill with the known distributions of these fishes (Chakrabarty et al., 2012). Additionally, these species exhibit a variety of life history patterns (Table S1) that could provide insight into different pathways of exposure to DWH oil.

2.2. Sample preparation

Most otolith preparation procedures took place in a Class 100 laminar flow bench to avoid contamination of otoliths with trace metals. To clean residual tissue off of otoliths, they were scrubbed using a soft-bristled brush, immersed in 36% ultrapure hydrogen peroxide for 3 min, rinsed three times in ultrapure water, and allowed to dry in clean vials for 24 h. Otoliths were embedded in Epoxies Etc. 20-3068 epoxy adhesive and mounted on trace-metal-clean petrographic slides using Crystal Bond™ 509 adhesive. Thin transverse sections (1 mm) were cut through the primordium region with a Buehler IsoMet® low speed saw. Otolith sections were polished until the core was reached using a sequence of 68, 13, and 3 μm grit waterproof silicon carbide papers wetted with ultrapure water. Polished sections were mounted on clean petrographic slides using Crystal Bond™ 509 adhesive, rinsed with ultrapure water, sonicated for 5 min, and air-dried for 24 h.

2.3. Data collection and processing

Otoliths were ablated in a sealed chamber using a PhotonMachines Analyte.193 excimer UV laser ablation (LA) system. An Agilent 7500CX Quadrupole Inductively Coupled Plasma-Mass Spectrometer (ICP-MS) was used to assay the ablated otolith material. For each sample, a suite of 9 isotopes was measured: ^{24}Mg, ^{51}V, ^{53}Cr, ^{57}Fe, ^{59}Co, ^{60}Ni, ^{63}Cu, ^{64}Zn, and ^{208}Pb. ^{43}Ca was also measured for use as an internal standard. These isotopes were selected for analysis because they are less likely to have inter-element isobaric interferences during analysis and they have been measured in the Macondo crude oil from the DWH oil spill (Liu et al., 2012).

The LA-ICP-MS instrumentation was tuned prior to data collection while ablating a National Institute of Standards (NIST) 612 glass wafer to maximize analytical sensitivity and minimize interferences. Background element counts were quantified prior to otolith ablation by collecting a gas blank for 60 s. A NIST 612 glass wafer was ablated two times for 60 s before and after each sample transect run to use as an external calibration reference material. Ablation of otoliths occurred as a line scan along a transect with a width of 64.1 μm extending from the primordium to the edge of the otolith along the sulcal groove. The pulse frequency of the laser was set at 10 Hz, while the laser travel speed was set to 10 μm/s. In most cases, 1–2 pre-ablation transects preceded the sampling transect to remove potential contaminants,

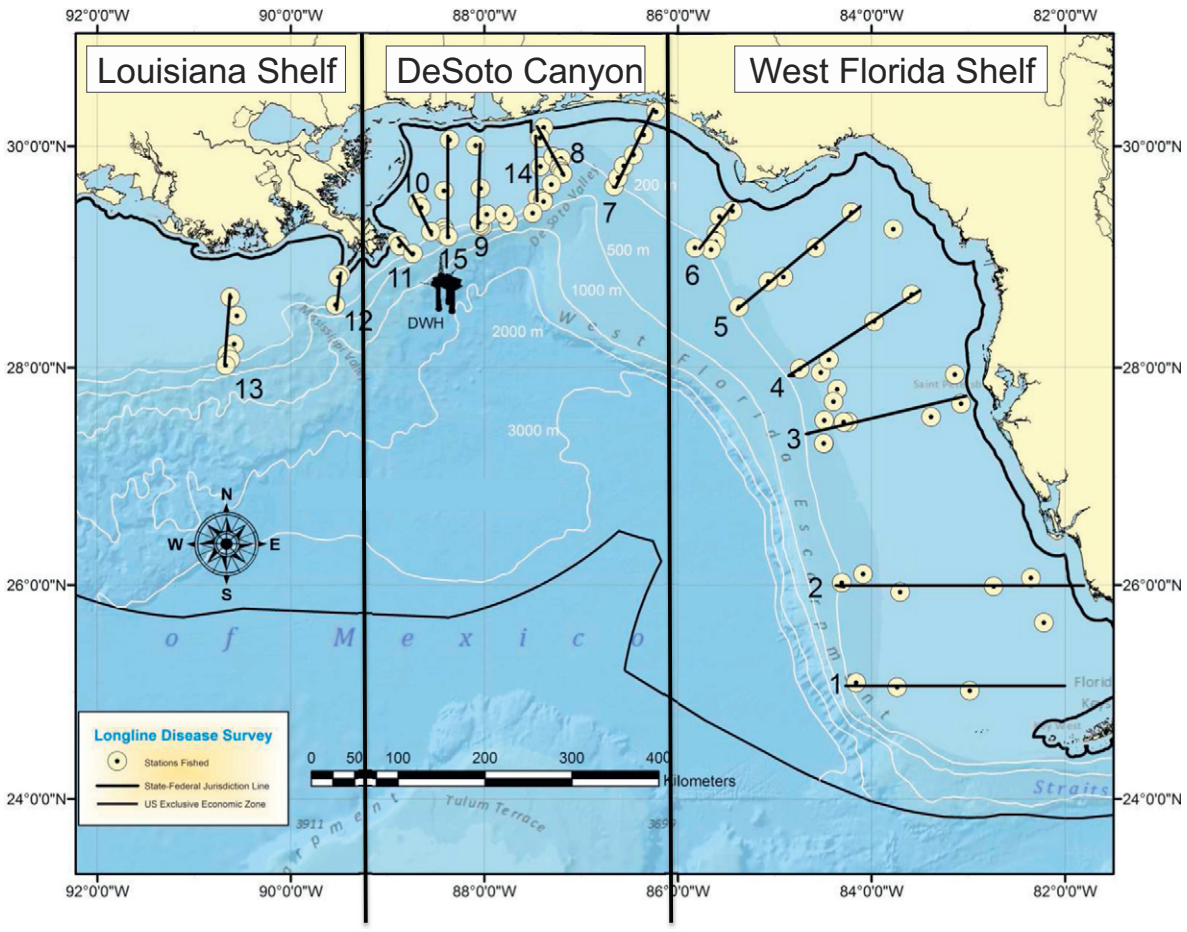

Fig. 1. Fish were collected at stations along the transects shown using baited demersal long lines during the three years that followed the DWH oil spill. The transects were separated into three geographic regions: Louisiana Shelf, DeSoto Canyon, and West Florida Shelf.

including Crystal Bond™ 509 adhesive. After each otolith was assayed, the ICP-MS continued to collect background levels for 60 s to ensure all sample material was flushed from the system. After otoliths were assayed with the LA-ICP-MS, each otolith was imaged using PAX-it imaging software and aged by two independent readers. Laser ablation transect length and annual increment widths were measured using ImageJ software.

The limits of detection were calculated using the Fathom Toolbox for Matlab (Jones, 2012; Jones, 2015) as three times the standard deviation of the gas blank. Limits of detection were adjusted for each sample based on ablation yield estimates following the methods of Longerich et al. (1996). Readings below detection limits were adjusted to zero. Mean metal concentrations and limits of detection (ppm) were calculated from counts-per-second data using established methods of geochemical data reduction (Longerich et al., 1996; Longerich et al., 1997; Halter et al., 2002; Heinrich et al., 2003; Jackson, 2008; Jones, 2012; Jones, 2015).

2.4. Statistical analysis

To address our first objective, which was to examine patterns of short- and long-term metal exposure, we examined annual metal concentrations for the years 2009–2011 within the otoliths of each species. Annual metal concentrations were determined by averaging metal concentrations corresponding to the annual increments from approximately 2009–2011, although the exact time periods for each species were based on the timing of otolith annulus deposition (Table S1). For instance, Red Grouper annulus deposition occurs from April–July; thus, the time period examined in Red Grouper occurred from approximately April–July 2009 to April–July 2011. The timing of annulus deposition for Southern Hake is unknown and therefore the best approximation of the time period investigated in this species is 2009–2011. For each species, we used the standardization procedure in PRIMER 7 to give equal weight to each metal by making the totals across samples all add to 100, which allowed us to standardize the data without generating negative values. A resemblance matrix was generated using Bray-Curtis similarity (Bray and Curtis, 1957); this resemblance measure was used because it is not affected by joint absences (Field et al., 1982), which were prevalent in this dataset.

We used hierarchical cluster analysis and the resulting divisions were tested using Type 1 similarity profile analyses (SIMPROF, (Clarke et al., 2008)) in PRIMER 7 to detect the presence of significant ($\alpha < 0.05$) multivariate structure within the annual (2009–2011) metal concentration datasets of each species. This method was used to investigate natural group structure within each species dataset without specifying a priori group membership. Heat maps (Wilkinson and Friendly, 2009) were constructed from the SIMPROF analyses to examine relative differences in metal concentrations among SIMPROF groups. Following the detection of significant multivariate structure using the SIMPROF test, the similarity percentages (SIMPER) exploratory analysis routine in PRIMER 7 was used to detect which metals contributed most to the SIMPROF group separation.

All of the remaining statistical tests were conducted using the Fathom Toolbox for Matlab (Jones, 2015) unless otherwise specified. Age-related changes in otolith microchemistry have been demonstrated for many species; therefore, we used analysis of covariance (ANCOVA) to address the potentially confounding effect of fish age on metal concentration. For those metals identified by SIMPER for each species, any

significant age effects on metal concentration detected using ANCOVA were consequently removed. For those metals identified by SIMPER for each species, the data were standardized by metal to *Z*-scores and SIMPROF groups were used as a priori groups to generate canonical analysis of principal coordinate (CAP) models for each species. The proportional chance criterion (PCC) test was used to assess the classification success rate of the CAP model in assigning SIMPROF group membership in comparison to a null model that assigns group membership by random allocation (McGarigal et al., 2000). We used CAP models to create CAP plots with corresponding variable importance vectors to visually assess the relative importance of the metals for the separation among SIMPROF groups.

We analyzed SIMPROF groups identified by the SIMPER and CAP analyses as containing relatively high levels of metals in order to investigate alternative explanations for the composition of these groups. Differences in all of the following variables were investigated as alternative explanations for the formation of these SIMPROF groups: collection location (Louisiana Shelf, DeSoto Canyon, and West Florida Shelf, Fig. 1); collection year (2011–2013); fish sex (male, female, or unknown); analyte year assignment (2009, 2010, and 2011); and the presence of external skin lesions (external breaks in the integument or severe skin irritation unrelated to mechanical damage, as originally classified by Murawski et al. (2014)). Non-random assignments of any of the variables listed above to a SIMPROF group were detected using a proportional randomization (PR) test developed for this purpose (Appendix A). We predicted that the presence of external skin lesions could be important in differentiating SIMPROF groups because stress has been observed to affect otolith microchemistry in other fish species (Kalish, 1992; Payan et al., 2004; Heagney et al., 2013). All graphs generated from SIMPROF analyses are labeled with fish lesion status to visualize any differences in lesion status among groups.

We evaluated the null hypothesis that each fish species was equally exposed to metals to investigate long-term trends in metal exposure. Lifetime metal concentrations were represented as the mean of entire otolith profiles (i.e., from the core to the edge of an otolith) for an individual. For each species, the SIMPROF test in PRIMER 7 was repeated using mean lifetime metal concentrations, a heat map of the SIMPROF groups was constructed, and SIMPER analysis was used to determine which metals contributed most to the separation among SIMPROF groups.

To address our second objective, which was to determine if there was a change in metal concentrations concurrent with the DWH oil spill, we assessed the null hypothesis that there was no effect of year (i.e., before, during, and after the DWH oil spill) on the concentrations of metals in fish otoliths. For each species, metal concentrations were standardized to *Z*-scores and a resemblance matrix was generated using Bray-Curtis similarity. We used a 2-way permutation-based multivariate analysis of variance (PERMANOVA; Anderson, 2001) to determine if there was a difference in the concentrations of the metals among years, with individual as a random factor to take into account the repeated measures nature of the data. SIMPROF groups with comparatively high concentrations of metals were also tested using a 2-way PERMANOVA to determine if exposure to metals changed in SIMPROF groups during the years bracketing the DWH oil spill (year: fixed factor, individual: random factor).

3. Results

3.1. Objective 1a: patterns of short-term metal exposure

We analyzed the otolith microchemistry of 222 fish consisting of six species collected throughout the northeastern GOM from 2011 to 2013 (Table 1). There appeared to be a trend of increasing metal concentrations for some of the fish species and metals examined from 2009 to 2011 (Fig. 2). The SIMPROF analyses of mean annual metal concentrations (2009–2011) identified distinct SIMPROF groups for four of the six species (Table 2, Figs. S2–S7). The metals ^{60}Ni, ^{64}Zn, and ^{63}Cu were most commonly responsible for the separation among distinct SIMPROF groups, as identified by SIMPER (Table 2).

3.2. Red Grouper

Red Grouper annual metal concentrations formed three SIMPROF groups with a similarity of 13% (SIMPROF: $p < 0.05$, Fig. S2). SIMPROF group B (Fig. 3A) was the largest group and was relatively 'clean' in comparison to the other two SIMPROF groups, which were characterized by comparatively high metal concentrations (Table 3). SIMPER identified ^{60}Ni, ^{63}Cu, and ^{64}Zn as the most important metals differentiating the SIMPROF groups (Table 2, Table S2). None of the important metals were found to significantly co-vary with age (ANCOVA: covariate $p > 0.05$).

The CAP plot (Fig. 3B) generated by a significant CAP model (classification success rate, CSR: 100%; proportional chance criterion, PCC: $p < 0.001$), indicated ^{60}Ni and ^{64}Zn characterized SIMPROF group C, while the single individual in group A had a relatively high concentration of ^{63}Cu. Because SIMPROF group C was identified as a relatively 'contaminated' group (i.e., high concentrations of the metals), it was further analyzed to determine if there were any characteristics (e.g., lesion status) that were over-represented in the group. Three variables were observed more frequently than would be expected by chance in SIMPROF group C: 2011 collection year, lesion status, and collection from the West Florida Shelf (PR: $p < 0.05$, Table 3).

3.3. Red Snapper

Red Snapper were not equally exposed to elements in the years prior to, during, and after the DWH oil spill (SIMPROF: $p < 0.05$, Fig. S4). The SIMPROF test of Red Snapper metal concentrations averaged over the years 2009–2011 identified 18 distinct groups; however, to facilitate interpretation of these results, 18 groups were reduced to nine by slicing the dendrogram at the maximum similarity level (i.e., 51%) that would not subdivide SIMPROF groups (Fig. S4). Most Red Snapper belonged to group I, a relatively 'clean' group with low levels of metals (Fig. 4A). There were two anomalous samples in the heat map, each of which formed a distinct SIMPROF group: A and B. All of the metals, except ^{57}Fe, were important in separating SIMPROF groups using SIMPER (Table 2). Of the metals identified by SIMPER, only ^{208}Pb significantly co-varied with age (ANCOVA: covariate $p = 0.002$); consequently, the effect of age was removed from the ^{208}Pb data to generate the Red Snapper CAP model.

Although nine Red Snapper groups were identified by the SIMPROF analysis, the CAP plot (Fig. 4B) and confusion matrix (Table 5) created using a highly significant CAP model (CSR: 76.4%; PCC: $p < 0.001$) appears to indicate that the most distinct separation occurred among groups D, E, and F. Group D was characterized by comparatively high concentrations of ^{60}Ni, ^{64}Zn, and ^{208}Pb (Fig. 4B) and consisted of a disproportionately large number of samples collected in 2011 (PR: $p < 0.05$, Table 4). Individuals from Group E, described by relatively high ^{53}Cr (Fig. 4A), were representative of the sample collections. Group F was characterized by high ^{60}Ni and ^{59}Co in comparison to the other SIMPROF groups and was over-represented by samples from 2009 and individuals collected in 2012 from DeSoto Canyon. SIMPROF groups C, G, H, and I were not strongly differentiated in the CAP analysis (Table 5, Fig. 4B) and were subsequently grouped together for the PR test. This combined group contained relatively high concentrations of ^{63}Cu and ^{51}V and was over-represented by individuals from 2012 collected on the Louisiana Shelf.

3.4. Southern Hake

We found that Southern Hake were not evenly exposed to oil-related elements in the years before, during, and after the DWH oil spill (SIMPROF: $p < 0.05$, Fig. S5). The SIMPROF test of Southern Hake

Table 1
Summary of target species collections. Transects occur throughout the northeastern Gulf of Mexico and their locations are noted in Fig. 1. "Collection years" column refers to the years during which samples were collected for analysis. The percentage of individuals in a species is given for each of the following categories: collection in the Louisiana Shelf (LA Shelf), DeSoto Canyon, and West Florida Shelf (WFL Shelf) regions; sex, designated as female, male, and unidentified sex (UI); and the presence of external skin lesions. The percentage of observations below the limits of detection (LOD) is given for each species.

Common name	Sample size	Collection year(s)	Depth (mean ± SD)	Age (mean ± SD)	Transect locations	LA shelf %	DeSoto Canyon %	WFL Shelf %	Female %	Male %	UI %	Lesioned %	Below LOD
Red Grouper	10	2011–2013	37.0 ± 20.0	6.6 ± 2.9	2, 4, 5, 8	0.0	40.0	60.0	90.0	0.0	10.0	10.0	18.1
Red Porgy	10	2011	42.0 ± 11.4	7.8 ± 4.8	6–8	0.0	80.0	20.0	50.0	50.0	0.0	0.0	23.6
Red Snapper	113	2011–2012	37.6 ± 12.7	6.5 ± 2.2	4, 8, 9, 10–15	37.2	41.6	21.2	52.2	46.0	1.8	7.1	18.2
Southern Hake	10	2011–2013	99.0 ± 22.3	7.5 ± 2.0	6–9, 13, 14	10.0	60.0	30.0	70.0	0.0	30.0	30.0	14.4
Tilefish	44	2011–2012	114.1 ± 25.8	11.4 ± 3.9	7–9, 11, 13–15	20.5	50.0	29.5	68.2	18.2	13.6	9.1	20.1
Yellowedge Grouper	35	2011–2013	88.3 ± 16.5	13.7 ± 6.1	3, 6–9, 11–15	14.3	68.6	17.1	94.3	2.9	2.9	5.7	22.6

identified three distinct groups at a minimum similarity of 41% (Table 2). The heat map illustrates that the lowest metal concentrations were observed in group C, while groups A and B had comparatively higher concentrations (Fig. 5A). The ANCOVA analysis did not identify any of the SIMPER metals, which included ^{51}V, ^{53}Cr, ^{60}Ni, ^{63}Cu, and ^{64}Zn (Table 2, Table S2), as significantly co-varying with age (ANCOVA: covariate $p > 0.05$).

The CAP plot that was created using a significant CAP model (CSR: 96.67%; PCC: $p < 0.001$) indicated group A was primarily characterized by ^{51}V and ^{63}Cu, while group B consisted of individuals with relatively high levels of ^{60}Ni and ^{64}Zn (Fig. 5B). The PR tests of SIMPROF group A revealed that the characteristics of individuals from group A were representative of the species (PR: all $p > 0.05$, Table 4). However, samples from SIMPROF group B were predominately collected during 2011 and were over-represented by lesioned individuals and females (PR: $p < 0.05$, Table 4).

3.5. Tilefish

In Tilefish, significant multivariate structure was detected in the annual, metal concentration dataset (Fig. S6). Of the three groups identified in the SIMPROF analysis, most samples were assigned to group C, which the heat map characterized as containing moderately low concentrations of metals (Fig. 6A). In comparison, the SIMPER analysis identified elevated concentrations of ^{63}Cu in SIMPROF group A, while group B had relatively high ^{60}Ni and ^{64}Zn concentrations (Table 2, Table S2). None of the important SIMPER metals were found to significantly co-vary with age (ANCOVA: covariate $p > 0.05$); therefore, unadjusted metal concentrations were used to construct a significant CAP model (CSR: 96.97%; PCC: $p < 0.001$).

The Tilefish CAP plot corroborated the patterns in metal concentrations among groups identified in the SIMPER analyses (Fig. 6B). To more clearly illustrate the differences between SIMPROF groups B and C, we plotted lifetime (i.e., core to edge) profiles of two individuals randomly selected from these two groups (Fig. 7). The profiles were linearly interpolated to fit on the same x-axis and smoothed by first applying an 11-point moving median, then an 11-point moving average following Sinclair et al. (1998), a method also recommended by Sanborn and Telmer (2003). The concentrations of ^{64}Zn, and to a lesser extent ^{60}Ni, were above the detection limits for the individual from SIMPROF group B, but not for the individual from SIMPROF group C. Thus, these profiles indicated a substantial difference in the concentrations of

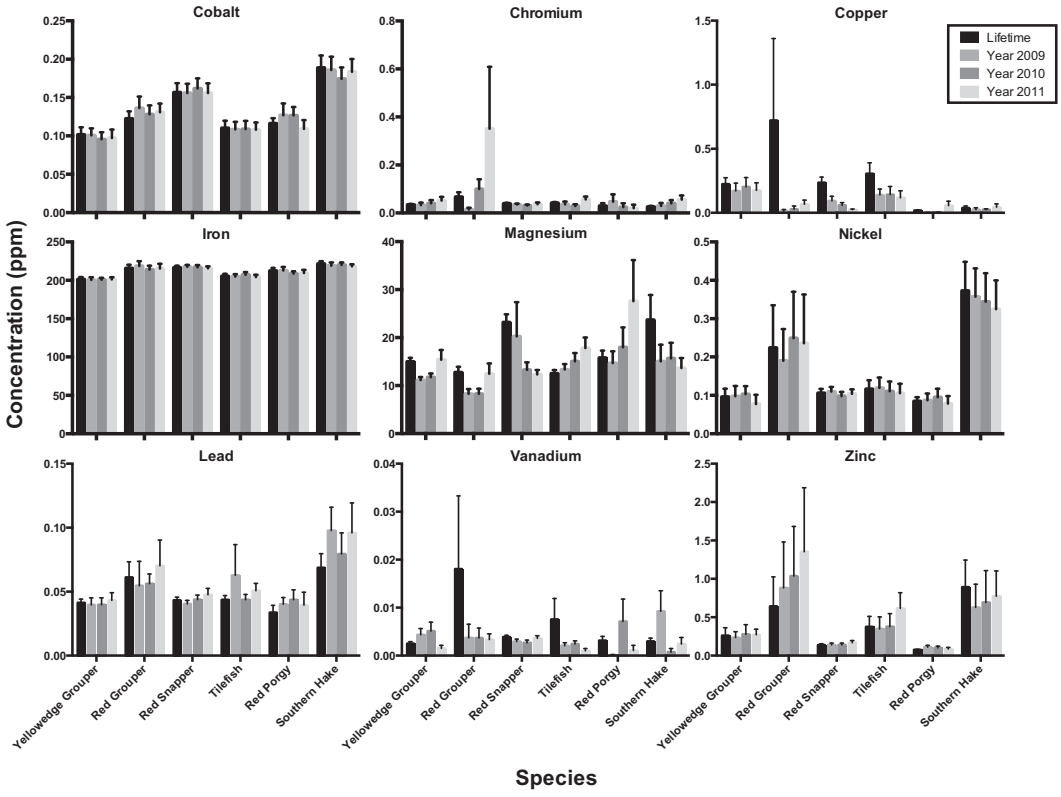

Fig. 2. Lifetime and annual (2009–2011) concentrations (mean ± s.e.m.) of the nine metals measured for each of the target species.

Table 2
Results of SIMPROF analyses of annual (2009–2011) and lifetime metal concentrations for the target species in this study. The "% similarity at first division" column refers to the first division in the dendrograms created by the SIMPROF analysis. SIMPER metals are those elements selected by SIMPER because they contributed most to the separation among SIMPROF groups. For those species that contained no significant SIMPROF groups, the selection of SIMPER metals and percent similarity at first division are not applicable (N/A).

Species	# SIMPROF groups	% Similarity at first division	SIMPER metals								
			^{24}Mg	^{51}V	^{53}Cr	^{57}Fe	^{59}Co	^{60}Ni	^{63}Cu	^{64}Zn	^{208}Pb
2009–2011											
Red Grouper	3	13						X	X	X	
Red Porgy	0	N/A	N/A	N/A	N/A	N/A	N/A	N/A	N/A	N/A	N/A
Red Snapper	9	13	X	X	X		X	X	X	X	X
Southern Hake	3	41		X	X			X	X	X	
Tilefish	3	30						X	X	X	
Yellowedge Grouper	0	N/A	N/A	N/A	N/A	N/A	N/A	N/A	N/A	N/A	N/A
Lifetime											
Red Grouper	2	38		X						X	
Red Porgy	0	N/A	N/A	N/A	N/A	N/A	N/A	N/A	N/A	N/A	N/A
Red Snapper	9	42	X	X	X		X	X	X	X	X
Southern Hake	2	56						X	X	X	
Tilefish	3	28		X				X		X	
Yellowedge Grouper	2	38						X		X	

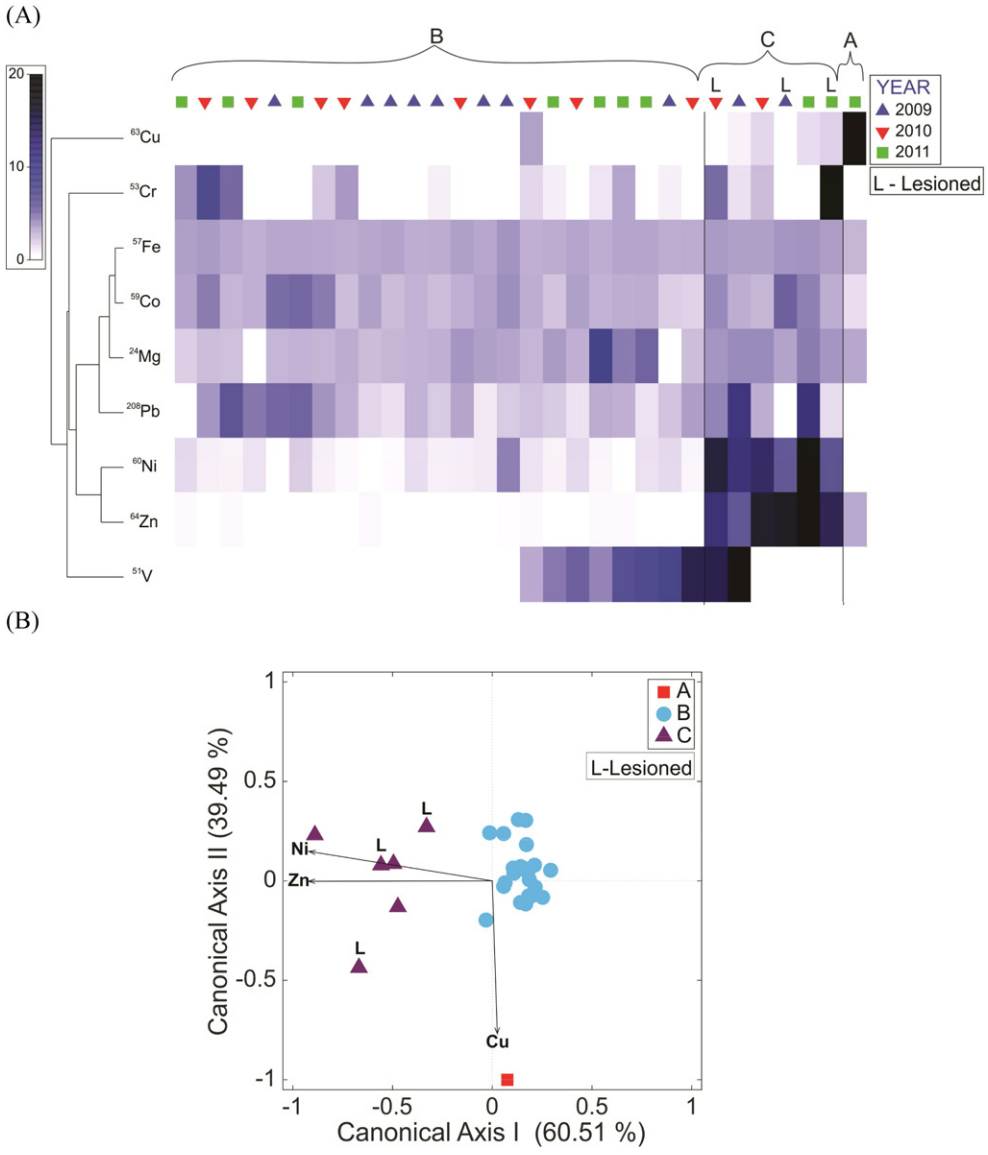

Fig. 3. Red Grouper mean analyte concentrations from 2009 to 2011. (A) Heat map of SIMPROF groups with rectangle shading based on a linear scale from absence (white) to the maximum concentration (black) (relative concentration). Symbols indicate year assignment of samples and letters indicate lesion status and significantly different groups of samples. (B) CAP plot of SIMPROF groups with corresponding variable importance vectors of the metals identified in the SIMPER test. Symbols indicate significantly different groups of samples and letters indicate lesion status.

Table 3
Target analyte concentrations (mean ± s.e.m.) (ppm) of all groups identified by the SIMPROF analyses of mean analytes from 2009 to 2011. *Indicates a group that contained only one individual.

Species	Group	^{24}Mg	^{51}V (ppb)	^{53}Cr	^{57}Fe	^{59}Co	^{60}Ni	^{63}Cu	^{64}Zn	^{208}Pb
Red Grouper	A*	9.58	0.00	0.00	174.2	0.05	0.00	13.58	1.12	0.00
	B	9.20 ± 1.17	2.59 ± 0.00	0.06 ± 0.02	211.63 ± 3.13	0.13 ± 0.01	0.07 ± 0.01	0.03 ± 0.02	0.10 ± 0.01	0.05 ± 0.01
	C	11.61 ± 0.39	7.25 ± 3.96	0.51 ± 0.35	236.74 ± 3.75	0.15 ± 0.02	0.83 ± 0.11	0.15 ± 0.04	5.05 ± 0.59	0.10 ± 0.03
Red Snapper	A*	812.21	5.81	0.19	185.66	0.06	0.06	0.10	2.19	0.03
	B*	24.50	0.00	0.00	185.7	0.08	0.00	0.00	0.00	0.49
	C	14.47 ± 3.39	3.22 ± 1.24	0.03 ± 0.01	202.68 ± 7.75	0.13 ± 0.05	0.10 ± 0.03	1.10 ± 0.24	0.15 ± 0.02	0.04 ± 0.01
	D	36.14 ± 7.27	3.24 ± 0.00	0.06 ± 0.02	216.65 ± 5.20	0.17 ± 0.02	0.25 ± 0.05	0.02 ± 0.01	0.91 ± 0.08	0.07 ± 0.01
	E	8.73 ± 1.04	2.76 ± 0.00	0.23 ± 0.03	224.44 ± 6.96	0.15 ± 0.03	0.09 ± 0.02	0.01 ± 0.00	0.05 ± 0.01	0.03 ± 0.01
	F	9.20 ± 0.22	0.00 ± 0.00	0.02 ± 0.01	269.76 ± 3.11	0.55 ± 0.02	0.31 ± 0.03	0.03 ± 0.02	0.00 ± 0.00	0.04 ± 0.01
	G	14.41 ± 2.43	5.06 ± 0.00	0.06 ± 0.02	201.57 ± 6.47	0.09 ± 0.02	0.05 ± 0.01	0.20 ± 0.01	0.18 ± 0.04	0.04 ± 0.01
	H	11.25 ± 0.74	11.09 ± 0.00	0.00 ± 0.00	221.83 ± 4.00	0.15 ± 0.02	0.10 ± 0.01	0.01 ± 0.00	0.10 ± 0.01	0.04 ± 0.00
	I	11.29 ± 0.48	1.00 ± 0.00	0.03 ± 0.00	210.89 ± 1.67	0.15 ± 0.01	0.07 ± 0.00	0.01 ± 0.00	0.09 ± 0.01	0.04 ± 0.00
Southern Hake	A	14.29 ± 0.80	27.78 ± 7.15	0.10 ± 0.02	220.30 ± 3.33	0.20 ± 0.01	0.35 ± 0.09	0.20 ± 0.02	1.86 ± 0.55	0.12 ± 0.03
	B	19.29 ± 2.08	1.53 ± 0.73	0.05 ± 0.01	224.28 ± 1.63	0.21 ± 0.01	0.49 ± 0.03	0.03 ± 0.01	0.91 ± 0.28	0.11 ± 0.01
	C	6.80 ± 1.02	4.13 ± 2.07	0.02 ± 0.01	209.73 ± 2.75	0.12 ± 0.01	0.08 ± 0.03	0.01 ± 0.00	0.09 ± 0.05	0.04 ± 0.01
Tilefish	A	8.87 ± 0.36	4.60 ± 0.00	0.03 ± 0.02	192.82 ± 3.55	0.07 ± 0.01	0.14 ± 0.01	1.70 ± 0.27	0.08 ± 0.02	0.02 ± 0.00
	B	12.97 ± 1.19	0.00 ± 0.00	0.01 ± 0.01	230.15 ± 6.84	0.14 ± 0.01	0.53 ± 0.07	0.16 ± 0.06	2.86 ± 0.74	0.14 ± 0.08
	C	15.94 ± 1.16	1.94 ± 0.00	0.04 ± 0.01	203.06 ± 1.83	0.11 ± 0.01	0.06 ± 0.01	0.06 ± 0.01	0.19 ± 0.03	0.04 ± 0.00

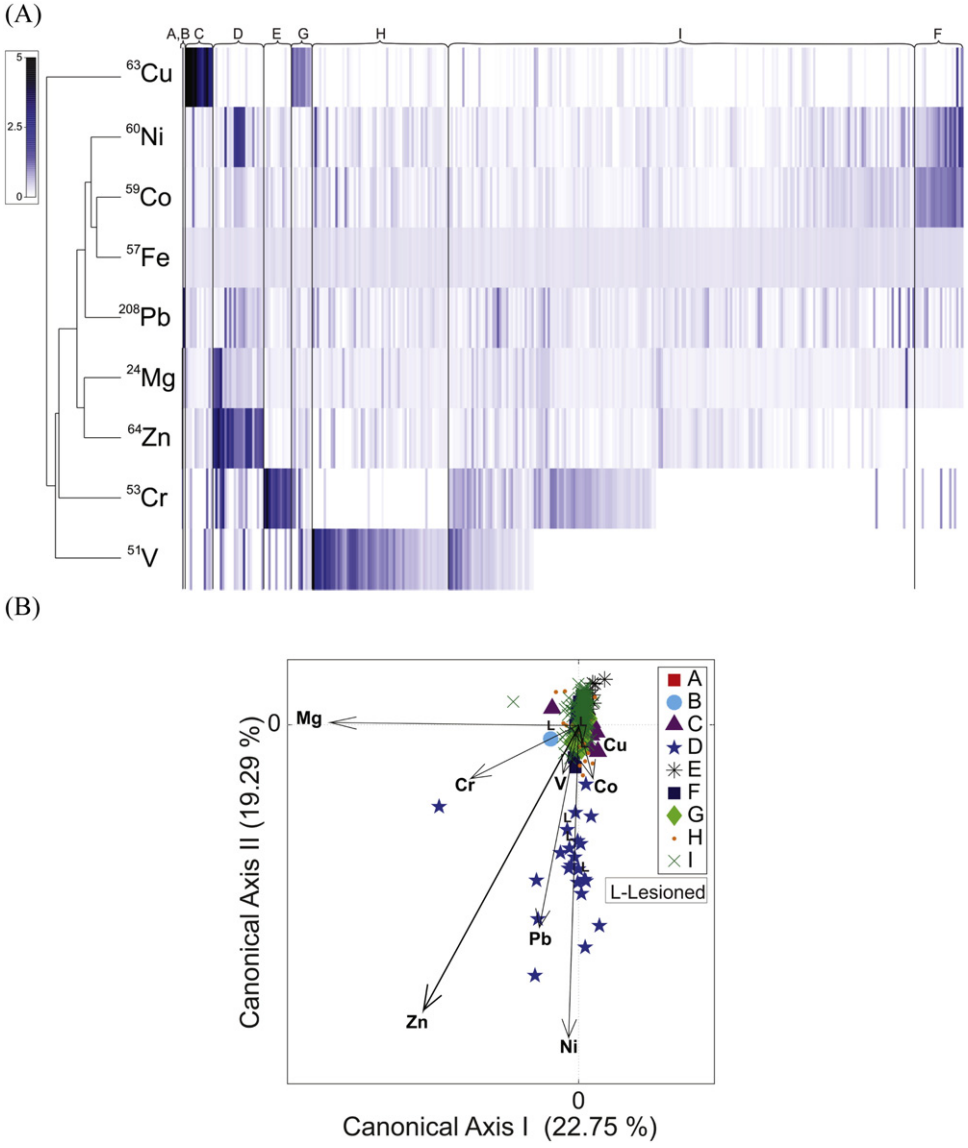

Fig. 4. Red Snapper mean analyte concentrations from 2009 to 2011. (A) Heat map of SIMPROF groups with rectangle shading based on a linear scale from absence (white) to the maximum concentration (black) (relative concentration). Letters indicate significantly different groups of samples. (B) CAP plot of SIMPROF groups with corresponding variable importance vectors of the metals identified in the SIMPER test. Symbols indicate significantly different groups of samples and letters indicate lesion status. SIMPROF group A is not shown in this plot for clarity.

Table 4
Results of the proportional randomization (PR) tests of selected groups from the SIMPROF analyses of mean, analytes from 2009 to 2011. *p*-Values from the PR tests are presented for the following five variables: sex (female, male, unidentified = UI), analyte year assignment (2009–2011), collection year (2011–2013), lesioned status (lesioned or non-lesioned), and collection location (Louisiana Shelf, DeSoto Canyon, and West Florida Shelf). Bold values represent significant *p*-values ($\alpha = 0.05$). Some group attributes (i.e., unidentified sex) were not observed within a group and accordingly are labeled "not applicable" (N/A).

Species	SIMPROF Group	High concentration element(s)	Female	Male	UI	Analyte 2009	Analyte 2010	Analyte 2011	Collection Year 2011	Collection Year 2012	Collection Year 2013	Non-lesioned	Lesioned	LA Shelf	DeSoto Canyon	West FL Shelf
Red Grouper	C	Ni, Zn	1.000	0.512	N/A	0.674	0.656	0.665	**0.002**	1.000	1.000	1.000	**0.010**	N/A	1.000	**0.037**
Red Snapper	C, G, H, and I	Cu, V	0.248	0.738	0.959	0.340	0.451	0.856	1.000	**0.001**	N/A	0.604	0.583	**0.026**	0.956	0.803
Red Snapper	D	Ni, Zn	0.989	0.125	0.057	0.908	0.154	0.617	**0.001**	1.000	N/A	0.941	0.200	0.144	0.984	0.313
Red Snapper	E	Cr	0.675	0.497	1.000	0.625	0.364	0.839	0.939	0.250	N/A	0.415	1.000	0.971	0.585	0.093
Red Snapper	F	Ni, Co	0.406	0.680	1.000	**0.002**	0.860	1.000	1.000	**0.003**	N/A	0.200	1.000	1.000	**0.002**	0.860
Southern Hake	A	Cu	0.483	1.000	N/A	0.547	1.000	0.561	0.481	1.000	1.000	0.470	1.000	1.000	1.000	0.076
Southern Hake	B	Ni, Zn	**0.001**	1.000	N/A	0.642	0.880	0.339	**0.001**	1.000	1.000	1.000	**0.006**	0.172	0.965	0.490
Tilefish	A	Cu	0.998	0.637	**0.020**	0.201	0.884	0.869	0.607	1.000	N/A	0.610	1.000	1.000	0.975	**0.028**
Tilefish	B	Ni, Zn	0.729	0.984	**0.015**	0.873	0.453	0.447	**0.001**	1.000	N/A	1.000	**0.001**	1.000	**0.001**	1.000

Table 5
Confusion matrix generated from the CAP analysis of nine Red Snapper SIMPROF groups. Most misclassifications occurred among SIMPROF groups C, G, H and I. SIMPROF groups A and B consisted of only 1 individual each.

Group	A	B	C	D	E	F	G	H	I
A	0	0	100	0	0	0	0	0	0
B	0	0	0	0	0	0	0	100	0
C	0	0	58.3	0	0	8.3	33.3	0	0
D	0	0	0	95.5	0	0	0	0	4.5
E	0	0	0	0	100	0	0	0	0
F	0	0	0	0	0	100	0	0	0
G	0	0	0	0	0	0	66.7	11.1	22.2
H	0	0	0	0	0	3.4	1.7	74.6	20.3
I	0	0	0	0	0	2	5.9	2.5	89.6

^{64}Zn, and to a lesser extent ^{60}Ni, between SIMPROF groups B and C. PR tests were used for groups A and B to determine if there were any characteristics over-represented in those groups. In both groups, fish of unidentified sex were represented more frequently than would be expected by chance (PR: $p < 0.05$, Table 4). Additionally, a significant proportion of group A was collected from the West Florida Shelf, while group B consisted of individuals from the DeSoto Canyon region and contained a significant number of lesioned fish (PR: $p < 0.05$, Table 4).

3.6. Yellowedge Grouper

The SIMPROF analysis failed to detect significant multivariate structure within Yellowedge Grouper metal concentrations averaged annually; however, the dendrogram indicated a separation, albeit non-significant, between lesioned and non-lesioned individuals (Fig. S7). Although all Yellowedge Grouper samples were deemed to be statistically similar, a non-metric multidimensional scaling (nMDS) plot of the Yellowedge Grouper resemblance matrix indicated an apparent separation of the lesioned group (Fig. 8A). Examination of the Yellowedge Grouper heat map revealed an apparent group of lesioned individuals that had relatively higher concentrations of ^{60}Ni and ^{64}Zn in comparison to the other samples (Fig. 8B).

3.7. Objective 1b: patterns of long-term metal exposure

The SIMPROF tests of mean, lifetime metal concentrations detected significant multivariate structure among individuals within each species, with the exception of Red Porgy (Table 2, Figs. S8–13). On average, lifetime metal concentrations within otoliths were highest in Red Grouper and lowest in Red Porgy (Fig. 9). The number of distinct groupings identified by the SIMPROF test varied between two and nine (Table 2). Close examination of the dendrograms generated by the cluster analysis with SIMPROF indicated the first division among groups occurred at a similarity between 30 and 55%. The metals responsible for the separation among distinct SIMPROF groups, as identified by SIMPER, varied among species, but ^{60}Ni, ^{64}Zn, ^{63}Cu, and ^{51}V were most frequently the important metals (Table 2, Table S3).

3.8. Objective 2: examination of otolith chemistry concurrent with DWH

There appeared to be a trend of increasing metal concentrations for some of the fish species and metals examined from 2009 to 2011 (Fig. 2); in particular, in the Red Grouper, there was a pattern of increasing concentrations of ^{24}Mg, ^{53}Cr, ^{60}Ni, ^{63}Cu, and ^{64}Zn in the years during and after the DWH oil spill compared to the year prior to the oil spill. However, the PERMANOVA analyses of the metal concentrations from 2009 to 2011 did not identify any significant differences in these concentrations among years for any of the species tested (Table 6, Test Type 1).

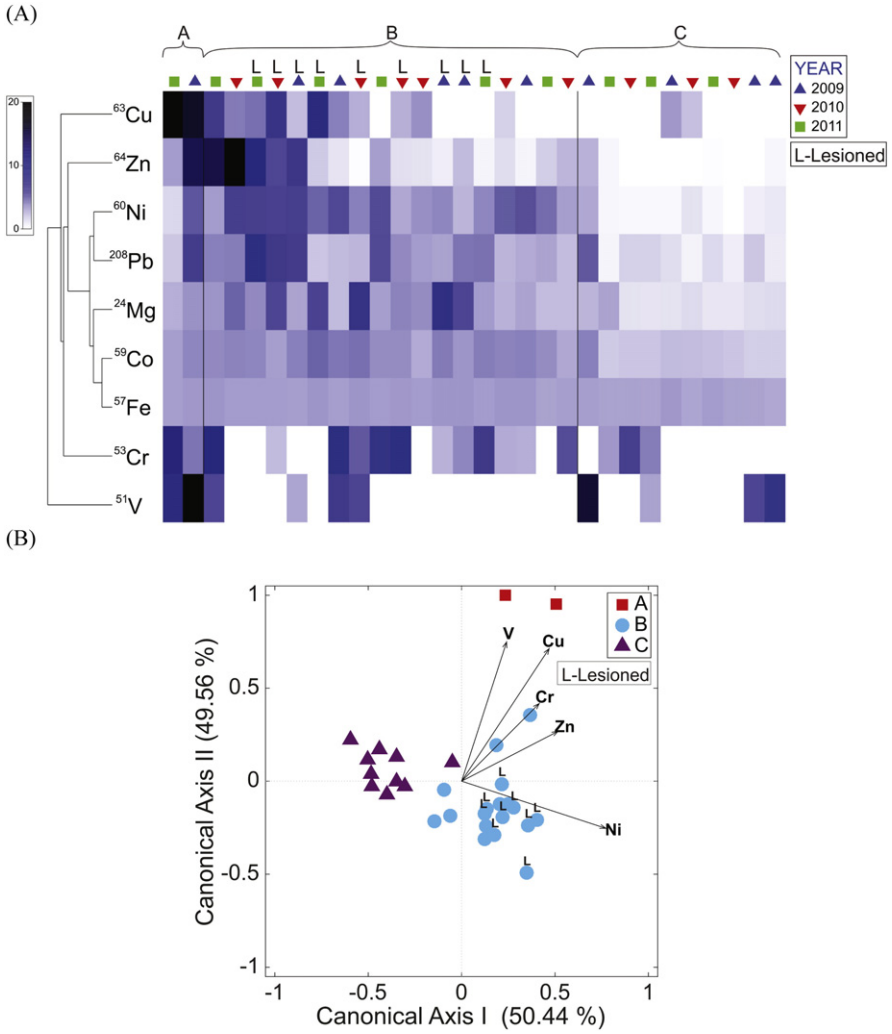

Fig. 5. Southern Hake mean analyte concentrations from 2009 to 2011. (A) Heat map of SIMPROF groups with rectangle shading based on a linear scale from absence (white) to the maximum concentration (black) (relative concentration). Symbols indicate year assignment of samples and letters indicate lesion status and significantly different groups of samples. (B) CAP plot of SIMPROF groups with corresponding variable importance vectors of the metals identified in the SIMPER test. Symbols indicate significantly different groups of samples and letters indicate lesion status.

We narrowed our PERMANOVA analyses to specific groups within each species that were identified by the SIMPROF analyses. The aim of these analyses was to highlight a potentially ephemeral metal exposure signature in some individuals that may have been unnoticed due to dilution of the signal by unexposed individuals. We focused the PERMANOVA analyses on the SIMPROF groups with the highest concentrations of metals. For each species, we combined individuals from the SIMPROF groups with high ^{60}Ni and ^{64}Zn concentrations with individuals in the high ^{63}Cu concentration SIMPROF groups. Again, the PERMANOVA analyses detected no significant differences in the concentrations of metals among years for all of the SIMPROF groups tested (Table 6, Test Type 2).

4. Discussion

4.1. Objective 1: patterns of metal exposure

There was a consistent pattern of metal exposure observed in both the short- and long-term metal histories of the offshore fish species examined. The analysis of long-term (i.e., lifetime) metal concentrations revealed that ^{60}Ni, ^{64}Zn, ^{63}Cu, and ^{51}V were repeatedly identified as the metals differentiating SIMPROF groups for most species. Over the short-term period from 2009 to 2011, the SIMPROF analyses consistently identified the following groups in most of the six species analyzed: a relatively clean SIMPROF group ("clean group") with comparatively low concentrations of the metals measured; a smaller group with a relatively high concentration of ^{63}Cu ("Cu group"); and a group characterized by high concentrations of ^{60}Ni and ^{64}Zn ("Ni-Zn group") that contained more lesioned fish than would be expected by chance. All of the SIMPROF groups identified in the short-term analyses were present before the DWH oil spill occurred. Taken together, the otolith metal histories suggest a long-term and heterogeneous exposure of at least half of the offshore fish species examined to ^{60}Ni, ^{64}Zn, ^{63}Cu, and ^{51}V prior to, during, and after the DWH oil spill.

The Cu group was identified in four of the six species. In Tilefish, the Cu group was over-represented by fish of unknown sex collected from the West Florida Shelf. There was only one individual in the Red Grouper Cu group, but it was also collected from the West Florida Shelf. In Red Snapper, the Cu group contained a disproportionate number of individuals from 2012 collected on the Louisiana Shelf. Finally, the Southern Hake Cu group primarily consisted of individuals collected during 2011. Thus, there was no defining characteristic (i.e., collection location, sex, etc.) that could clarify why individuals in this group were exposed to relatively high ^{63}Cu concentrations.

In contrast, two variables were consistently over-represented in the Ni-Zn group: lesioned status and collection during the year 2011. These variables, however, are confounded because most lesioned individuals analyzed were collected during 2011, with only a few lesioned

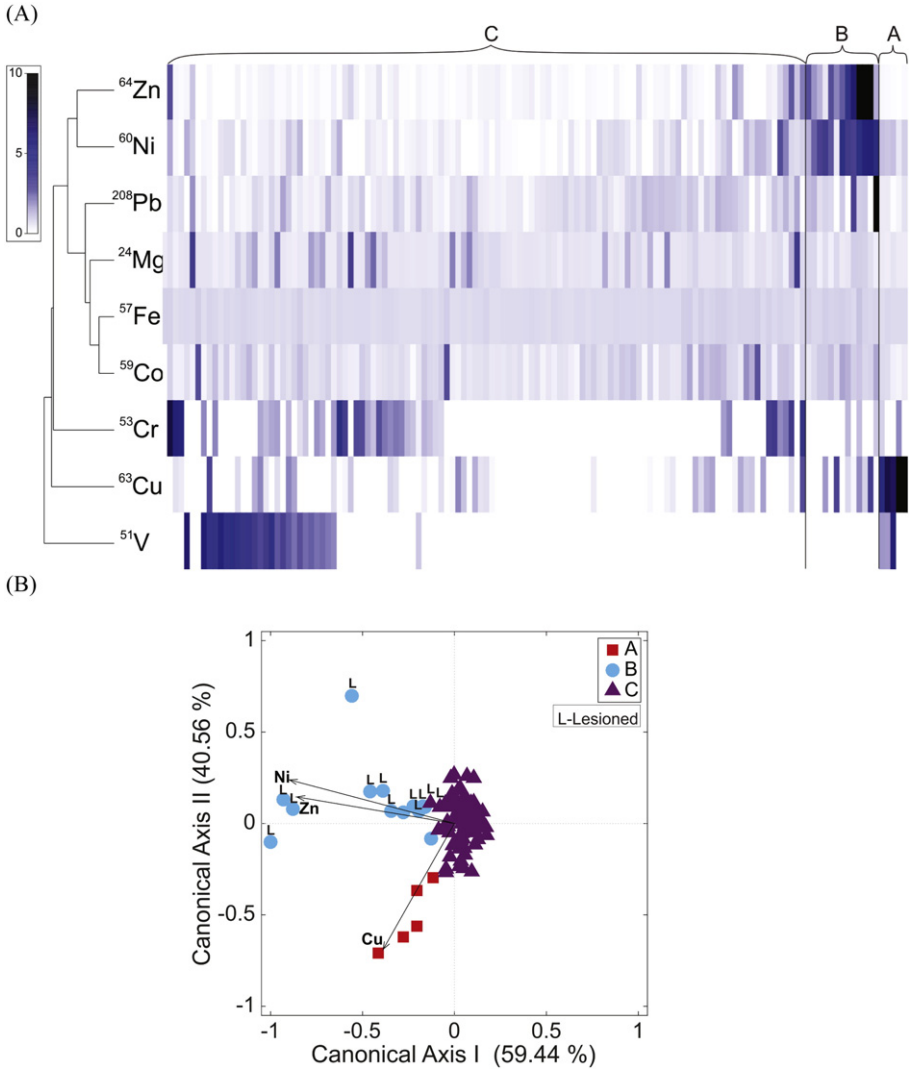

Fig. 6. Tilefish mean analyte concentrations from 2009 to 2011. (A) Heat map of SIMPROF groups with rectangle shading based on a linear scale from absence (white) to the maximum concentration (black) (relative concentration). Letters indicate significantly different groups of samples. (B) CAP plot of SIMPROF groups with corresponding variable importance vectors of the metals identified in the SIMPER test. Symbols indicate significantly different groups of samples and letters indicate lesion status.

individuals collected during 2012–2013. Within the Tilefish, the Ni-Zn group disproportionately consisted of individuals of unknown sex from the DeSoto Canyon study area, while Red Grouper in the Ni-Zn group were disproportionately collected from the West Florida Shelf (Red Grouper become much less abundant west of the West Florida Shelf). Although the Yellowedge Grouper Ni-Zn group was not statistically different from the other individuals in the sample, this "group" consisted of the only lesioned Yellowedge Grouper that were analyzed. Thus, the only consistent characteristic of the Ni-Zn group among species was the presence of dermal lesions, although this factor was not significant for the Red Snapper.

4.2. Proximate and ultimate causes of lesion formation

Chronic exposure of fish to sublethal metal concentrations can result in reductions in the following health indicators: growth, condition factor, hepatosomatic index, and gonadosomatic index (Pereira et al., 1993; Clements and Rees, 1997; Bervoets and Blust, 2003; Maes et al., 2005; Bervoets et al., 2013), suppression of the immune response (Oneill, 1981; Zelikoff, 1993; Bols et al., 2001), and lesion formation (Mallatt, 1985; Kotsanis et al., 2000). Zelikoff (1993) demonstrated that heavy-metal pollutants ^{60}Ni and ^{64}Zn alter immunoregulatory functions in a variety of fish species. The majority of the lesioned fish collected in the present study had relatively high concentrations of otolith ^{60}Ni and ^{64}Zn, suggesting metal-induced immunomodulation may have occurred in these fish. Alternatively, Ni and Zn bioavailability may have been greater in lesioned fish if they were exposed to oil.

Murawski et al. (2014) identified an elevated frequency of skin lesions in offshore NGoM fish species related to polycyclic aromatic hydrocarbon (PAH) exposure following the DWH oil spill. The prevalence of skin lesions observed on GoM fishes has continued to decline every year since the DWH oil spill occurred (Murawski, unpublished data), further suggesting that the cause of these skin lesions in fish from the NGoM is likely of toxicopathic origin. We suspect that the lesioned fish in the Ni-Zn groups may have been immunosuppressed prior to the DWH oil spill, and were thus more vulnerable to the effects of the spilled PAHs.

Apart from the 699,700 metric tons (±10%) of oil released into the GoM by the DWH oil spill, an oil-pollution budget for the GoM identified that an estimated 3571 tons of oil is spilled into the GoM annually due to oil and gas infrastructure (e.g., leaks and discharges from platforms and pipelines) (Ocean Studies Board and Marine Board, 2003). Grizzle (1986) observed higher lesion prevalence in several fish species, including Southern Hake, in close proximity to oil and gas platforms. This high lesion frequency was attributed by Grizzle (1986) to exposure to toxicants originating from drilling fluids, drill cuttings, cooling water,

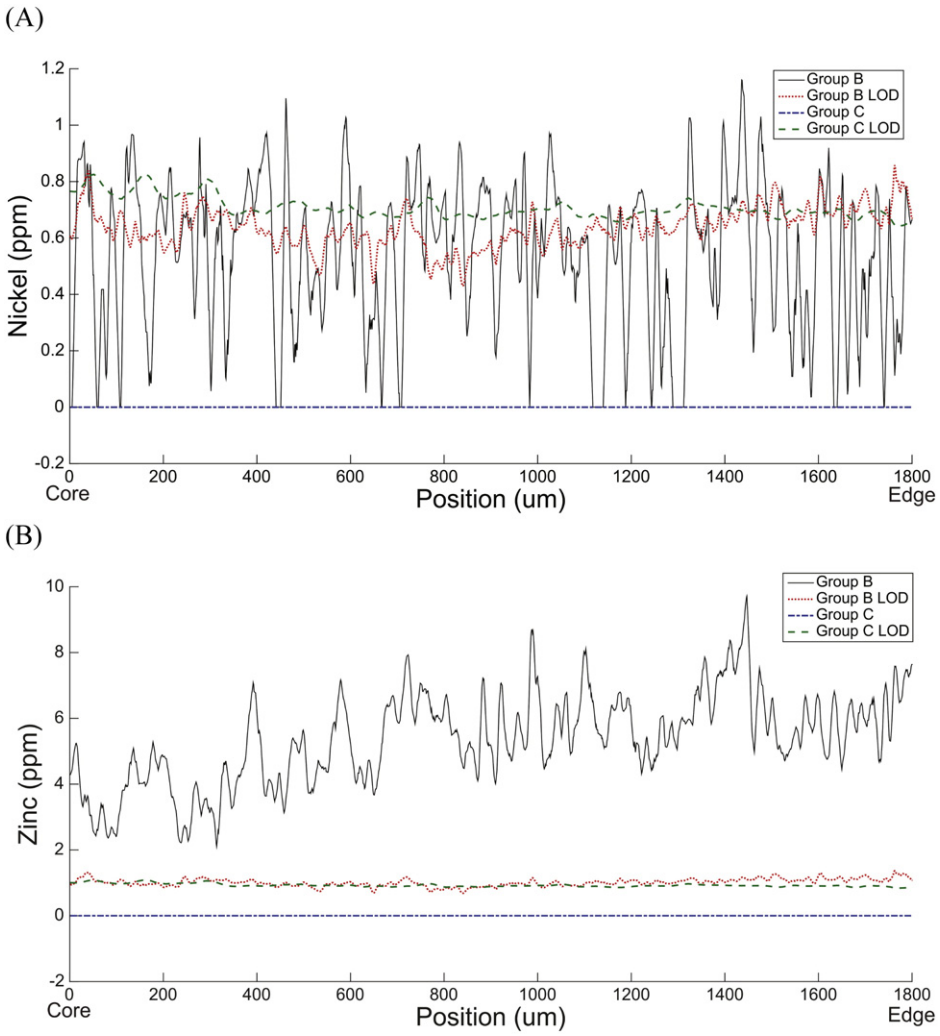

Fig. 7. Linearly interpolated profiles, from otolith core to edge, from two Tilefish otoliths from SIMPROF groups B and C showing the concentrations of (A) Ni, and (B) Zn. LOD represents the limits of detection. Profiles were smoothed by first applying an 11-point moving median and then an 11-point moving average.

water originating from the well, drilling-related shipping activity, and/or the physical presence of structures and pipelines.

4.3. Trace metals near oil and gas platforms

Several of the important trace metals in this study (^{60}Ni, ^{64}Zn, ^{63}Cu, and ^{51}V) have been detected in higher concentrations in sediments near oil platforms and are associated with oil production processes (Tillery and Thomas, 1980, as cited in (Neff, 1987)). In a synthesis of the literature on benthic meiofauna and macroinfauna responses to pollution in the GoM, Peterson et al. (1996) concluded that toxicity responses, which were observed up to 100–200 m away from oil and gas platforms, were primarily due to the heavy metals in drilling mud and produced waters associated with platforms.

Previous studies have detected unique, metal signatures in the otoliths of Red Snapper collected from oil and gas platforms in the NGoM (Nowling et al., 2011; Sluis and Cowan, 2013). Nowling et al. (2011) detected higher concentrations of ^{206}Pb and ^{51}V in the otoliths of Red Snapper collected from platform habitats, while Sluis and Cowan (2013) identified the following suite of metals unique to fish otoliths collected near oil and gas platforms: ^{138}Ba, ^{59}Co, ^{56}Fe, ^{55}Mn, ^{206}Pb, ^{51}V, ^{63}Cu, ^{65}Cu, ^{64}Zn, and ^{66}Zn. In the Red Snapper from this study, the Ni-Zn group that was identified also contained relatively high concentrations of ^{208}Pb. Hence, the high concentrations of ^{60}Ni, ^{64}Zn, and ^{63}Cu observed in the otoliths of some of the individuals in this study may indicate that those individuals lived near oil and gas platforms; yet, there are many additional, potential sources of these metals in the GoM.

4.4. Gulf-wide sources of trace metals

The primary sources of metals that could contribute to localized increases in these metals in the GoM include: atmospheric deposition, river discharge, or anthropogenic input (De Groot et al., 1976; Windom, 1992). Historically, anthropogenic inputs of metals to some GoM estuaries have been shown to exceed natural, riverine inputs due to weathering of continental rocks (Summers et al., 1996). An evaluation of NGoM estuarine sediments found that 39% of sites with anthropogenically-enriched sediments were near human population centers, industrial facilities, or military installations, 54% were near agricultural watersheds, and 7% included the Mississippi River (Summers et al., 1996).

Two distinct sediment zones exist along the continental shelf of the northern GoM, affecting trace metal concentrations in these zones: (1) silicate sediments derived from weathering of continental rocks west of the Mississippi River, and (2) calcium carbonate sediments derived from the shells of planktonic foraminifera and coccolithophores east of the Mississippi River (Martinec et al., 2014). Trace metals concentrations (Cr, Cu, Fe, Ni, Pb, V, and Zn) west of the Mississippi River correlate with Al and longitude, suggesting that these metals have a lithogenic origin, without anthropogenic input (Martinec et al., 2014). The Louisiana/

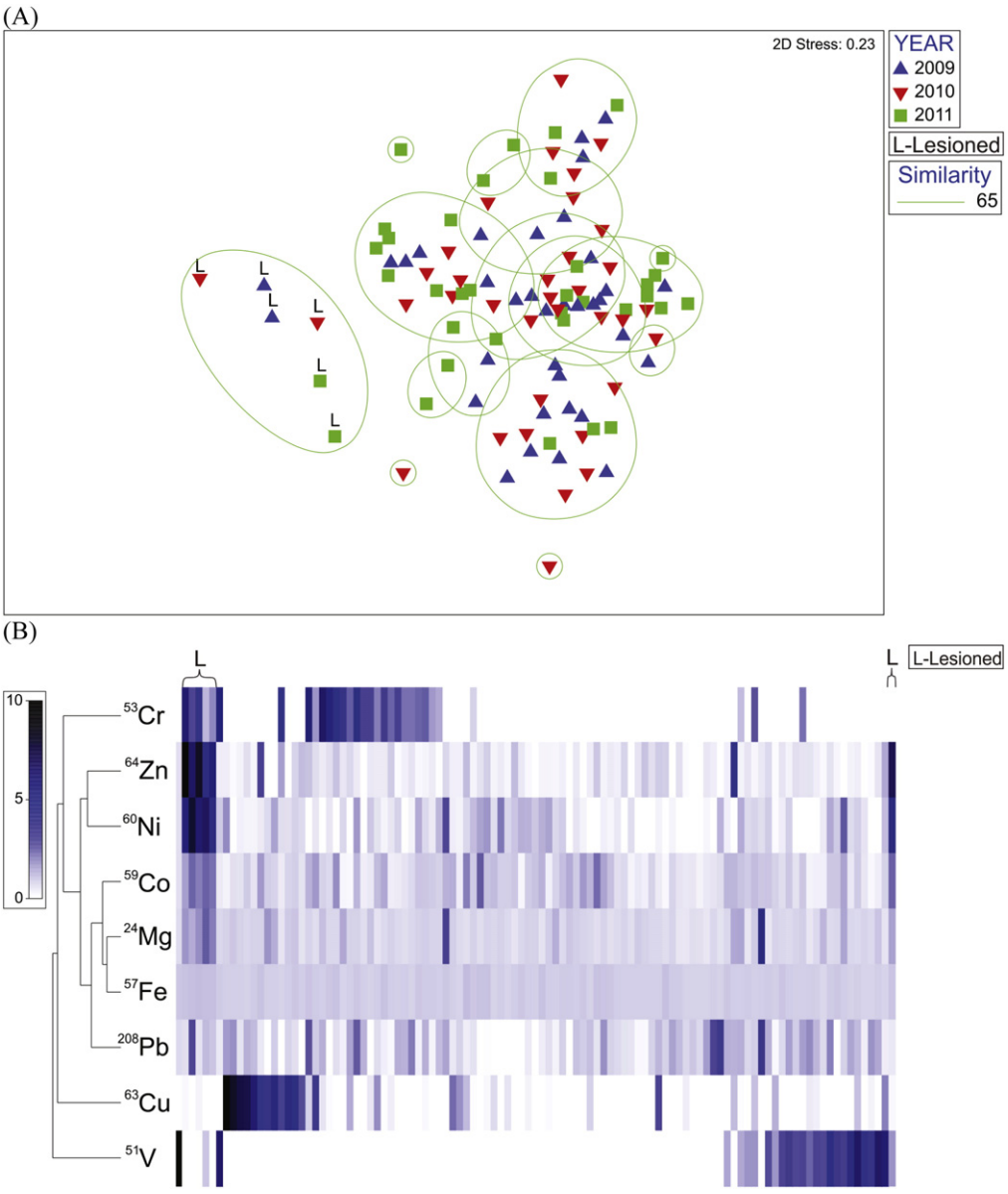

Fig. 8. Yellowedge Grouper mean analyte concentrations from 2009 to 2011. (A) Nonmetric multidimensional scaling (nMDS) plot of Yellowedge Grouper mean analyte concentrations from 2009 to 2011. Groups with a non-significant 65% similarity level are indicated on the plot. (B) Heat map of SIMPROF groups with rectangle shading based on a linear scale from absence (white) to the maximum concentration (black) (relative concentration). Letters indicate lesioned status.

Texas current is likely responsible for carrying silty and clayey sediments westward from the Mississippi River (Kourafalou and Androulidakis, 2013). Several trace metals in the NGoM (Ni, Pb, Cd, Cu, and Mn) are enriched compared to Mississippi-derived material and do not correlate well with Al; Wade et al. (1980) suggested that the enrichment of these metals may be due to natural diagenetic processes rather than anthropogenic inputs. East of the Mississippi River, trace metal concentrations in sediments are comparatively low because carbonate sediments are precipitated by living organisms from chemical species in seawater, which is depleted in trace metals; although, concentrations of Sr, Ca, and Mg are elevated in these regions due to the availability of carbonate material (Table 7) (Holmes, 1973; Martinec et al., 2014).

The annual flux of metals investigated in this study to the GoM from the Mississippi River totals 13.03 billion kg (Trefry, 1977) (Table 7). During the oil spill, the State of Louisiana opened freshwater diversions along the Mississippi River in an effort to prevent oil from reaching coastal marshes (State of Louisiana, 2010). The discharge of the Mississippi River from July to September 2010, exceeded the 20-year mean (O'Connor et al., 2016) and potentially contributed a second source of trace metals to the northeastern Gulf. Whether this discharge reached the offshore environment sampled in this study is unknown. Comparatively, the input of metals from the DWH oil spill contributed <1% of the total annual flux of these metals to the GoM from the Mississippi River (Table 7).

Additionally, an annual oil budget in the GoM identified all of the following additional annual inputs of oil into the GoM that could contribute to metals in the GoM: 70,000 tons from natural oil seeps (~73%); 18,700 tons from oil combustion byproducts (~20%); 4090 tons from transportation activities (~4%); and 2710 tons from oil and gas extraction activities (~3%) (Ocean Studies Board and Marine Board, 2003). Yet, Murawski et al. (2014) noted that in the northeastern GoM, oil inputs from natural oil seeps likely account for less than ~30%, and not ~73%, of the oil budget because most natural seeps primarily occur in the northwestern GoM. We are unaware of any studies investigating trace metals that are contributed to the GoM from natural oil seeps; therefore, while seeps may contribute to the metal exposure of marine organisms, the extent of these effects is currently unknown.

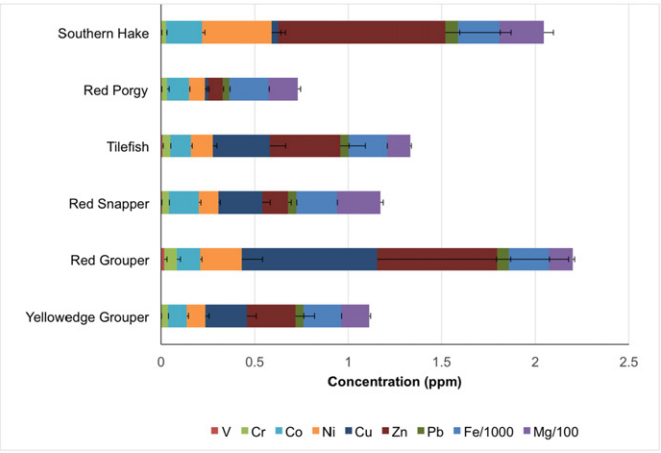

Fig. 9. Lifetime concentrations (mean ± s.e.m.) of the metals measured for each of the target species.

4.5. Life-history patterns and exposure vectors

The differences in otolith chemistry observed among the species examined here may be related to differences in life history patterns and exposure vectors. In the Red Porgy, both the lifetime and short-term analyses revealed no significant multivariate structure in the data. Additionally, Red Porgy had, on average, the lowest concentrations of metals in their otoliths (Fig. 9). Red Porgy and Red Snapper are the shallowest dwelling species investigated in this study (Table S1) and both are highly reef-associated. Red Snapper, unlike Red Porgy, are frequently observed to be closely associated with oil and gas platforms (Stanley and Wilson, 1990; Stanley and Wilson, 1997).

The four other species examined in this study, for which a high Ni-Zn group was generally observed, are deeper-dwelling shelf species that associate closely with sediment (Table S1). Tilefish and Red Grouper have been observed manipulating sediment with their mouths and fins to create burrows and expose rocky bottom habitat, while Yellowedge Grouper are known to utilize burrows created by Tilefish. Fish that burrow in and/or manipulate the sediment, or utilize burrows, may be exposed to metals associated with sediments. This exposure route could be either uptake of metals through the integument and gills, and/or through increased benthivory and incidental ingestion of sediment particles that contain metals. Different patterns of habitat use, including varying degrees of sediment association, likely exposed the fish species in this study to different sources and concentrations of metals.

Table 6
Results from the 2-way PERMANOVA analyses of metal concentration from 2009 to 2011 for all individuals in a species (Test Type 1) and for individuals in SIMPROF groups with the highest concentrations of metals (Test Type 2).

Species	Test Type	DF	Factor	F-ratio	*p*-Value
Red Grouper	1	2	Year	0.912	0.566
	1	9	Individual	2.568	0.001
	2	2	Year	5.807	0.110
	2	2	Individual	45.729	0.017
Red Porgy	1	2	Year	1.120	0.331
	1	9	Individual	2.039	0.001
Red Snapper	1	2	Year	1.490	0.091
	1	112	Individual	4.785	0.001
	2	2	Year	1.513	0.531
	2	9	Individual	0.743	0.980
Southern Hake	1	2	Year	1.304	0.218
	1	9	Individual	5.741	0.001
	2	2	Year	1.059	0.425
	2	6	Individual	2.787	0.047
Tilefish	1	2	Year	1.571	0.087
	1	43	Individual	2.590	0.001
	2	2	Year	0.587	0.788
	2	8	Individual	2.049	0.500
Yellowedge Grouper	1	2	Year	1.658	0.070
	1	34	Individual	5.228	0.001

4.6. Objective 2: examination of otolith chemistry concurrent with DWH

The short-term analysis of trends in otolith metal concentrations revealed no significant differences among the years prior to, during, or after the DWH oil spill for all of the species analyzed. Indeed, even when the analyses were limited to those individuals in the Ni-Zn and Cu groups (to eliminate a possible signal dilution) there was no significant change in metal concentrations among years. The results from this study are in agreement with previous studies, which also observed no change in the trace metal content of marine or estuarine organisms during or after the DWH oil spill (Carmichael et al., 2012; Apeti et al., 2013; Fitzgerald and Gohlke, 2014; Nelson et al., 2014). In contrast, studies of offshore microbes (Lu et al., 2012) and sperm whales (Wise et al., 2014) in the GoM have suggested relatively high metal exposure in these organisms, potentially as a result of exposure to the DWH oil spill.

Previous studies have detected increases in the trace-metal concentrations in the water column, sediments, and marine organisms following the Gulf War, Prestige, and Erika oil spills (Fowler et al., 1993; Al-Abdali et al., 1996; Massoud et al., 1998; Chiffoleau et al., 2004; Prego et al., 2006; Santos-Echeandia et al., 2008; Moreno et al., 2011). Macondo crude oil is relatively depleted in trace metals in comparison to many other crude oils (Joung and Shiller, 2013). One potential explanation for the lack of a trace-metal signature in some marine organisms exposed to the DWH oil spill is the relatively low concentration of trace metals in the Macondo crude oil.

4.7. Physiological regulation of otolith chemistry

Over one-third of all proteins in fish require a metal cofactor (Rosenzweig, 2002); yet, the potential toxicity of these essential metals suggests that tight physiological control of these elements is necessary. Of the metals investigated in this study, several (^{57}Fe, ^{59}Co, ^{63}Cu, and ^{64}Zn) are recognized as essential metals that fish are able to regulate in order to maintain homeostasis as long as concentrations are not exceptionally high (Wood et al., 2012). The remaining metals in the study are either non-essential (^{60}Ni and ^{208}Pb) or have not been demonstrated to be under strict physiological control in marine fishes (^{24}Mg, ^{51}V, and ^{53}Cr) (Wood et al., 2012). In this study, we observed that lesioned fish contained comparatively high concentrations of both an essential and a non-essential metal (^{63}Cu and ^{60}Ni, respectively), potentially indicating prolonged exposure to these heavy metals. An alternative explanation is that normal homeostatic regulation of these elements was inhibited by prolonged exposure to heavy metals, which has been shown to disturb ion regulation (Larsson et al., 1981; Kalish, 1992; Bonga, 1997).

Otolith microchemistry is not a function of ambient water chemistry alone, but may instead be influenced by temperature and salinity (Elsdon and Gillanders, 2002; Martin and Wuenschel, 2006), species-specific processes (Reis-Santos et al., 2008; Chang and Geffen, 2013), and biochemical controls (Campana, 1999; Hamer and Jenkins, 2007). The relative importance of the physiological regulation of element uptake in fish otoliths has only been recently recognized (Sturrock et al., 2014), and currently relatively little is known about the physiological regulation of element incorporation into otoliths in relation to their concentration in the environment. In principle, species that are phylogenetically close will have the most analogous physiological processes and more similar otolith microchemistries (Patterson et al., 2014). Thus, the differences in otolith microchemistry observed among species in this study are likely due in part to species-specific physiological differences in element regulation.

Table 7
Concentrations (ppm) and fluxes (10^6 kg) of trace metals investigated in this study in the GoM and Macondo crude oil.

Metal	Ref	Cr	Co	Cu	Fe	Pb	Mg	Ni	V	Zn
Comparison data for metals in sediments and water column										
NW shelf and slope	1	47 ± 2.05	8 ± 1.41	10 ± 1.70	15,100 ± 2.09	24 ± 1.77	7400 ± 1.98	19 ± 2.07	73 ± 2.01	309 ± 2.36
NE shelf and slope	1	31 ± 2.89	7 ± 1.44	9 ± 1.85	12,100 ± 3.33	23 ± 1.99	12,500 ± 2.62	16 ± 2.48	36 ± 2.47	55 ± 2.63
South Florida shelf and slope	1	26 ± 1.88	2 ± 3.27	NA	3710 ± 3.74	NA	24,100 ± 1.37	5 ± 3.52	19 ± 2.29	11 ± 2.26
NGOM slope sediments	2	54	NA	27	0.028	17	NA	38	100	81
Deep Water (1000–1350 m)	3	0.16	8.3×10^{-4}	0.083	0.051	NA	NA	0.276	1.579	NA
Crude oil and dispersant concentrations										
MC252 crude	4	9.4	0.2	0.5	7.9	0.3	6.4	1.5	0.2	18
MC252 mousse	4	7.4–9.4	0.2–0.7	1.7–4.0	49.9–955	0.6–1.5	309–2899	4.2–7.7	1.0–1.7	13.3–51.8
Corexit	5,6	0.03		0.1				0.14		
Annual flux of metals to the GoM										
Annual Flux (particulate and dissolved)	7	22.3	NA	14.1	12,905.7	13.3	NA	16.6	NA	59.7
Metal input from MC252 oil and dispersant	NA	7.3	0.2	0.4	6.2	0.2	5.0	1.2	0.2	14.0

1. Geometric mean (± geometric deviations) metal concentrations in surficial sediments on the continental shelf and slope in the NGoM (Holmes, 1973).
2. Mean metal concentrations in surficial sediments on the continental slope in the NGoM (Wade et al., 1980).
3. Mean metal concentrations (ppb) from water collected at depths of 1000–1350 m (Joung and Shiller, 2013).
4. Mean metal concentrations in Macondo crude oil and range of values from Macondo mousses (Liu et al., 2012).
5,6. Mean metal concentrations in Corexit dispersant (USEPA, 1995; Steffy et al., 2013).
7. Annual flux of metals from the Mississippi River to the GoM (Trefry, 1977).

5. Conclusions

The present study is the first to fully utilize the time-keeping properties of otoliths to investigate otolith metal concentrations in fish before and after an oil spill. Its major findings are 1) in most of the species examined, there was a group of individuals that contained a record of long-term and relatively high concentrations of ^{60}Ni and ^{64}Zn in their otoliths; 2) these high ^{60}Ni and ^{64}Zn concentrations were present in otoliths prior to the start of the DWH oil spill and did not appear to have changed during or after the oil spill; and 3) the high Ni-Zn group was strongly characterized by individuals with external skin lesions. These findings identify a long-term source of trace-metal stress in the northern Gulf of Mexico that has implications for fish health.

Acknowledgements

We thank the field team for collecting samples, including: K. Deak, E. Herdter, S. Gilbert, S. Grasty, S. Snyder, and A. Wallace. Gratitude is extended to Orian Tzadik, Matthew McCarthy, and two anonymous reviewers for comments on the manuscript. This research was made possible in part by grants from The Gulf of Mexico Research Initiative/C-IMAGE I and II (SA 15-16), the National Fisheries Institute, and the State of Louisiana (S203-4S-2121). Data are publicly available through the Gulf of Mexico Research Initiative Information & Data Cooperative (GRIIDC) at https://data.gulfresearchinitiative.org (doi:10.7266/N7XS5SFZ).

Appendix A. Supplementary data

Supplementary data to this article can be found online at http://dx.doi.org/10.1016/j.marpolbul.2017.01.066.

References

Al-Abdali, F., Massoud, M.S., Al-Ghadban, A.N., 1996. Bottom sediments of the Arabian Gulf - III. Trace metal contents as indicators of pollution and implications for the effect and fate of the Kuwait oil slick. Environ. Pollut. 93 (3):285–301. http://dx.doi.org/10.1016/S0269-7491(96)00046-2.

Amiard, J.C., Bacheley, H., Barille, A.L., Geffard, A., Himery, N., 2004. Temporal changes in nickel and vanadium concentrations and in condition index and metallothionein levels in three species of molluscs following the "Erika" oil spill. Aquat. Living Resour. 17 (3):281–288. http://dx.doi.org/10.1051/alr:2004037.

Anderson, M.J., 2001. A new method for non-parametric multivariate analysis of variance. Austral Ecol. 26 (1):32–46. http://dx.doi.org/10.1111/j.1442-9993.2001.01070.pp.x.

Apeti, D., Whitall, D., Lauenstein, G., McTigue, T., Kimbrough, K., Jacob, A., Mason, A., 2013. Assessing the impacts of the Deepwater Horizon oil spill: the National Status and Trends Program response. A Summary Report of Coastal Contamination. Silver Spring, MD. http://aquaticcommons.org/id/eprint/14686.

Bervoets, L., Blust, R., 2003. Metal concentrations in water, sediment and gudgeon (*Gobio gobio*) from a pollution gradient: relationship with fish condition factor. Environ. Pollut. 126 (1):9–19. http://dx.doi.org/10.1016/S0269-7491(03)00173-8.

Bervoets, L., Knapen, D., De Jonge, M., Van Campenhout, K., Blust, R., 2013. Differential hepatic metal and metallothionein levels in three feral fish species along a metal pollution gradient. PLoS One 8 (3). http://dx.doi.org/10.1371/journal.pone.0060805.

Bols, N.C., Brubacher, J.L., Ganassin, R.C., Lee, L.E.J., 2001. Ecotoxicology and innate immunity in fish. Dev. Comp. Immunol. 25 (8–9):853–873. http://dx.doi.org/10.1016/S0145-305X(01)00040-4.

Bonga, S.E.W., 1997. The stress response in fish. Physiol. Rev. 77 (3), 591–625.

Bray, J.R., Curtis, J.T., 1957. An ordination of the upland forest communities of southern Wisconsin. Ecol. Monogr. 27 (4):326–349. http://dx.doi.org/10.2307/1942268.

Camilli, R., Reddy, C.M., Yoerger, D.R., Van Mooy, B.A.S., Jakuba, M.V., Kinsey, J.C., McIntyre, C.P., Sylva, S.P., Maloney, J.V., 2010. Tracking hydrocarbon plume transport and biodegradation at Deepwater Horizon. Science 330 (6001):201–204. http://dx.doi.org/10.1126/science.1195223.

Campana, S.E., 1999. Chemistry and composition of fish otoliths: pathways, mechanisms and applications. Mar. Ecol. Prog. Ser. 188:263–297. http://dx.doi.org/10.3354/meps188263.

Campana, S.E., Neilson, J.D., 1985. Microstructure of fish otoliths. Can. J. Fish. Aquat. Sci. 42 (5):1014–1032. http://dx.doi.org/10.1139/f85-127.

Campana, S.E., Gagne, J.A., McLaren, J.W., 1995. Elemental fingerprinting of fish otoliths using ID-ICPMS. Mar. Ecol. Prog. Ser. 122 (1–3):115–120. http://dx.doi.org/10.3354/meps122115.

Carmichael, R.H., Jones, A.L., Patterson, H.K., Walton, W.C., Perez-Huerta, A., Overton, E.B., Dailey, M., Willett, K.L., 2012. Assimilation of oil-derived elements by oysters due to the Deepwater Horizon oil spill. Environ. Sci. Technol. 46 (23):12787–12795. http://dx.doi.org/10.1021/Es302369h.

Chakrabarty, P., Lam, C., Hardman, J., Aaronson, J., House, P.H., Janies, D.A., 2012. Species map: a web-based application for visualizing the overlap of distributions and pollution events, with a list of fishes put at risk by the 2010 Gulf of Mexico oil spill. Biodivers. Conserv. 21 (7):1865–1876. http://dx.doi.org/10.1007/s10531-012-0284-4.

Chang, M., Geffen, A., 2013. Taxonomic and geographic influences on fish otolith microchemistry. Fish Fish. 14 (4):458–492. http://dx.doi.org/10.1111/j.1467-2979.2012.00482.x.

Chiffoleau, J.F., Chauvaud, L., Amouroux, D., Barats, A., Dufour, A., Pecheyran, C., Roux, N., 2004. Nickel and vanadium contamination of benthic invertebrates following the "Erika" wreck. Aquat. Living Resour. 17 (3):273–280. http://dx.doi.org/10.1051/alr:2004032.

Clarke, K.R., Somerfield, P.J., Gorley, R.N., 2008. Testing of null hypotheses in exploratory community analyses: similarity profiles and biota-environment linkage. J. Exp. Mar. Biol. Ecol. 366 (1–2):56–69. http://dx.doi.org/10.1016/j.jembe.2008.07.009.

Clements, W.H., Rees, D.E., 1997. Effects of heavy metals on prey abundance, feeding habits, and metal uptake of brown trout in the Arkansas River, Colorado. Trans. Am. Fish. Soc. 126 (5):774–785. http://dx.doi.org/10.1577/1548-8659(1997)126%3C0774:Eohmop%3E2.3.Co;2.

De Groot, A., Salomons, W., Allersma, E., 1976. Processes affecting heavy metals in estuarine sediments. In: Burton, J., Less, P. (Eds.), Estuarine Chemistry. Academic Press, London, pp. 131–157.

Dubansky, B., Whitehead, A., Miller, J.T., Rice, C.D., Galvez, F., 2013. Multitissue molecular, genomic, and developmental effects of the Deepwater Horizon oil spill on resident gulf killifish (*Fundulus grandis*). Environ. Sci. Technol. 47 (10):5074–5082. http://dx.doi.org/10.1021/es400458p.

Elsdon, T.S., Gillanders, B.M., 2002. Interactive effects of temperature and salinity on otolith chemistry: challenges for determining environmental histories of fish. Can. J. Fish. Aquat. Sci. 59 (11):1796–1808. http://dx.doi.org/10.1139/F02-154.

Field, J.G., Clarke, K.R., Warwick, R.M., 1982. A practical strategy for analyzing multispecies distribution patterns. Mar. Ecol. Prog. Ser. 8 (1):37–52. http://dx.doi.org/10.3354/meps008037.
Fingas, M., 2011. Introduction to oil chemistry and properties. In: Fingas, M. (Ed.), Oil Spill Science and Technology. Elsevier, Burlington, MA:pp. 51–59 http://dx.doi.org/10.1016/B978-1-85617-943-0.10003-6.
Fitzgerald, T.P., Gohlke, J.M., 2014. Contaminant levels in Gulf of Mexico reef fish after the Deepwater Horizon oil spill as measured by a fishermen-led testing program. Environ. Sci. Technol. 48 (3):1993–2000. http://dx.doi.org/10.1021/Es4051555.
Fowler, S.W., Readman, J.W., Oregioni, B., Villeneuve, J.P., Mckay, K., 1993. Petroleum-hydrocarbons and trace-metals in nearshore gulf sediments and biota before and after the 1991 war - an assessment of temporal and spatial trends. Mar. Pollut. Bull. 27: 171–182. http://dx.doi.org/10.1016/0025-326x(93)90022-C.
Gohlke, J.M., Doke, D., Tipre, M., Leader, M., Fitzgerald, T., 2011. A review of seafood safety after the Deepwater Horizon blowout. Environ. Health Perspect. 119 (8):1062–1069. http://dx.doi.org/10.1289/ehp.1103507.
Grizzle, J.M., 1986. Lesions in fishes captured near drilling platforms in the Gulf of Mexico. Mar. Environ. Res. 18 (4):267–276. http://dx.doi.org/10.1016/0141-1136(86)90026-7.
Hall, R., Zook, E.G., Meaburn, G., 1978. National Marine Fisheries Service Survey of Trace Elements in the Fishery Resource. (Seattle, WA. http://hdl.handle.net/1969.3/20105).
Halter, W.E., Pettke, T., Heinrich, C.A., Rothen-Rutishauser, B., 2002. Major to trace element analysis of melt inclusions by laser-ablation ICP-MS: methods of quantification. Chem. Geol. 183 (1–4):63–86. http://dx.doi.org/10.1016/s0009-2541(01)00372-2.
Hamer, P.A., Jenkins, G.P., 2007. Comparison of spatial variation in otolith chemistry of two fish species and relationships with water chemistry and otolith growth. J. Fish Biol. 71 (4):1035–1055. http://dx.doi.org/10.1111/J.1095-8649.2007.01570.X.
Heagney, E.C., Gillanders, B.M., Suthers, I.M., 2013. The effect of parasitism by a blood-feeding isopod on the otolith chemistry of host fish. Mar. Freshw. Res. 64 (1): 10–19. http://dx.doi.org/10.1071/Mf12123.
Heinrich, C.A., Pettke, T., Halter, W.E., Aigner-Torres, M., Audetat, A., Gunther, D., Hattendorf, B., Bleiner, D., Guillong, M., Horn, I., 2003. Quantitative multi-element analysis of minerals, fluid and melt inclusions by laser-ablation inductively-coupled-plasma mass-spectrometry. Geochim. Cosmochim. Acta 67 (18): 3473–3497. http://dx.doi.org/10.1016/s0016-7037(03)00084-x.
Holmes, C., 1973. Distribution of Selected Elements in Surficial Marine Sediments of the Northern Gulf of Mexico Continental Shelf and Slope. US Government Printing Office, pp. 2330–7102 (Washington, DC).
Jackson, S.E., 2008. Calibration strategies for elemental analysis by LA-ICP-MS. In: Sylvester, P. (Ed.), Laser Ablation-ICP-MS in the Earth Sciences. Current Practices and Outstanding Issuesvolume Short Course Series Volume 40. Mineralogical Association of Canada, Vancouver, B.C. :pp. 169–188. http://hdl.handle.net/1959.14/85596.
Jones, D., 2012. Processing LA-ICP-MS Otolith Microchemistry Data Using the Fathom Toolbox for Matlab. University of South Florida, St. Petersburg, FL, College of Marine Science (http://marine.usf.edu/user/djones).
Jones, D.L., 2015. Fathom Toolbox for Matlab: Software for Multivariate Ecological and Oceanographic Data Analysis. College of Marine Science, University of South Florida, St. Petersburg, FL, USA (http://www.marine.usf.edu/user/djones/matlab/matlab.html).
Joung, D., Shiller, A.M., 2013. Trace element distributions in the water column near the Deepwater Horizon well blowout. Environ. Sci. Technol. 47 (5):2161–2168. http://dx.doi.org/10.1021/es303167p.
Joye, S.B., MacDonald, I.R., Leifer, I., Asper, V., 2011. Magnitude and oxidation potential of hydrocarbon gases released from the BP oil well blowout. Nat. Geosci. 4 (3):160–164. http://dx.doi.org/10.1038/Ngeo1067.
Kalish, J.M., 1992. Formation of a stress-induced chemical check in fish otoliths. J. Exp. Mar. Biol. Ecol. 162 (2):265–277. http://dx.doi.org/10.1016/0022-0981(92)90206-P.
Kotsanis, N., Iliopoulou-Georgudaki, J., Kapata-Zoumbos, K., 2000. Changes in selected haematological parameters at early stages of the rainbow trout, *Oncorhynchus mykiss*, subjected to metal toxicants: arsenic, cadmium and mercury. J. Appl. Ichthyol. 16 (6): 276–278. http://dx.doi.org/10.1046/j.1439-0426.2000.00163.x.
Kourafalou, V.H., Androulidakis, Y.S., 2013. Influence of Mississippi River induced circulation on the Deepwater Horizon oil spill transport. J. Geophys. Res. Oceans 118 (8): 3823–3842. http://dx.doi.org/10.1002/jgrc.20272.
Larsson, A., Bengtsson, B.E., Haux, C., 1981. Disturbed ion balance in flounder, *Platichthys flesus* L exposed to sublethal levels of cadmium. Aquat. Toxicol. 1 (1):19–35. http://dx.doi.org/10.1016/0166-445x(81)90004-7.
Liu, Z.F., Liu, J.Q., Zhu, Q.Z., Wu, W., 2012. The weathering of oil after the Deepwater Horizon oil spill: insights from the chemical composition of the oil from the sea surface, salt marshes and sediments. Environ. Res. Lett. 7 (3). http://dx.doi.org/10.1088/1748-9326/7/3/035302.
Longerich, H.P., Jackson, S.E., Gunther, D., 1996. Laser ablation inductively coupled plasma mass spectrometric transient signal data acquisition and analyte concentration calculation. J. Anal. At. Spectrom. 11 (9):899–904. http://dx.doi.org/10.1039/Ja9961100899.
Longerich, H.P., Jackson, S.E., Gunther, D., 1997. Laser ablation-inductively coupled plasma-mass spectrometric transient signal data acquisition and analyte concentration calculation. Errata. J. Anal. At. Spectrom. 12, 391.
Lu, Z.M., Deng, Y., Van Nostrand, J.D., He, Z.L., Voordeckers, J., Zhou, A.F., Lee, Y.J., Mason, O.U., Dubinsky, E.A., Chavarria, K.L., Tom, L.M., Fortney, J.L., Lamendella, R., Jansson, J.K., D'haeseleer, P., Hazen, T.C., Zhou, J.Z., 2012. Microbial gene functions enriched in the Deepwater Horizon deep-sea oil plume. ISME J. 6 (2):451–460. http://dx.doi.org/10.1038/ismej.2011.91.
Lubchenco, J., McNutt, M.K., Dreyfus, G., Murawski, S.A., Kennedy, D.M., Anastas, P.T., Chu, S., Hunter, T., 2012. Science in support of the Deepwater Horizon response. Proc. Natl. Acad. Sci. U. S. A. 109 (50):20212–20221. http://dx.doi.org/10.1073/Pnas.1204729109.
Maes, G.E., Raeymaekers, J.A.M., Pampoulie, C., Seynaeve, A., Goemans, G., Belpaire, C., Volckaert, F.A.M., 2005. The catadromous European eel *Anguilla anguilla* (L.) as a model for freshwater evolutionary ecotoxicology: relationship between heavy metal bioaccumulation, condition and genetic variability. Aquat. Toxicol. 73 (1): 99–114. http://dx.doi.org/10.1016/j.aquatox.2005.01.010.
Mallatt, J., 1985. Fish gill structural changes induced by toxicants and other irritants: a statistical review. Can. J. Fish. Aquat. Sci. 42 (4):630–648. http://dx.doi.org/10.1139/f85-083.
Martin, G.B., Wuenschel, M.J., 2006. Effect of temperature and salinity on otolith element incorporation in juvenile gray snapper *Lutjanus griseus*. Mar. Ecol. Prog. Ser. 324: 229–239. http://dx.doi.org/10.3354/Meps324229.
Martinec, C.C., Miller, J.M., Barron, N.K., Tao, R., Yu, K., Stewart, P.M., Nichols, A.C., Steffy, D.A., Landers, S.C., 2014. Sediment chemistry and meiofauna from the northern Gulf of Mexico continental shelf. Int. J. Oceanography 2014.
Massoud, M.S., Al-Abdali, F., Al-Ghadban, A.N., 1998. The status of oil pollution in the Arabian gulf by the end of 1993. Environ. Int. 24 (1–2):11–22. http://dx.doi.org/10.1016/S0160-4120(97)00117-7.
McGarigal, K., Cushman, S., Stafford, S., 2000. Multivariate Statistics for Wildlife and Ecology Research. Springer-Verlag New York Inc. http://dx.doi.org/10.1007/978-1-4612-1288-1.
Morales-Nin, B., Geffen, A.J., Cardona, F., Kruber, C., Saborido-Rey, F., 2007. The effect of Prestige oil ingestion on the growth and chemical composition of turbot otoliths. Mar. Pollut. Bull. 54 (11):1732–1741. http://dx.doi.org/10.1016/J.Marpolbul.2007.07.007.
Moreno, R., Jover, L., Diez, C., Sanpera, C., 2011. Seabird feathers as monitors of the levels and persistence of heavy metal pollution after the Prestige oil spill. Environ. Pollut. 159 (10):2454–2460. http://dx.doi.org/10.1016/j.envpol.2011.06.033.
Muhling, B.A., Roffer, M.A., Lamkin, J.T., Ingram, G.W., Upton, M.A., Gawlikowski, G., Muller-Karger, F., Habtes, S., Richards, W.J., 2012. Overlap between Atlantic bluefin tuna spawning grounds and observed Deepwater Horizon surface oil in the northern Gulf of Mexico. Mar. Pollut. Bull. 64 (4):679–687. http://dx.doi.org/10.1016/j.marpolbul.2012.01.034.
Murawski, S.A., Hogarth, W.T., Peebles, E.B., Barbeiri, L., 2014. Prevalence of external skin lesions and polycyclic aromatic hydrocarbon concentrations in Gulf of Mexico fishes, post-Deepwater Horizon. Trans. Am. Fish. Soc. 143 (4):1084–1097. http://dx.doi.org/10.1080/00028487.2014.911205.
Neff, J.M., 1987. Biological effects of drilling fluids, drill cuttings, and produced waters. In: Boesch, D.F., Rabalais, N.N. (Eds.), Long-Term Environmental Effects of offshore Oil and Gas Development. Elsevier Applied Science, London, UK:pp. 469–538 http://dx.doi.org/10.1086/416424.
Nelson, T.R., DeVries, D.R., Wright, R.A., Gagnon, J.E., 2014. *Fundulus grandis* otolith microchemistry as a metric of estuarine discrimination and oil exposure. Estuar. Coasts:1–15 http://dx.doi.org/10.1007/s12237-014-9934-y.
Nowling, L., Gauldie, R.W., Cowan, J.J.H., Carlo, E.D., 2011. Successful discrimination using otolith microchemistry among samples of Red Snapper *Lutjanus campechanus* from artificial reefs and sample of *L. campechanus* taken from nearby oil and gas platforms. Open Fish Sci. J. 4:1–9. http://dx.doi.org/10.2174/1874401X01104010001.
Ocean Studies Board and Marine Board, 2003. Oil in the Sea III. Inputs, Fates, and Effects. National Academies Press, Washington, DC. http://dx.doi.org/10.17226/10388.
O'Connor, B.S., Muller-Karger, F.E., Nero, R.W., Hu, C., Peebles, E.B., 2016. The role of Mississippi River discharge in offshore phytoplankton blooming in the northeastern Gulf of Mexico during August 2010. Remote Sens. Environ. 173:133–144. http://dx.doi.org/10.1016/j.rse.2015.11.004.
Oneill, J.G., 1981. The humoral immune-response of *Salmo trutta* L and *Cyprinus carpio* L exposed to heavy metals. J. Fish Biol. 19 (3):297–306. http://dx.doi.org/10.1111/j.1095-8649.1981.tb05833.x.
Pannella, G., 1971. Fish otoliths - daily growth layers and periodical patterns. Science 173 (4002):1124–1131. http://dx.doi.org/10.1126/science.173.4002.1124.
Patterson III, W.F., Barnett, B.K., Sluis, M.Z., Cowan Jr., J.H., Shiller, A.M., 2014. Interspecific variation in juvenile snapper otolith chemical signatures in the northern Gulf of Mexico. Aquat. Biol. 21 (1):1–10. http://dx.doi.org/10.3354/ab00567.
Payan, P., De Pontual, H., Edeyer, A., Borelli, G., Boeuf, G., Mayer-Gostan, N., 2004. Effects of stress on plasma homeostasis, endolymph chemistry, and check formation during otolith growth in rainbow trout (*Oncorhynchus mykiss*). Can. J. Fish. Aquat. Sci. 61 (7):1247–1255. http://dx.doi.org/10.1139/f04-059.
Pereira, J.J., Mercaldoallen, R., Kuropat, C., Luedke, D., Sennefelder, G., 1993. Effect of cadmium accumulation on serum vitellogenin levels and hepatosomatic and gonadosomatic indexes of winter flounder (*Pleuronectes americanus*). Arch. Environ. Contam. Toxicol. 24 (4):427–431. http://dx.doi.org/10.1007/BF01146157.
Peterson, C.H., Kennicutt, M.C., Green, R.H., Montagna, P., Harper, D.E., Powell, E.N., Roscigno, P.F., 1996. Ecological consequences of environmental perturbations associated with offshore hydrocarbon production: a perspective on long-term exposures in the Gulf of Mexico. Can. J. Fish. Aquat. Sci. 53 (11):2637–2654. http://dx.doi.org/10.1126/science.108428210.1139/Cjfas-53-11-2637.
Prego, R., Cobelo-Garcia, A., Marmolejo-Rodriguez, J., Santos-Echeandia, J., 2006. Trace elements in the Prestige fuel-oil spill: levels and influence on Laxe Ria sediments (NW Iberian peninsula). Cienc. Mar. 32 (1b):179–186. http://dx.doi.org/10.7773/cm.v32i12.1028.
Reis-Santos, P., Vasconcelos, R.P., Ruano, M., Latkoczy, C., Gunther, D., Costa, M.J., Cabral, H., 2008. Interspecific variations of otolith chemistry in estuarine fish nurseries. J. Fish Biol. 72 (10):2595–2614. http://dx.doi.org/10.1111/J.1095-8649.2008.01871.X.
Rooker, J.R., Kitchens, L.L., Dance, M.A., Wells, R.J.D., Falterman, B., Cornic, M., 2013. Spatial, temporal, and habitat-related variation in abundance of pelagic fishes in the Gulf of Mexico: potential implications of the Deepwater Horizon oil spill. PLoS One 8 (10). http://dx.doi.org/10.1371/journal.pone.0076080.
Rosenzweig, A.C., 2002. Metallochaperones: bind and deliver. Chem. Biol. 9 (6):673–677. http://dx.doi.org/10.1016/S1074-5521(02)00156-4.
Sanborn, M., Telmer, K., 2003. The spatial resolution of LA-ICP-MS line scans across heterogeneous materials such as fish otoliths and zoned minerals. J. Anal. At. Spectrom. 18 (10):1231–1237. http://dx.doi.org/10.1039/B302513F.

Santos-Echeandia, J., Prego, R., Cobelo-Garcia, A., 2008. Influence of the heavy fuel spill from the Prestige tanker wreckage in the overlying seawater column levels of copper, nickel and vanadium (NE Atlantic ocean). J. Mar. Syst. 72 (1–4):350–357. http://dx.doi.org/10.1016/j.jmarsys.2006.12.005.

Sinclair, D.J., Kinsley, L.P.J., McCulloch, M.T., 1998. High resolution analysis of trace elements in corals by laser ablation ICP-MS. Geochim. Cosmochim. Acta 62 (11): 1889–1901. http://dx.doi.org/10.1016/s0016-7037(98)00112-4.

Sluis, M., Cowan, J.H., 2013. Platform Recruited Reef Fish, Phase II: Do Platforms Provide Habitat that Increases the Survival of Reef Fishes? Department of Interior, New Orleans, LA

Snyder, S.M., Pulster, E.L., Wetzel, D.L., Murawski, S.A., 2015. PAH exposure in Gulf of Mexico demersal fishes, post-Deepwater Horizon. Environ. Sci. Technol. 49 (14): 8786–8795. http://dx.doi.org/10.1021/acs.est.5b01870.

Stanley, D.R., Wilson, C.A., 1990. A fishery-dependent based study of fish species composition and associated catch rates around oil and gas structures off Louisiana. Fish. Bull. 88 (4), 719–730.

Stanley, D.R., Wilson, C.A., 1997. Seasonal and spatial variation in the abundance and size distribution of fishes associated with a petroleum platform in the northern Gulf of Mexico. Can. J. Fish. Aquat. Sci. 54 (5):1166–1176. http://dx.doi.org/10.1139/cjfas-54-5-1166.

State of Louisiana, 2010. Office of Coastal Protection and Resotration officials open Davis Pond diversion to full capacity to help curb oil penetration into coastal marshes. http://emergency.louisiana.gov/Releases/05102010-ocpr.html.

Steffy, D.A., Nichols, A.C., Morgan, L.J., Gibbs, R., 2013. Evidence that the Deepwater Horizon oil spill caused a change in the nickel, chromium, and lead average seasonal concentrations occurring in sea bottom sediment collected from the eastern Gulf of Mexico continental shelf between the years 2009 and 2011. Water Air Soil Pollut. 224 (11). http://dx.doi.org/10.1007/S11270-013-1756-1.

Sturrock, A.M., Trueman, C.N., Milton, J.A., Waring, C.P., Cooper, M.J., Hunter, E., 2014. Physiological influences can outweigh environmental signals in otolith microchemistry research. Mar. Ecol. Prog. Ser. 500:245–264. http://dx.doi.org/10.3354/Meps10699.

Summers, J.K., Wade, T.L., Engle, V.D., Malaeb, Z.A., 1996. Normalization of metal concentrations in estuarine sediments from the Gulf of Mexico. Estuaries 19 (3):581–594. http://dx.doi.org/10.2307/1352519.

Tillery, J.B., Thomas, R.E., 1980. Heavy metal contamination from petroleum platforms in the central Gulf of Mexico. Page 562 in Research on Environmental Fate and Effects of Drilling Fluids and Cuttings Volume 1. American Petroleum Institute, Washington, D.C.

Trefry III, J., 1977. The Transport of Heavy Metals by the Mississippi River and their Fate in the Gulf of Mexico. Texas A&M University.

USEPA, 1995. Corexit 9500 A. Technical Bulletin #D-4. http://www.epa.gov/emergency-response/corexitr-ec9500a.

Valentine, D.L., Fisher, G.B., Bagby, S.C., Nelson, R.K., Reddy, C.M., Sylva, S.P., Woo, M.A., 2014. Fallout plume of submerged oil from Deepwater Horizon. Proc. Natl. Acad. Sci. 111 (45):15906–15911. http://dx.doi.org/10.1073/pnas.1414873111.

Varanasi, U., Stein, J., Nishimoto, M., 1989. Biotransformation and disposition of polycyclic aromatic hydrocarbons (PAH) in fish. In: Varanasi, U. (Ed.), Metabolism of Polycyclic Aromatic Hydrocarbons in the Aquatic Environment. CRC Press, Inc., Boca Raton, Florida, pp. 1–40.

Wade, T.L., Soliman, Y., Sweet, S.T., Wolff, G.A., Presley, B.J., 1980. Trace elements and polycyclic aromatic hydrocarbons (PAHs) concentrations in deep Gulf of Mexico sediments. Deep Sea Res. Pt II 55 (24):2585–2593. http://dx.doi.org/10.1016/j.dsr2.2008.07.006.

Wilkinson, L., Friendly, M., 2009. The history of the cluster heat map. Am. Stat. 63 (2): 179–184. http://dx.doi.org/10.1198/tas.2009.0033.

Windom, H.L., 1992. Contamination of the marine environment from land-based sources. Mar. Pollut. Bull. 25 (1–4):32–36. http://dx.doi.org/10.1016/0025-326x(92)90180-E.

Wise, J.P.J., Wise, J.T.F., Wise, C.F., Wise, S.S., Gianios, C., Xie, H., Thompson, W.D., Perkins, C., Falank, C., Wise, J.P.S., 2014. Concentrations of the genotoxic metals, chromium and nickel, in whales, tar balls, oil slicks, and released oil from the Gulf of Mexico in the immediate aftermath of the Deepwater Horizon oil crisis: is genotoxic metal exposure part of the Deepwater Horizon legacy? Environ. Sci. Technol. 48 (5): 2997–3006. http://dx.doi.org/10.1021/Es405079b.

Wood, C.M., Farrell, A.P., Brauner, C.J., 2012. Homeostasis and Toxicology of Essential Metals. volume 31. Academic Press.

Zelikoff, J.T., 1993. Metal pollution-induced immunomodulation in fish. Annu. Rev. Fish Dis. 3:305–325. http://dx.doi.org/10.1016/0959-8030(93)90041-9.